

**Epigenetic and Transcriptional Regulation of
Cortico-Ponto-Cerebellar
Circuit Formation**

Inauguraldissertation

Zur

Erlangung der Würde eines Doktors der Philosophie
vorgelegt der
Philosophisch-Naturwissenschaftlichen Fakultät
der Universität Basel

Von

Dominik Gerhard Kraus
aus Sulzbach-Rosenberg/Deutschland

Basel, 2016

Originaldokument gespeichert auf dem Dokumentenserver der Universität Basel
edoc.unibas.ch

Genehmigt von der Philosophisch-Naturwissenschaftlichen Fakultät

auf Antrag von:

Prof. Dr. Filippo Rijli

(Dissertationsleiter)

Prof. Dr. Peter Scheiffele

(Koreferent)

Basel, den 23. Februar 2016

Prof. Dr. Jörg Schibler

(Dekan)

| | |
|---|----|
| Summary | 4 |
| Abbreviations | 6 |
| 1. Introduction | 8 |
| 1.1. Patterning the nervous system..... | 8 |
| 1.1.1. Retinoic acid (RA) signaling | 11 |
| 1.1.2. Wnt signaling | 14 |
| 1.2. Neuronal circuit formation..... | 16 |
| 1.3. Regulation of Hox gene expression | 19 |
| 1.3.1. Collinearity of Hox gene expression | 20 |
| 1.3.2. Signaling molecules and transcription factors relevant for Hox gene expression .. | 22 |
| 1.3.3. Regulation of Hox gene expression: Epigenetics..... | 24 |
| 1.3.4. Higher order chromatin organization underlying Hox gene expression | 27 |
| 1.4. Role of Hox genes during development..... | 29 |
| 1.4.1. Hox genes and hindbrain segmentation..... | 30 |
| 1.4.2. Function of Hox genes during circuit formation | 31 |
| 1.5. The rhombic lip..... | 34 |
| 1.6. The precerebellar system | 36 |
| 1.6.1. Specification of the different components of the precerebellar system | 37 |
| 1.6.2. Migration and nucleation of pontine nuclei neurons..... | 38 |
| 1.6.3. Circuitry of the pontine nuclei: Input connectivity | 41 |
| 1.6.4. Circuitry of the pontine nuclei: Output connectivity..... | 44 |
| 1.6.5. Function of the pontine nuclei..... | 46 |
| 1.7. Aim of this thesis | 48 |
| 2. Material and Methods | 49 |
| 2.1. Animals | 49 |
| 2.1.1. Generation of the <i>Math1::Cre</i> line..... | 49 |
| 2.1.2. Generation of the <i>Jmjd3</i> knock-in line | 49 |
| 2.1.3. Generation of the <i>ROSA26::CAG(lox-stop-lox)3xFlag-Hoxa5-IRES-GFP</i> knock-in line | 50 |
| 2.1.4. Generation of the <i>ROSA26::(lox-stop-lox)Hoxa5-IRES-GFP</i> BAC transgenic line... | 50 |
| 2.1.5. Generation of the <i>Tau::(lox-stop-lox)Rabies-glycoprotein-IRES-nls-LacZ</i> line..... | 51 |

| | |
|---|----|
| 2.1.6. Other mouse lines used in this study | 51 |
| 2.1.7. Retinoic acid and tamoxifen treatment..... | 51 |
| 2.2. In utero electroporation | 52 |
| 2.3. Histological analysis, immunostaining, and in situ hybridization | 52 |
| 2.4. Fluorescent activated Cell Sorting (FACS) | 53 |
| 2.5. Quantitative PCR (qPCR) | 53 |
| 2.6. Chromatin immunoprecipitation (ChIP) | 54 |
| 2.7. 4C sequencing | 55 |
| 2.7.1. 4C template preparation | 55 |
| 2.7.2. 4C PCR, mapping and analysis of 4C data | 55 |
| 2.8. RNA sequencing | 56 |
| 2.9. Virus and retrograde tracing experiments | 56 |
| 2.10. Imaging and picture processing | 56 |
| 2.11. Statistical analysis | 57 |
| 3. Results | 58 |
| 3.1. Antagonistic Wnt and RA signaling results in postmitotic induction of <i>Hox PG5</i> in a specific subset of PN neurons..... | 58 |
| 3.2. Depletion of Polycomb-dependent H3K27me3 repressive mark is necessary but not sufficient for <i>Hox PG5</i> expression in the precerebellar system | 65 |
| 3.3. Three Dimensional (3D) conformational change of chromatin organization upon RA mediated <i>Hox PG5</i> induction | 71 |
| 3.4. <i>Hoxa5</i> expression is sufficient to drive neurons into a posterior position in the PN...73 | |
| 3.5. PN neuron subpopulations have distinct, Hox dependent transcriptional programs ...75 | |
| 3.6. Ectopic expression of <i>Hoxa5</i> rearranges PN neuron output connectivity | 78 |
| 3.7. Relative A-P position of neurons within the PN is predictive for their cortical input connectivity | 80 |
| 3.8. <i>Hoxa5</i> overexpression is sufficient to reorganize input connectivity of PN neurons..84 | |
| 4. Discussion | 88 |
| 4.1. A-P identity is specified post-mitotically in PN neurons..... | 88 |
| 4.2. H3K27me3 dependent and independent mechanisms of <i>Hox PG5</i> gene repression ...90 | |
| 4.3. Higher order chromatin reorganisation upon RA treatment in the nervous system.....91 | |
| 4.4. <i>Hoxa5</i> regulates positional and transcriptional identity of specific PN neurons subsets. | 92 |

Table of Contents

| | |
|---|-------------------------------------|
| 4.5. Hoxa5 is sufficient to orchestrate PN neuron input-output connectivity | 93 |
| 4.6. Implications for somatosensory map transformation | 96 |
| 4.7. Outlook..... | 97 |
| Statement of contribution..... | 99 |
| Bibliography | 100 |
| Acknowledgments..... | 129 |
| Curriculum vitae | Error! Bookmark not defined. |

Summary

The precerebellar system constitutes an array of nuclei located in the mammalian hindbrain and conveys movement and balance information from the cortex, spinal cord and periphery to the cerebellum (Sotelo, 2004). Within this system, the pontine nuclei (PN), including pontine gray and reticulotegmental nuclei, mostly relay cortical information (Schwarz and Thier, 1999). During the processing through the cortex, PN and cerebellum, continuous maps of sensorimotor information are transformed into a complex fractured map (Leergaard et al., 2006). To date, however, there is a paucity of knowledge on the molecular and cellular mechanisms organizing this complex circuitry. Previous work suggests an intrinsic topographic organization, according to rostro-caudal progenitor origin, that is maintained during migration and nucleation of the PN (Di Meglio et al., 2013). As a result, one of the hallmarks of the PN topography is a well-defined population of *Hox paralogous group 5* (PG5) expressing neurons in the posterior part of the PN. However, the molecular mechanisms governing the spatial expression pattern of *Hox PG5* genes in the PN and their functional impact on circuit formation remain largely unknown.

The first part of this thesis focuses on the molecular mechanisms of *Hox PG5* induction in the precerebellar system. We find that the precise spatio-temporal expression pattern of *Hox PG5* genes rely on the integration of environmental signaling and the resulting modifications of the epigenetic landscape. Unlike transcripts of more anterior Hox genes, expression of *Hox PG5* genes is entirely excluded from progenitors in the rhombic lip (RL) and only induced in a subset of postmitotic neurons. Mapping and manipulation of signaling pathways show that the restriction of *Hox PG5* induction to the ventrally located (i.e. posterior RL-derived) postmitotic pontine neuron subsets is due to an interplay between retinoic acid (RA) and Wnt environmental signaling. Assessment of histone profiles at Hox loci indicate that the induction of *Hox PG5* genes through RA is tightly linked to a depletion of the histone mark H3K27me3. However, conditional inactivation of *Ezh2*, a member of the polycomb repressive complex 2 responsible for setting the H3K27me3 mark (Margueron and Reinberg, 2011), does not result in a de-repression of *Hox PG5* genes in the progenitor domain. In contrast, removal of H3K27me3 in *Ezh2* depleted PN neurons leads to an ectopic induction of *Hox PG5* in rostral PN neuron subsets of the migratory stream showing an enhanced response to RA (Di Meglio et al., 2013). Moreover, high levels of RA-induced *Hox PG5* expression in postmitotic PN neurons require Jmjd3, one of the enzymes known to catalyze the removal of

methyl groups at H3K27 (Agger et al., 2007; De Santa et al., 2007). We show that Jmjd3 is physically present at RA responsive elements in proximity to the *Hoxa5* promoter supporting the direct involvement of Jmjd3 in *Hox PG5* induction. Thus, a central function of H3K27me3 regulation during late stages of precerebellar development is the establishment of a threshold for RA mediated activation of *Hox PG5* genes to allow for diversification of PN neurons. Finally, we show how the integration of environmental signaling on the epigenetic level results in distinct changes of the three dimensional (3D) organization of chromatin at *Hox PG5* loci *in vivo*. Together, the late specification of PN neurons employs a sophisticated sequence of interactions between signaling pathways such as RA and Wnt, and histone modifying enzymes like Ezh2 and Jmjd3.

The second part of the thesis addresses the functional significance of *Hox PG5* genes in sub-circuit formation of PN neurons. Using multiple conditional overexpression strategies, we show that the expression of *Hoxa5* is sufficient to shape the input-output relationship of PN neurons. *Hoxa5* expressing neurons migrate into a posterior position in the PN and induce a distinct transcriptional program specific for topographic circuit formation. Together, this indicates a crucial role of *Hoxa5* in the specification of the positional identity of PN subsets. We further describe a genetically identified *Hox PG5* negative PN subset that primarily projects to the paraflocculus, a lobule in the cerebellum heavily concerned with visually related tasks. Conditional overexpression of *Hoxa5* in this PN subset leads to the ectopic targeting of several other lobes in the cerebellum concerned with processing of somatosensory information. This matches with the input connectivity of the PN that has been shown to be antero-posteriorly patterned, such that visual/medioposterior projections target the anterior, *Hox PG5* negative, and somatosensory projections target the posterior, *Hox PG5* positive part of the PN (Di Meglio et al., 2013; Leergaard and Bjaalie, 2007). Consequently, *Hoxa5* overexpressing PN neurons are largely devoid of input from the visual cortex and primarily engage in a somatosensory hindlimb specific circuitry. One single Hox gene is thus sufficient to position neurons in the posterior aspects of the PN, change their transcriptional program and rearrange both, output connectivity to the cerebellum and input connectivity from the cortex. These findings extend the function of Hox genes to orchestrating topographic circuit formation in the PN. Further, the presented results point towards an involvement of Hox genes in the longstanding problem of fracturing of the somatosensory map that is realized between the cortex and the cerebellum.

Abbreviations

| | |
|--------|---|
| 3-D | three dimensional |
| 4C | Circular chromosome conformation capture |
| 4C-seq | 4C followed by high throughput sequencing |
| A-P | antero-posterior |
| Ac | acetylation |
| AES | anterior extramural stream |
| ARE | autoregulatory element |
| AVCN | antero-ventral cochlear nucleus |
| BAC | bacterial artificial chromosome |
| bHLH | basic helix-loop-helix |
| BMP | Bone morphogenetic protein |
| ChIP | Chromatin immunoprecipitation |
| cKO | conditional knockouts |
| CNS | central nervous system |
| CRE | cross-regulatory element |
| CST | cortico-spinal tract |
| D-V | dorso-ventral |
| dnRAR | dominant negative retinoic acid receptor |
| dPrV | dorsal principal trigeminal nucleus |
| Dsh | Dishevelled |
| E | embryonic day |
| ECN | external cuneate nuclei |
| ESC | embryonic stem cell |
| FACS | fluorescence activated cell sorting |
| FC | fold change |
| FDR | false discovery rate corrected |
| FGF | fibroblast growth factor |
| FISH | fluorescent <i>in situ</i> hybridisation |
| FMN | Facial nucleus |
| Fz | Frizzled |
| GFP | green fluorescent protein |
| GO | gene ontology |
| Gsk3 | glycogen synthase 3 |
| H3 | Histone 3 |
| IFV | interfascicular trigeminal nucleus |
| IO | inferior olivary complex |
| IRES | internal ribosome entry site |
| K4 | lysine residue 4 |
| K9 | lysine residue 9 |
| K27 | lysine residue 27 |
| LI | linear nucleus |

Abbreviations

| | |
|--------------------|--------------------------------------|
| IRL | lower rhombic lip |
| LRN | lateral reticular nuclei |
| M-L | medio-lateral |
| Me3 | tri-methylation |
| NA | numerical aperture |
| nls | nuclear localisation sequence |
| P | postnatal day |
| PBS | phosphate buffer |
| PcG | polycomb group |
| PCP | planar cell polarity |
| PES | posterior extramural stream |
| PFL | paraflocculus |
| RFP | red fluorescent protein |
| PG5 | paralogous group 5 |
| PGN | pontine gray nucleus |
| PML | paramedian lobule |
| PN | pontine nuclei |
| PRC | polycomb repressive complex |
| PVCN | posterior-ventral cochlear nucleus |
| qPCR | quantitative PCR |
| r | rhombomere |
| RA | retinoic acid |
| Rabies- ΔG | glycoprotein-deleted rabies viruses |
| RAR | retinoic acid receptor |
| RARE | retinoic acid responsive element |
| Rbp4 | retinol binding protein 4 |
| RL | rhombic lip |
| RT | reverse transcription |
| RTN | reticulotegmental nuclei |
| S1 | primary somatosensory cortex |
| SL | simple lobule |
| SSH | sonic hedgehog |
| Tcf | T cell factor |
| TGF- β | transforming growth factor beta |
| TrxG | trithorax |
| V1 | primary visual cortex |
| vPrV | ventral principal trigeminal nucleus |
| vs | versus |

1. Introduction

How does a single cell, the fertilized oocyte, transform into a full organism with its cell types, tissues, organs, and organ systems? This question has fascinated developmental biologists ever since. Especially in the mammalian nervous system with its more than 12^{10} neurons and $10^{14} - 10^{15}$ synapses many questions regarding the assembly of neuronal circuits are still unanswered. Major functions of the central nervous system (CNS), e.g. sensory perception and motor coordination, depend on the fact that basic connectivity patterns between diverse neuronal populations are hard wired.

1.1. Patterning the nervous system

Initially, the mammalian CNS starts from a uniform population of epithelial progenitors, the neural plate, that induce a neural program. This plate folds into a tubular structure, the neural tube, which will give rise to the brain and spinal cord. The rostral part of the neural tube broadens into several dilatations that eventually form the three primary cerebral vesicles, corresponding to the prospective fore-brain (prosencephalon), midbrain (mesencephalon) and hindbrain (rhombencephalon). Later during development, the prosencephalon is further subdivided into the telencephalon and diencephalon and the rhombencephalon gives rise to the metencephalon and myelencephalon. At this stage, the CNS is patterned into its six major regions being present in a mature mammalian organism. These regions are then further patterned along the dorso-ventral (D-V) as well as antero-posterior (A-P) axis to ultimately give rise to a fully functioning CNS.

Any kind of patterning, from the very early specification of the neural plate to the formation of cortical regions depend on reciprocal interactions of cells through cell surface or diffusible molecules, so called morphogens (Turing, 1952). Morphogens and cell-cell interactions, e.g. through Notch signaling, play an important role in defining polarity, during cell differentiation, and the spatial specification of cell fates in the developing embryo (Feller et al., 2008; Hunter et al., 2006). The basic principle of morphogens is that long-range signaling molecules are present in a graded manner along different axes of tissues in an organism. Depending on the position of cells along this gradient, different transcriptional programs get switched on, resulting in diversification of cells along the respective gradient (Figure 1) (Wolpert, 1969). Additionally, the response of cells is dependent on many other factors including the duration of exposure as well as the state of the cell at the moment of exposure.

Despite the longstanding history of experiments indicating the existence of inductive molecules (Lewis, 1904) the first clear link between a gradient and pattern formation was published only in 1988 with the discovery of the Bicoid protein in *Drosophila* by Nüsslein-Volhard (Driever and Nusslein-Volhard, 1988a, b). Thereafter many other bona fide morphogens including RA (Durston et al., 1989), sonic hedgehog (SHH) (Echelard et al., 1993), transforming growth factor beta (TGF- β) (Ferguson and Anderson, 1992) and Wnt/beta-catenin (Neumann and Cohen, 1997) were discovered. Only for this thesis relevant morphogens will be described in more detail later on.

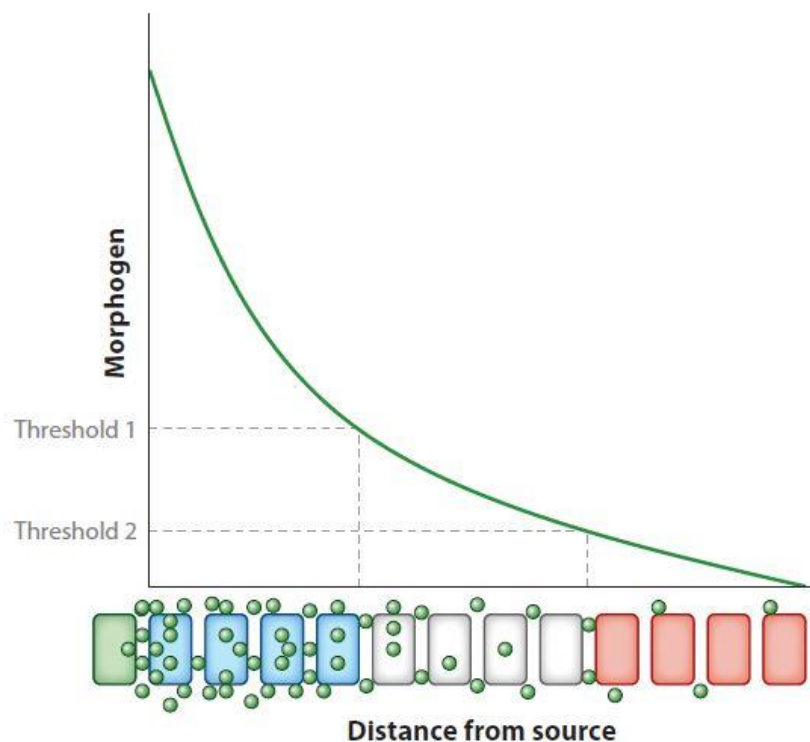


Figure 1: The French flag model by Lewis Wolpert. Morphogens (green circles), secreted from a localized source (green box), form a gradient over a certain tissue. Cells along this gradient will adopt different fates (blue, white and red boxes) dependent on whether the morphogen concentration reaches a given threshold. (Rogers and Schier, 2011)

There are many mechanisms which contribute to the formation of morphogenetic gradients (Dubrulle and Pourquie, 2004; Grieneisen et al., 2012) but the most widely known mechanism is through secretion from a localized group of cells followed by non-directional diffusion through the adjacent tissue and removal of the morphogen by immobilization, degradation, or endocytosis. This source-sink mechanism of gradient formation was first suggested as a theoretical model by Crick in 1970 (Crick, 1970), further refined by Gregor et

al. in 2007 (Gregor et al., 2007) and remains to be the best model to explain the gradient formation of many morphogens.

Morphogens interact with cells along their gradients through binding to receptors displayed either on cell surfaces or intracellularly. Receptor-ligand binding elicits a signaling cascade ultimately resulting in transcriptional changes in the respective cell. Different levels of morphogens dictate a certain cell fate through the regulation of gene expression. Thereby, the absolute number of ligand bound receptors seems to be decisive (Dyson and Gurdon, 1998) rather than the ratio between bound and unbound receptors despite possible exceptions (Casali and Struhl, 2004). Morphogen signaling usually does not elicit an “all-or-none” event. Rather multiple responses are generated from different morphogen concentrations. Signal transduction follows mostly a linear rule, meaning an x-fold increase of receptor occupancy results in a roughly x-fold in- or decrease in the expression of the regulated genes (Ashe and Briscoe, 2006; Shimizu and Gurdon, 1999; Stamatakis et al., 2005). However, certain target genes show distinct expression domains along a morphogen gradient suggesting that cells have the capacity to interpret morphogen signaling. One of several ways to explain the formation of specific expression domains is through differential DNA binding affinities to *cis*-regulatory elements. This model implicates that high-threshold genes are under the transcriptional control of low-affinity regulatory elements ensuring expression only at high morphogen levels and vice versa (Ashe and Briscoe, 2006). Another way to form distinct expression domains is through pre-patterning of the tissue by transcriptional activators or repressors that act in a combinatorial manner with morphogens to regulate target gene expression (Szymanski and Levine, 1995). This pre-patterning may be achieved through feed-forward loops or through the activity of other morphogens. Over the last decade, it also became more and more appreciated that pre-patterning might be reflected on the epigenetic level through nucleosome positioning (Kim and O'Shea, 2008) or chromatin modifications (Dahle et al., 2010). Finally, time of exposure of a cell to a given morphogen seems to have an impact on the interpretation of morphogen signaling in some occasions as well (Rogers and Schier, 2011).

Together, the described mechanisms give rise to an astonishing precision and robustness that is of paramount importance for the reliable development of embryos considering the perturbations that might arise through its journey.

1.1.1. Retinoic acid (RA) signaling

Deficiencies in vitamin A (retinol) during gestation have been linked to a plethora of developmental malformation since the early 19th century (Sommer, 2008). The acidic metabolite of vitamin A and its main biologically active derivate is RA. The functional aspects of vitamin A and RA biochemistry got sorted out in the 1960s-1980s. However, it was not before 1987 that RA was described to be present in a graded manner in the developing limb bud indicating that RA is a substance with morphogenetic properties (Thaller and Eichele, 1987). Since then RA has been implicated in a number of patterning events during embryonic development with the hindbrain being the most extensively studied one (Glover et al., 2006).

Availability of RA is entirely dependent on the uptake of vitamin A through dietary, as vitamin A is an essential vitamin that cannot be synthesized *de novo*. In mammals, the delivery of vitamin A from the liver to peripheral tissues via the vascular system is usually mediated through its binding to Rbp4 (O'Byrne and Blaner, 2013). Vitamin A can be taken up by target tissues through the transmembrane protein Stra6 (Kawaguchi et al., 2007) but can also enter cells without specific transporters due to its liposoluble character. The oxidation of vitamin A to retinaldehyde through alcohol or retinol dehydrogenases is the first step in the biosynthesis of RA (Figure 2). The most well-known enzyme catalyzing this step is Rdh10 which has been shown to be essential for embryonic development (Sandell et al., 2007). The expression pattern of *Rdh10* may already convey spatiotemporal specificity to RA signaling (Cammass et al., 2007; Romand et al., 2008). The final step of RA biosynthesis, the oxidation of retinaldehyde, is mediated by three different retinaldehyde dehydrogenases out of which Raldh2 is the one with the widest implication for the developing embryo (Niederreither et al., 1997; Niederreither et al., 1999; Niederreither et al., 2003). Raldh1 and 3 instead seem to be rather specifically required for the development of the eyes and the olfactory system (Dupe et al., 2003; Molotkov et al., 2006). Localized sources of RA exist due to the restricted expression patterns of Raldh enzymes. However, the tissue specific oxidative metabolism of RA has been shown to be equally important for the formation of RA gradients (White and Schilling, 2008). RA is catabolized to 4-hydroxy-RA by enzymes of the cytochrome P450 subfamily 26 (White et al., 1996). *Cyp26* genes display complex expression patterns in various organs, usually complementary to *Raldh* expression. For instance, the anterior expression of *Cyp26s* (Fujii et al., 1997) and posterior presence of *Raldh2* (Niederreither et

al., 1997) suggest an anterior-low to posterior-high RA gradient in the hindbrain. Furthermore, inactivation of *Cyp26s* results in phenotypes closely resembling the effects of exogenous RA availability underlining their importance for normal RA signaling (Abu-Abed et al., 2001; Yashiro et al., 2004). Interestingly, *Cyp26a1* has been shown to be a direct target of RA indicating an auto-regulatory negative feedback loop (White et al., 2007).

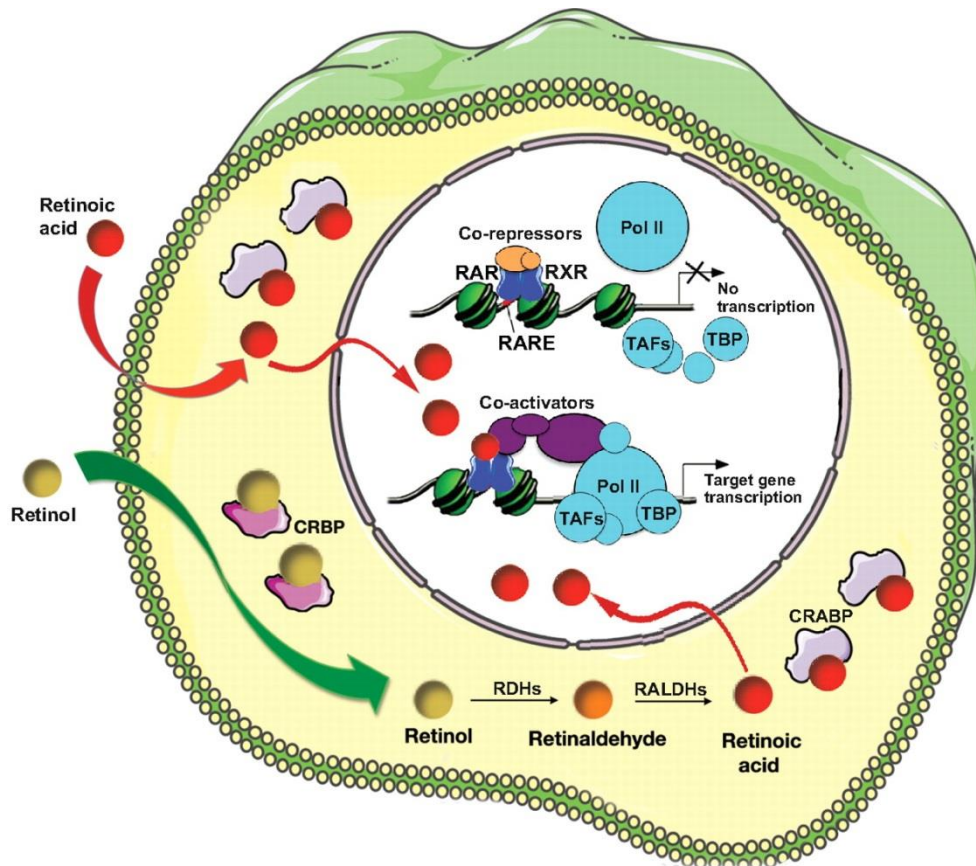


Figure 2: Retinoic acid (RA) signaling pathway. RA is synthesized from retinol by Rdhs and Raldhs. Upon reaching the nucleus, RA binds to and induces a conformational change of RAR/RXR heterodimers. As a consequence, the covalently bound co-repressors are released and the RAR/RXR heterodimer associates with co-activators. Ultimately, the transcription machinery is recruited and the target gene is transcribed. Cellular binding proteins, such as Crbp and Crabp might be involved in regulating the intracellular retinol or RA concentration. (Rhinn and Dolle, 2012)

First hints on RA's mode of action came from pioneering studies in the late 1960s that discovered a direct effect of RA on RNA and protein synthesis (De Luca et al., 1969; Johnson et al., 1969; Zachman, 1967). The notion that other lipophilic hormones exert their physiological action through nuclear receptors was extrapolated to RA and led to the identification of the first retinoic acid receptor (RAR), RAR α (Giguere et al., 1987; Petkovich

et al., 1987). Within the next three years, the two other members of the RAR family, RAR β (Brand et al., 1988) and RAR γ (Zelent et al., 1989), as well as the three members of the second family of nuclear retinoid receptors, the RXRs (α , β and γ) (Mangelsdorf et al., 1992; Mangelsdorf et al., 1990; Yu et al., 1991) were identified and cloned. Functionally, RARs and RXRs act as heterodimers through binding to so called retinoic acid responsive element (RARE) DNA motifs (Figure 2) (Leid et al., 1992; Mark et al., 2009). There is a large amount of redundancy within the respective families. Depending on the existence of their ligand RAR/RXR heterodimers regulate both transcriptional repression and activation. This is molecularly explained by the RA independent DNA binding capacity of the heterodimers and their ligand-induced conformational changes (Chambon, 1996) that select for the binding of either co-repressors (Mengeling et al., 2012; Perissi et al., 1999) or co-activators (Figure 2) (Lefebvre et al., 2005). Co-activator binding recruits proteins with chromatin remodeling activities. This leads to chromatin decompaction and the formation of nucleosome-free regions. Especially the modifications on histone 3 (H3) residues lysine 4 (K4) and lysine 27 (K27) are dynamically regulated upon RA exposure (Kashyap et al., 2011; Kashyap et al., 2013; Laursen et al., 2013). This ultimately initiates the transcription at target genes (Rosenfeld et al., 2006).

RA plays numerous roles during embryonic development (Niederreither and Dolle, 2008). The best-studied structure in terms of RA morphogenetic gradient function represents the developing hindbrain (Gavalas and Krumlauf, 2000; Glover et al., 2006). More than 30 years ago, it was discovered that exogenous amounts of RA during embryogenesis lead to teratogenic effects in the hindbrain (Morriss, 1972). Subsequent studies described the disruptive effect of manipulated RA signaling on the patterning of the hindbrain. It emerged that excessive amounts of RA result in a posteriorisation of the hindbrain (Durstun et al., 1989), while RA deficiency impairs normal posterior hindbrain development and leads to an expansion of more anterior structures (Gale et al., 1999). These findings are consistent with the previously described notion of a posterior to anterior gradient of RA. Despite association of most RA functions with patterning of the A-P axis there is evidence for further roles in D-V patterning (Wilson et al., 2004) as well as the specification of individual neuronal subtypes (Linville et al., 2004). Besides many other genes, such as signaling factors, transcription factors and nuclear as well as membrane receptors, Hox genes have been identified and shown to be key targets of RA (Papalopulu et al., 1991b; Simeone et al., 1991; Stornaiuolo et

al., 1990). Their regulation accounts for some of the patterning functions of RA as described in more details later in this thesis.

1.1.2. Wnt signaling

Wnt genes were initially discovered more than 30 years ago as wingless in *Drosophila* (Sharma and Chopra, 1976) and *Int1* (Nusse and Varmus, 1982) in mice. Only years later, it was discovered that these genes are orthologues and the names were combined to Wnt (Cabrera et al., 1987; Rijsewijk et al., 1987). Today, 19 Wnt genes are known in mice and humans. The Wnt signal transduction pathway is highly conserved throughout evolution highlighting its importance for the development of many species (Richards and Degnan, 2009). Many of the Wnt signaling components were identified through forward genetic screens and functional mapping in *Drosophila*. In these studies, most of what we know nowadays as Wnt/ β -catenin pathway was described including the transmembrane receptor Frizzled (Fz) (Bhanot et al., 1996), and intracellular signaling components like Dishevelled (Dsh) (Perrimon and Mahowald, 1987), β -catenin (Wieschaus and Riggleman, 1987), glycogen synthase kinase 3 (Gsk3) (Siegfried et al., 1992) and T cell factor (Tcf) (Brunner et al., 1997).

Wnt gradient formation is yet not very well understood. However, evidence in the literature suggest that it requires the secretion of Wnt by defined subsets of cells, the transport and the endocytosis of Wnt by neighboring cells. The idea that Wnt might not be passively secreted through the secretory pathway but actually through specialized machineries came from experiments showing that secreted Wnts are highly hydrophobic due to the acylation and N-glycosylation at conserved amino acids (Harterink and Korswagen, 2012). The acylation of Wnts is recognized by the transmembrane protein Wntless which directs Wnts to the plasma membrane through the Golgi (Bartscherer et al., 2006; Herr and Basler, 2012). This modification makes Wnts insoluble and thus forces them to stay bound to the plasma membrane after secretion (Pfeiffer et al., 2002), making it unlikely that passive diffusion would play a major role in the formation of Wnt gradients. Instead, extracellular matrix components like the Dally-like protein (Gallet et al., 2008), transport through lipoprotein particles and extracellular transport proteins are discussed to be relevant for Wnt gradient formation (Esteve et al., 2011; Neumann et al., 2009; Panakova et al., 2005).

Wnt signaling is mediated by three downstream pathways, the canonical and the two non-canonical pathways termed planar cell polarity (PCP) and Ca^{2+} pathway (Figure 3). Centre of the canonical pathway is the regulation of β -catenin. The canonical pathway is activated through binding of Wnt to Fz receptors and Lrp5/6 co-receptors at the plasma membrane (Bhanot et al., 1996; Tamai et al., 2000). Binding of Wnt to these receptors recruits the cytoplasmic scaffold Dsh and leads to its phosphorylation (Chen et al., 2003; Yanagawa et al., 1995). Phosphorylated Dsh thereafter associates with the Axin-Gsk3 complex (Itoh et al., 2000) which leads to the inhibition of β -catenin phosphorylation and thus to its stabilization and accumulation (Tolwinski and Wieschaus, 2004). Upon translocation to the nucleus, β -catenin interacts with the Tcf/lef family of DNA-binding proteins (Behrens et al., 1996; Molenaar et al., 1996) and regulates the expression of downstream target genes amongst which *Axin2* is one of the most general ones (Yan et al., 2001). In the absence of Wnt, β -catenin is part of a complex composed of APC, Axin, Gsk3 and Ck1 α (Hart et al., 1998; Kishida et al., 1998). Gsk3 and Ck1 α phosphorylate β -catenin (Yanagawa et al., 2002; Yost et al., 1996), which leads to subsequent polyubiquitination and degradation through the 26S proteasome (Aberle et al., 1997). As for RA, chromatin remodeling plays a major part in the transcriptional activation of target genes through the Wnt/ β -catenin signaling pathway (Logan and Nusse, 2004).

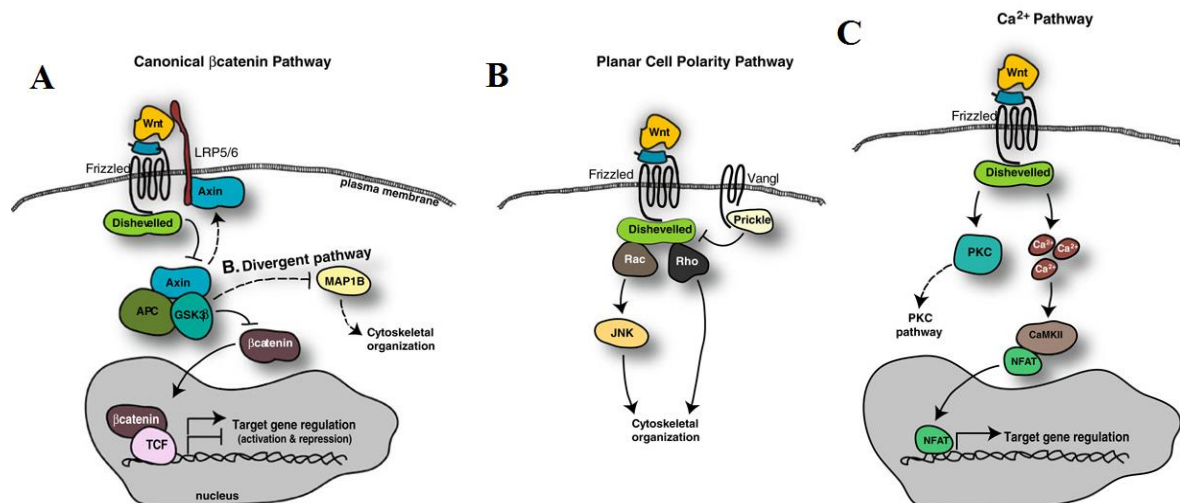


Figure 3: Wnt signaling pathways. (A) Signaling through the canonical Wnt pathway stabilizes β -catenin, which translocates into the nucleus and regulates target gene expression via interactions with DNA binding proteins such as Tcf. (B) The planar cell polarity (PCP) pathway mostly affects the cytoskeletal organization. (C) Wnt signaling through the Ca^{2+} pathway leads to a transient increase in intracellular Ca^{2+} levels, which has broad effects including target gene regulation. Adapted from: (Mulligan and Cheyette, 2012)

The non-canonical pathways are also initiated through Wnt binding to Fz and Dsh recruitment but then diverge in the intracellular components involved. The PCP pathway acts on the actin cytoskeleton and microtubule dynamics which is important for cell migration and planar to epithelial cell polarity (Komiya and Habas, 2008). The Wnt/Ca²⁺ pathway increases intracellular Ca²⁺ levels which is relevant for cell migration and adhesion, target gene regulation as well as for providing a negative feedback to the canonical pathway (Kuhl et al., 2000).

The role of Wnts in patterning the embryo can be observed as early as the 2- to 4-cell stage where β -catenin shows a differential intracellular distribution between dorsal and ventral (Larabell et al., 1997). This observation established Wnts as key player in providing dorsal identity in the early embryo (Hikasa and Sokol, 2013). The expression of several Wnt ligands in posterior (Krauss et al., 1992; Moon et al., 1993) and Wnt antagonists in anterior (Wang et al., 1997; Yamamoto et al., 2005) suggested an additional role in A-P axis specification which was experimentally shown by Itoh and Sokol (Itoh and Sokol, 1997). Further, Wnt signaling has been implicated in the development of numerous CNS structures including forebrain, midbrain and hindbrain where it regulates processes involving cell fate specification, cell proliferation, cell migration and axon growth and guidance (Mulligan and Cheyette, 2012).

1.2. Neuronal circuit formation

Besides axis patterning and cell fate specification, one of the major challenges during CNS development is the meaningful guidance of axons from the location of cell bodies to target neurons. For certain neurons in humans, the distance between cell body and axon terminal may span more than 1 meter. Considering these distances, it is highly remarkable how neurons find and connect to their targets with extreme precision. As all vital functions have to be in place in a newborn, the basic connectivity plan has to be hardwired during embryonic development. However, it has been shown throughout the CNS that early connections are subjected to activity dependent refinement. These refinement processes play a major role for many neuronal processes including learning and memory.

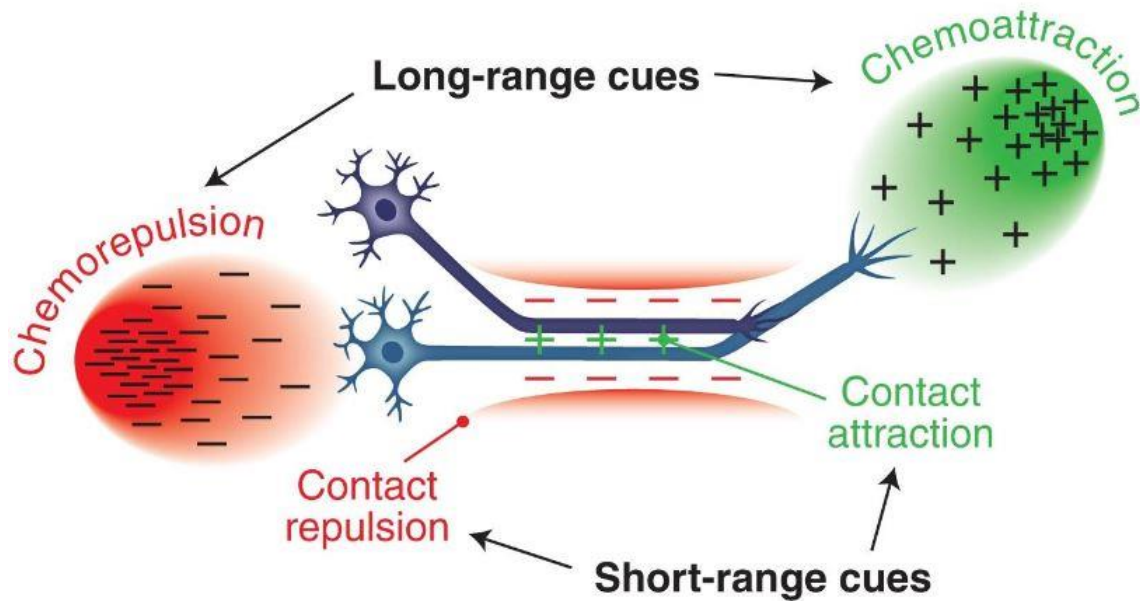


Figure 4: Mechanisms of axon guidance. The axonal path of neurons can be influenced by either diffusible molecules or through contact-mediated effects. While diffusible molecules function as long-range cues, cell-cell contact is often required for short-range cues. Both can function as either attractive or repulsive cues to the neuronal process. (Kolodkin and Tessier-Lavigne, 2011)

The process of finding the appropriate target, called axon guidance, starts with the formation of a flattened, fan-shaped structure at the tip of an outgrowing axon, termed growth cone (Tamariz and Varela-Echavarría, 2015). This growth cone is a highly dynamic, actin-supported extension that allows the developing neurite to scan the environment for appropriate cues that have the capacity to determine its further path. Positive or attractive cues attract axons towards the signal while negative or repulsive cues guide the axon away from the signal or even lead to a collapse of the growth cone resulting in growth arrest (Figure 4) (Tessier-Lavigne and Goodman, 1996). Besides imposing an axonal trajectory, such factors might also influence other processes such as the bundling or fasciculation of several axons into nerves and the final synapse formation onto target neurons. Especially for long distance projections, the final trajectory of an axon might be influenced by several guidance factors. Thereby, it is common that a variety of attractive and repulsive cues provided by guidepost cells work together to precisely navigate the growth cone (Kolodkin and Tessier-Lavigne, 2011). Moreover, axons might gain or lose responsiveness to certain factors along the way or might even change the interpretation of a cue (Kaprielian et al., 2001). In general, these cues can function either over long distances (long-range chemoattraction/chemorepulsion) or through cell-cell interactions (contact-mediated

repulsion/attraction). Long-range cues are usually secreted molecules that act to some extent in a concentration dependent manner (Tessier-Lavigne, 1994). As these are characteristics that are inherent to morphogens, it is not surprising that a number of morphogens such as BMPs and Wnts have been shown to act on growth cones as well. The most well-known long-range cues besides morphogens comprise the families of Netrin, Slits and some Semaphorins. Contact mediated cues may be provided by the extracellular matrix through which an axon extends or by nearby cells. Extracellular matrix proteins that are used by growth cones are laminins or tenascins. Examples of cell surface molecules are Ephrins, Cadherins, Semaphorins and cell adhesion molecules of the immunoglobulin superfamily (Kolodkin and Tessier-Lavigne, 2011). All of these molecules exert their action through the selective binding to receptors present on the growth cone. Upon binding, intracellular signaling cascades are elicited, which can influence the cytoskeleton of the growth cone, lead to local translation or degradation of proteins or to the expression of new receptors. The contact-mediated attraction through so called pioneer axons is a particular mechanism that minimizes errors and allows later developing axons to simply follow a pre-existing route to target cells (Raper and Mason, 2010).

The connectivity between structures can be organized in many different ways. For instance, monoamine-neurotransmitter systems have a high degree of convergence of synaptic input and at the same time strong divergence of output (Beier et al., 2015; Schwarz et al., 2015). Those neuronal populations integrate and broadcast information relatively unspecific to large parts of the CNS and are involved in the regulation of entire brain states rather than specific functions. Neural maps are a commonly used principle to ensure the orderly transmission of information for sensory modalities and motor control (Luo and Flanagan, 2007). The most well known example of such a map is the somatosensory homunculus in S1. Herein, different body parts are represented in accordance to their relative position towards each other thereby preserving spatial order. Information is organized in a topographic manner in these so called continuous maps. For their assembly complementary positional labels in gradients need to be present in the projecting cells as well as in the target tissue. These inversed gradients of ligand and receptor ensure that projecting axons find their correct position. Ephrin-As and their receptors EphA are the best studied example for orchestrating topographic map formation (McLaughlin and O'Leary, 2005). The more axes a map has the more receptor-ligand systems have to be in place. Another described neural map is the discrete one. Discrete maps are characterized by a point-to-point connectivity where discrete qualities are reflected

in the input as well as in the target area. Thereby, the spatial organization must not necessarily be maintained. The olfactory system is an example for such an organization in discrete functional units (Murthy, 2011). The whisker system combines the two principles by embedding discrete units into the larger somatosensory map. Sorting of axons for the formation of discrete maps is achieved through mutual attraction of axons from the same unit and/or the repulsion of axons from different units as well as the unique match of cues between the axons and the target. Refinement through correlated neural activity is common to both systems to account for potential inaccurateness during the assembly of the circuitry.

1.3. Regulation of Hox gene expression

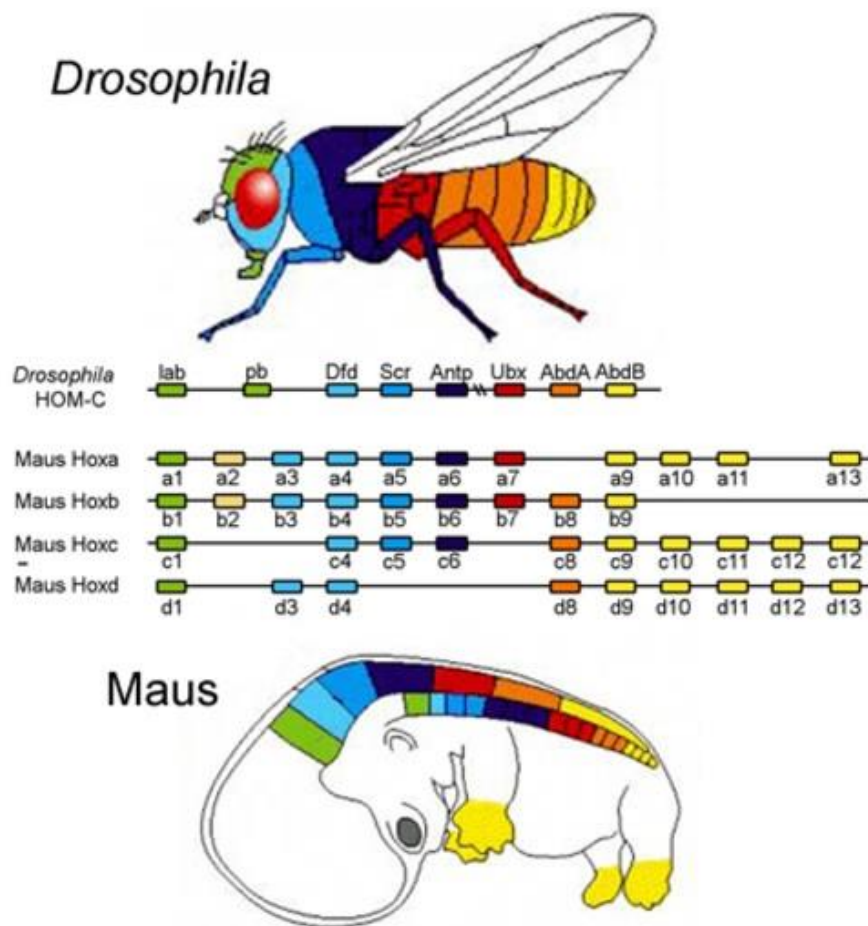


Figure 5: Hox cluster organization and spatial collinearity in *Drosophila* and mammals. Schematic illustration of the single Hox cluster in *Drosophila* and the four clusters in mammals. Homologies between *Drosophila* and mammalian Hox genes are indicated by color. Hox gene expression in the developing embryo follows a spatial collinearity as illustrated by the color coded expression pattern of Hox genes. Adapted from Max-Planck-Institute for molecular Genetic (http://www.molgen.mpg.de/92271/research_report_331001)

The formation of many body structures requires the differential and nested induction of key transcription factors along the neuraxis. One important class of such factors is homeodomain proteins. The common feature of these proteins is a 60 amino acid long homeobox domain that binds DNA. Especially the specification of identity along the A-P axis is dependent on homeodomain transcription factors such as Otx, Emx, Pax, and En transcription factors for the pros- and mesencephalon (Kumamoto and Hanashima, 2014; Vollmer and Clerc, 1998). Hox or homeotic genes, a subfamily of homeodomain genes, play an essential role in the hindbrain and spinal cord (Narita and Rijli, 2009). The term “homeotic” was introduced over 100 years ago by William Bateson and used to describe a phenomenon in which “something is changed into the likeness of something else” (Bateson, 1894). In the following decades, mutations which result in such homeotic transformations were discovered in *Drosophila* with Ed Lewis describing a whole set of mutations affecting almost the entire A-P axis (Lewis, 1978). All of these mutations were found to reside in a single gene complex, termed bithorax (Figure 5). Since then, Hox genes have been described to be one of the unifying mechanisms of Bilaterian development (Holland, 2013). Starting from one single ur-hox gene, unequal crossing over events and divergence lead to eight Hox genes in one cluster found for instance in *Drosophila* (Gehring et al., 2009). This ancestral Hox gene cluster was further expanded during evolution to vertebrates and entirely duplicated twice, most likely due to full genome duplication, giving rise to 39 Hox genes in four Hox clusters found in mice and humans (Figure 5) (Hart et al., 1987).

1.3.1. Collinearity of Hox gene expression

During vertebrate development, the A-P axis is, with the exception of the cephalic part, segmented into segregated compartments of mesodermal precursor cells called somites (Hirsinger et al., 2000). Despite being very similar initially, each of these somites eventually develops into a unique part of the embryo. Hox transcription factors convey the information into which precise anatomical structures each segment has to differentiate (Krumlauf, 1994). One particularly intriguing feature of these Hox genes during development is that the arrangement of Hox genes within their respective cluster reflects the timing of onset of their expression (temporal collinearity) as well as their expression domain (spatial collinearity) along the A-P axis (Figure 5) (Kmita and Duboule, 2003). Thus, anteriorly located Hox genes are expressed earlier and in more anterior somites as compared to more posteriorly located Hox genes. This leads to a unique combination of Hox genes being expressed in each somite

(Kessel and Gruss, 1991). The identity of the respective segment is thereby specified by the most posterior Hox gene expressed, a phenomenon termed ‘posterior prevalence’ (Duboule and Morata, 1994). Temporal collinearity critically depends on the intactness of the Hox cluster (Seo et al., 2004). This indicates a tight correlation between the physical location of each Hox gene and its expression. Despite the precise mechanisms, controlling the temporal collinearity being incompletely understood, literature suggests that regulatory elements and epigenetic mechanisms are involved. A series of relocation experiments showed that Hox genes moved to a more posterior location in the cluster adopt the expression pattern corresponding to the new location (vanderHoeven et al., 1996). This argued for a progressive opening of chromatin in a 3’-5’ direction that allows for the sequential expression of Hox genes. A number of experimental approaches demonstrated that *cis*-regulatory elements in close proximity to Hox genes play a pivotal role for their expression. For instance, relocation of *Hoxb1* to the 5’ end of the *Hoxd* cluster not only recapitulated its normal expression pattern but also induced chromatin decondensation showing that collinearity was broken (Kmita et al., 2000). Further, mutations of *cis*-regulatory elements within the clusters alter the temporal collinearity (Zakany et al., 1996). Besides local *cis*-regulatory elements within the cluster, global enhancers located up- and downstream of the *Hoxd* cluster were identified to significantly contribute to collinearity. First evidence for such enhancers came from experiments in which premature activation of 5’ Hox genes was observed upon deletion of more 3’ Hox genes (Tarchini and Duboule, 2006). These global control regions are believed to act in an antagonistic manner with one of them opening the cluster starting from 3’ and the other one exerting silencing properties to ensure collinearity (Deschamps, 2007). Together, temporal collinearity seems to depend on the *cis*-regulatory environment of individual Hox genes, their relative position within the cluster and regulatory elements outside the cluster. The translation of the temporal collinearity to a spatial collinearity is suggested to be mediated through the Hox dependent control of cell ingression during gastrulation (Iimura and Pourquie, 2006). Ectopic overexpression of posterior Hox genes retained cells longer in the epiblast than overexpression of anterior cells. This effect is discussed to be dependent on the regulation of cell adhesion molecules. Posterior prevalence is one of the mechanisms that contribute to the establishment of the spatial collinearity. However, the *cis*-regulatory landscape in close proximity of individual Hox genes is also relevant, as spatial collinearity is observed in species with an entirely disintegrated cluster (Seo et al., 2004).

1.3.2. Signaling molecules and transcription factors relevant for Hox gene expression

Many signaling molecules have been implicated in the regulation of Hox gene expression over the past decades. Most prominently numerous studies demonstrated a profound role of RA in the induction of Hox genes (Gavalas, 2002). Initial experiments indicated that RA acts on different Hox genes in a concentration dependent manner. Cell culture experiments demonstrated that 3' Hox genes respond earlier and at lower concentrations as compared to their 5' counterparts within the same cluster (Papalopulu et al., 1991a; Simeone et al., 1990). Furthermore, RA treatment leads to a collinear activation of Hox genes suggesting a potential involvement of RA in the temporal collinearity of Hox gene activation. However, results in *Raldh2* knockout mice, which show a rather normal activation of Hox genes, are in contradiction to these findings leaving it still an open discussion to which extent RA is required for the collinear activation for Hox genes *in vivo* (Niederreither et al., 1999). Regulatory studies discovered that RA acts on Hox gene expression directly through the binding to RAREs located at various places in the Hox clusters (Figure 6) (Glover et al., 2006; Mahony et al., 2011b). Intriguingly, these RAREs show a very high degree of conservation across species, emphasizing their relevance for Hox expression. Certain Hox genes were additionally associated with several RAREs, each of which has a distinct role for precise regulation of Hox expression during certain stages and within distinct tissues of the embryo during development (Huang et al., 2002; Huang et al., 1998; Marshall et al., 1994). Moreover, certain RAREs have been reported to have repressive instead of activating properties (Studer et al., 1994). Mutational studies of single and multiple RAREs *in vivo* further demonstrated their importance, as the resulting phenotypes were reminiscent of the phenotypes of full inactivation of the cognate gene (Dupe et al., 1997; Studer et al., 1998). RA, however, has mostly been shown to regulate the expression of *Hox PG1-6* genes with less clear effects on more caudal Hox genes. Instead, fibroblast growth factor (FGF) signaling significantly contributes to the expression of *Hox PG4-10* genes in the spinal cord, partly in concert with RA for *Hox PG4-6* and with growth differentiation factor-11 for *Hox PG6-11* (Philippidou and Dasen, 2013). FGFs are furthermore discussed to regulate certain aspects of Hox expression in the hindbrain. However, it is not fully understood whether this is a direct or indirect regulation (Alexander et al., 2009). Finally, Wnt signaling has been shown to impinge on Hox expression (Ikeya and Takada, 2001). In general, the effect of Wnt seems to

be rather activating in respect to Hox gene expression in the mesoderm as well as during somite specification (Lengerke et al., 2008).

Three of the above mentioned pathways, RA, FGF and Wnt also regulate Cdx homeodomain factors which induce the expression of posterior Hox genes (Alexander et al., 2009). Different *Cdx* mutations induce anterior homeotic transformations (van den Akker et al., 2002) and relevant *Cdx* consensus motifs have been identified in *cis*-regulatory regions of *Hox PG7* and *PG8* genes (Charite et al., 1998). During hindbrain patterning, *Krox20* regulates Hox expression patterns in rhombomere (r) 3 and 5 (Figure 6). *Krox20* has also been shown to be directly involved in the activation of both *Hoxa2* and *Hoxb2* in r3 and *Hoxb3* in r5. Furthermore, *Krox20* represses *Hoxb1* in both r3 and r5 (Figure 6). In turn, Hox genes provide feedback to *Krox20* in terms of a positive regulatory loop to maintain its expression. In r5 and r6, *Kreisler* controls the expression of *Hoxa3* and *Hoxb3*. *Cis*-regulatory sequences mediating this effect have been identified upstream of both genes.

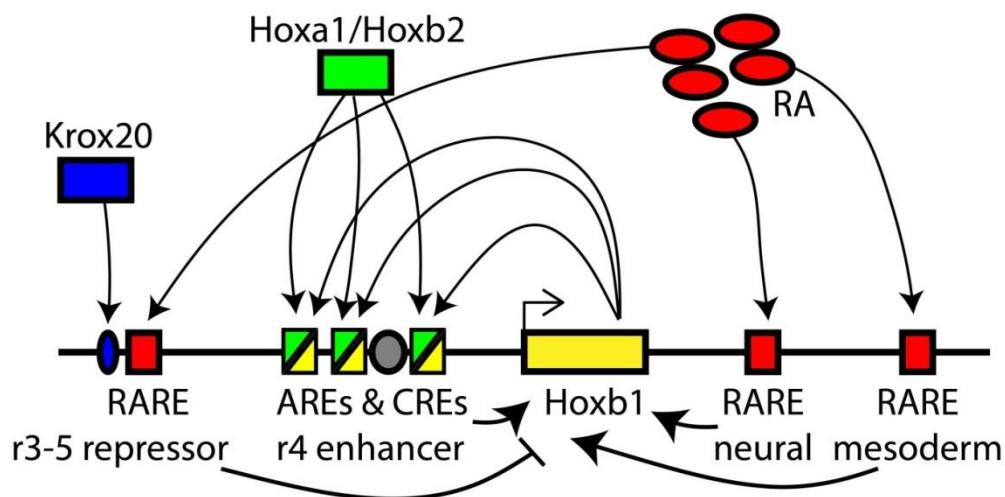


Figure 6: Regulation of Hox gene expression as exemplified by the *Hoxb1* gene. *Trans*-acting factors as well as *cis*-regulatory elements relevant for the regulation of different aspects of *Hoxb1* expression during development. ARE: auto-regulatory element; CRE cross-regulatory element; RA: retinoic acid; RARE; retinoic acid responsive element. Figure by D. Kraus based on (Tumpel et al., 2009)

Once induced, Hox genes show auto- and cross-regulatory properties in conjunction with their Pbx co-factors (Figure 6). Examples of Hox genes with identified auto-regulatory elements include *Hoxb1*, *Hoxa3*, *Hoxb3* and *Hoxb4* (Alexander et al., 2009). Cross-regulation has been demonstrated across PGs as well as within PGs (Maconochie et al., 1997; Manzanares et al., 2001). These regulations, together with signaling molecules, trigger entire

cascades where the initial induction of a certain Hox gene through RA leads to the subsequent expression of a number of Hox genes to specify the identity of the respective segment.

1.3.3. Regulation of Hox gene expression: Epigenetics

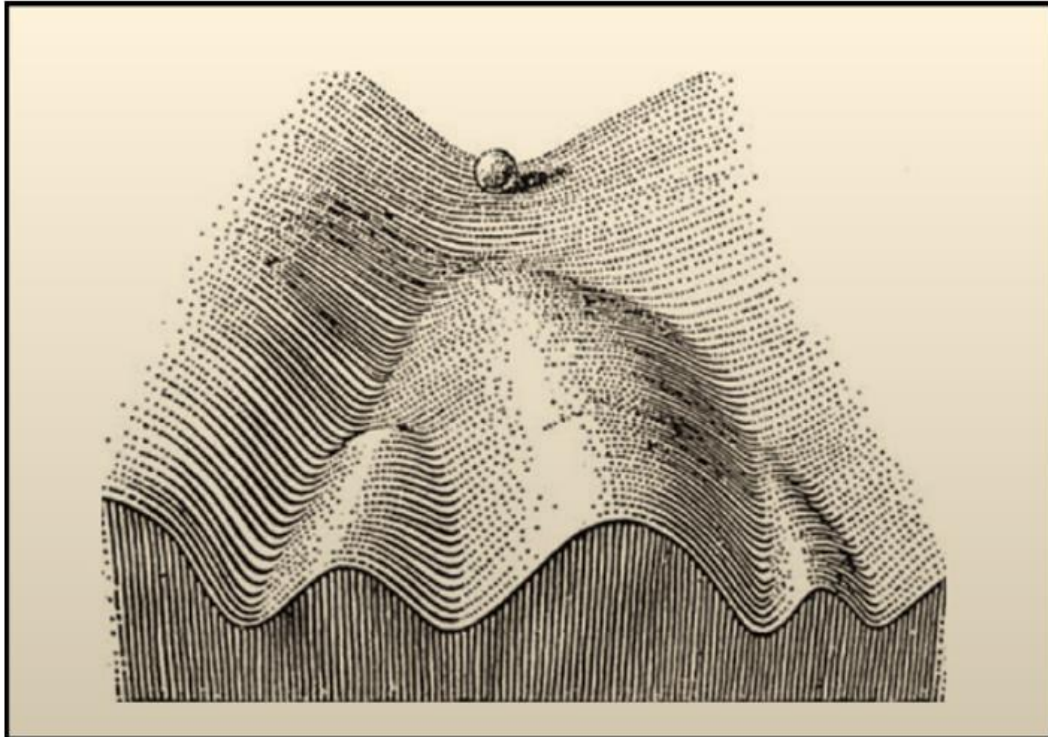


Figure 7. Waddington’s classical epigenetic landscape. The process of cellular decision-making during differentiation as initially proposed by Conrad Waddington. As the cell moves through development, it reaches several points at which it has to commit to one or another fate. (Waddington, 1957)

The term epigenetics was coined by C. H. Waddington in 1942 (Waddington, 1942). He used the term in those times to conceptually describe the interaction between genes and the environment to produce a certain phenotype. His drawing of a marble rolling down a hill with certain paths that can possibly be chosen is one of the most commonly used pictures until today to explain the concept of cell fate choice (Figure 7). Literally translated, epigenetics means “in addition to genetics” and the contemporary definition of the term is the study of heritable changes in gene function that cannot be explained by changes in the DNA sequence. Mechanistically, epigenetics works in many different ways, with covalent modifications of either DNA or histones being one of the most well studied. On the DNA level, cytosine methylations and hydroxymethylations are by far the most studied modifications (Schubeler,

2015). In contrast, a huge variety of modifications is described for the four core histone proteins (Perla Cota, 2013). These modifications include ubiquitinations, phosphorylations, methylations as well as acetylations of different residues on the N-terminal histone tails. They usually act in concert to regulate the structure of the chromatin, the accessibility of DNA and the expression of genes. Modifications that promote gene expression are commonly referred to as “open chromatin” while “closed chromatin” interferes with the expression of genes (Kmita and Duboule, 2003). Trimethylation (me₃) of H3K4 and acetylation (ac) of H3K9 are examples for modifications associated with active genes. H3K9me₃ as well as H3K27me₃ on the other hand are correlated with transcriptional repression (Urvalek et al., 2014).

The progressive opening of the Hox clusters during their temporally colinear activation as described above also refers to a consecutive change of histone modifications from a closed to an open state (Figure 9A) (Kashyap et al., 2011). It is interesting to note, that already Ed Lewis identified Polycomb as a major regulator of Hox gene expression in his screen in *Drosophila* (Lewis, 1978). After decades of research we now know that Polycomb group (PcG) proteins are negative regulators of Hox gene expression that mediate their effect by the deposition of the K3K27me₃ mark (Margueron and Reinberg, 2011). Mutations in Polycomb lead to a loss of spatial restriction of Hox gene expression with posterior Hox genes becoming active in more anterior parts of the embryo as initially demonstrated in *Drosophila* and subsequently in many other species (Di Meglio et al., 2013; Moazed and O'Farrell, 1992). The repressive function of Polycomb is counteracted by the trithorax group (TrxG) of proteins, whose main action is to ensure the stable activation of genes in their respective expression domains (Geisler and Paro, 2015). In *Drosophila*, TrxG proteins were shown to be essential for the correct expression of different Hox genes (Ingham, 1985). TrxG proteins thereby act as methylases of the H3K4 residue leading to its trimethylation, a hallmark of active genes. In mammals, the polycomb repressive complexes 1 and 2 (PRC1 & 2) exert a silencing function on Hox and other genes. PRC2 silences genes via K3K27me₃ deposition (Figure 8) and PRC1, which is recruited by K3K27me₃, induces a further compaction of chromatin and the additional ubiquitination of the H2AK119 residue (Kalb et al., 2014; Wang et al., 2004). PRC1 and 2 are both multiprotein complexes consisting of histone modifying enzymes, scaffold proteins and histone binding proteins. The enzymes that mediate the histone modifications in the respective complexes are the SET domain-containing histone methyltransferases Ezh1 and 2 (Margueron and Reinberg, 2011). The deletion of different members, including Ezh1 and 2, from both complexes leads to homeotic transformations due

to Hox de-repression (Cao et al., 2005; Schwarz et al., 2014). The main mammalian PRC counterparts are MLL complexes as well as the NURF and SWI/SNF complexes (Schuettengruber et al., 2011). While the latter two are ATP dependent chromatin remodeling complexes that open chromatin through nucleosome positioning, the MLL complexes function through H3K4 trimethylation (Figure 8). MLL1, 2 and 3 are the SET domain-containing enzymes in these complexes which are required for the methylation of the lysine residue (Del Rizzo and Trievel, 2011). Highlighting the relevance of the PcG and TrxG complexes, the progressive opening and thus the transcriptional status of Hox genes can be described by assessing the H3K27me3 and H3K4me3 levels at the respective gene (Noordermeer et al., 2011; Soshnikova and Duboule, 2009). Transcribed genes contain high H3K4me3 and low H3K27me3 levels while the opposite is true for repressed genes. Over the course of activation of a Hox cluster, the H3K27me3 mark that initially covers the entire cluster successively disappears and high H3K4me3 levels are gained (Figure 9A). In embryonic stem cells (ESCs), treatment with RA is sufficient to induce the shift from H3K27me3 to H3K4me3 at Hox genes as they become transcriptionally active (Kashyap et al., 2011). One long-standing question in the field was whether the removal of the H3K27me3 mark is a passive process or if it is catalyzed by enzymes. In 2007 several groups reported the identification of two proteins, Utx1 and Jmjd3, with H3K27me3 demethylase activity (Agger et al., 2007; De Santa et al., 2007; Lan et al., 2007; Lee et al., 2007). Both Jmjd3 and Utx1 were described to be relevant for Hox gene expression and the knockout of either one affects Hox expression levels in the developing embryo. Again, RA signaling had been brought into context with these demethylases. The RA induced activation of Hox genes not only leads to a dissociation of the PRC2 complex but also triggers Jmjd3 and Utx1 association to remove the repressive H3K27me3 mark. This active demethylation process is thought to be required for a precise spatio-temporal activation of Hox genes by ensuring the rapid erasure of the repressive mark over large domains. Another mechanism that is discussed to be relevant for the fast onset of stable expression of developmental regulators is the simultaneous occurrence of the H3K27me3 and H3K4me3 mark. Domains that are covered by both marks are termed bivalent and are found for instance at Hox genes in ESCs (Soshnikova and Duboule, 2009). These bivalent domains are thought to infer a not expressed, but at the same time primed state that allows for a fast acquaintance of transcriptional activity (Bernstein et al., 2006).

Induction of Hox expression however is not only accompanied by a decrease in H3K27me3 and an increase in H3K4me3 but also by a number of other epigenetic changes. The H3K27 residue can for instance be present in an acetylated form, which coincides with transcriptional activity (Pasini et al., 2010). CBP/p300 mediates the acetylation and is a well-known co-factor of RA mediated regulation (Tie et al., 2012). H3K9 and H3K14 acetylation are further known epigenetic marks that are gained at Hox genes upon onset of expression (Kashyap et al., 2011).

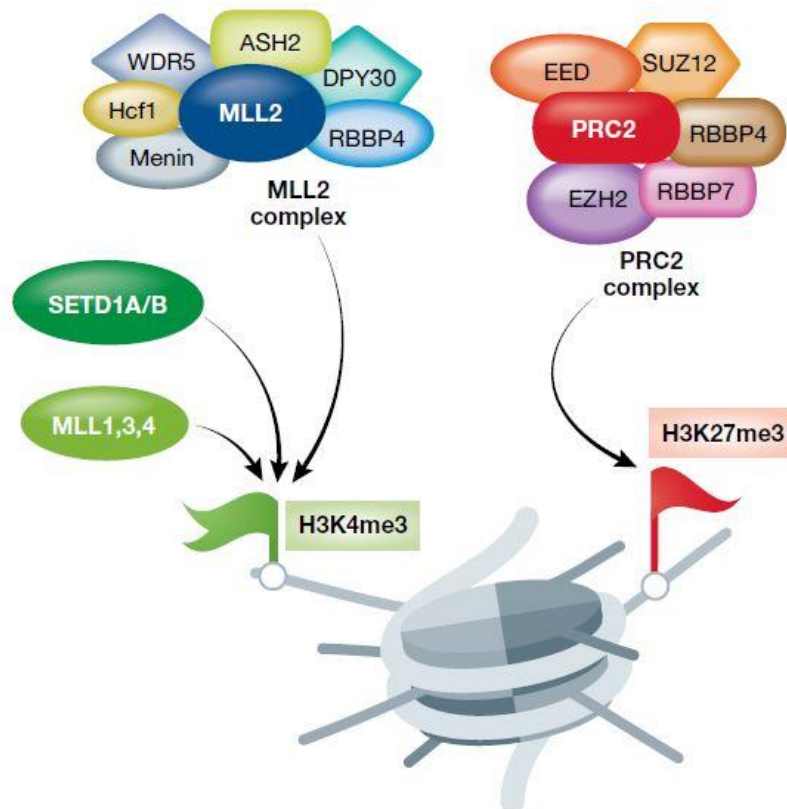


Figure 8: PRC2 and MLL complexes. Shown is the main scaffolding, histone binding and catalytically active proteins of both complexes. The MLL complex regulates the tri-methylation of H3K4 and the PRC2 complex the tri-methylation of H3K27. (Harikumar and Meshorer, 2015)

1.3.4. Higher order chromatin organization underlying Hox gene expression

Chromatin accessibility and higher order chromatin organization have recently gained much attention as transcriptional activity has been tightly linked with the organization of chromatin at regulatory sites. PcG and TrxG complexes and their respective marks act in parts through the regulation of differential compaction of chromatin. About a decade ago, it was first described that the induction of Hox gene expression is accompanied by changes in higher

order chromatin organization (Chambeyron and Bickmore, 2004). These early studies were utilizing fluorescent *in situ* hybridization techniques (FISH) to label Hox loci within the nucleus of different cells *in vivo* and *in vitro*. While the inter-probe distance was minimal in cells, where the cluster is in an inactive state, the distance significantly increased with the activation of Hox genes. For instance, RA mediated differentiation of ESCs was sufficient to induce such a decompaction, closely mimicking the processes during embryonic development (Chambeyron and Bickmore, 2004; Chambeyron et al., 2005).

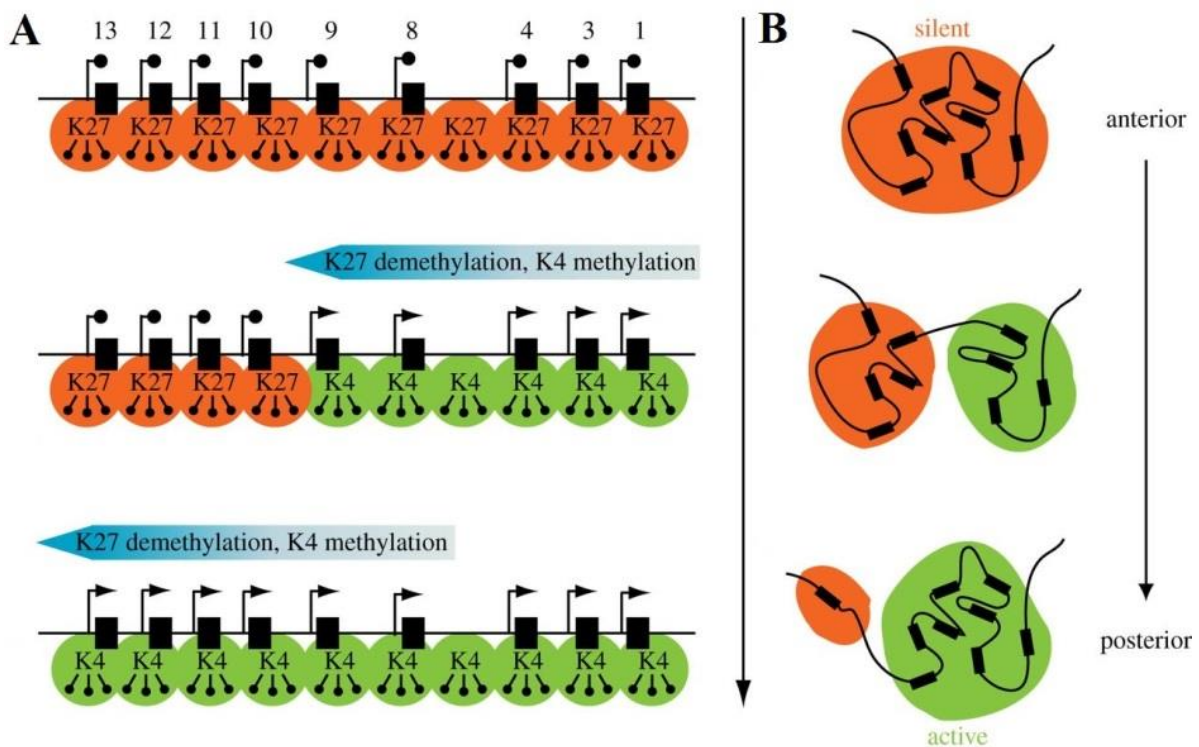


Figure 9: Dynamic regulation of histone modifications and the resulting higher order chromatin organization of Hox cluster. (A) Spatial and temporal colinear expression of Hox genes is accompanied by a transition of H3K27me3 to K3K4me3 levels. From an initial repression and the occupancy of the entire cluster with H3K27me3 more and more Hox genes acquire high H3K4me3 level and become transcriptionally active. (B) On the higher order chromatin level the Hox cluster is segregated into distinct spatial compartments dependent on their transcriptional and epigenetic status. Adapted from (Montavon and Duboule, 2013)

The development of chromosome capture techniques coupled to high throughput sequencing allowed for a more precise assessment of contacts formed between different genomic loci and the resulting higher order structure of chromatin (Simonis et al., 2007; van de Werken et al., 2012). Circular chromosome conformation capture (4C) experiments not only confirmed the interaction between Hox genes and long-range regulatory elements but also identified an additional set of distant enhancers. Besides these chromatin loops, 4C also allowed to

monitor the local 3D chromatin dynamics of Hox clusters during development. This revealed the existence of distinct spatial conformations across Hox clusters dependent on its transcriptional state (Figure 9B) (Andrey et al., 2013; Ferraiuolo et al., 2010; Noordermeer et al., 2011). Entirely inactive Hox clusters are organized in one large 3D compartment. Strikingly, the borders of the domain coincide with the domain covered by the repressive H3K27me3 mark. In partially active Hox clusters, the active and inactive genes group in distinct 3D compartments, precisely overlapping with the H3K4me3 and H3K27me3 domains respectively. These observations suggest a potential mechanistic implication of epigenetic signatures in higher order chromatin conformation (Noordermeer et al., 2011). The size of the two compartments furthermore reflected the number of active or inactive Hox genes. Accordingly, the active domain extends towards the posterior end of the A-P axis of the embryo. Spatial collinearity might therefore in parts be dependent on these 3D compartments. A dynamic shift of local compartments could also account for temporal collinearity. Despite the lack of experimental evidence, the sequential transition of Hox genes from the passive to the active domain could act as a clock that allows Hox gene activation only in a collinear fashion. It has been suggested that this bimodal organization of Hox clusters, which leads to a physical separation of active and inactive genes, helps to increase the local concentration of activating or repressing factors in each compartment. CTCF binding has been implicated in defining chromatin compartments. CTCF binds to multiple regions within the Hox clusters and depletion of binding sites results in posterior spread of Hox gene activation in ESCs upon RA mediated differentiation (Narendra et al., 2015).

1.4. Role of Hox genes during development

As indicated earlier, the main function of Hox genes is to pattern the body along the A-P axis. A combinatorial Hox code, specific to each body segment, determines the fate of the respective segment. Hox genes thus provide positional identity to each segment. Hox genes are expressed and are functionally relevant in all three germ layers (Young et al., 2009). One process highlighting the role of Hox genes is the formation of the axial skeleton. From the fifth somite onwards, each segment contributes to the formation of two vertebral elements. Each vertebra along the A-P axis is morphologically unique. Transplantation as well as gain- and loss-of-function experiments provided evidence for the central role of Hox genes in assigning the positional identity and thus unique morphology to each segment (Wellik, 2009). Besides the A-P axis also the proximal-to-distal (P-D) axis has been shown to be Hox

dependent. However, opposed to the A-P axis, loss-of-function of certain Hox genes does not lead to a homeotic transformation but rather a loss or malformation of affected skeletal elements within the P-D axis (Davis et al., 1995; Fromental-Ramain et al., 1996). Thus, Hox genes have a growth regulating role in P-D axis development (Dolle et al., 1993). This effect is thought to rely on the regulation of Shh signaling in the zone of polarizing activity and FGF signaling in the apical ectodermal ridge, the two major signaling centers during P-D axis development (Zakany and Duboule, 2007).

1.4.1. Hox genes and hindbrain segmentation

One of the best-studied processes with respect to a functional involvement of Hox genes is hindbrain segmentation. The hindbrain is transiently patterned from a smooth, featureless sheet of neurons into seven discrete units known as rhombomeres (Lumsden and Krumlauf, 1996). These lineage restricted cellular compartments confine the movement of cells to one single rhombomere. Notably, cells in two adjacent compartments are not separated by a mechanical or physical boundary (Guthrie and Lumsden, 1991). Instead, cells from adjacent compartments have different cell adhesive properties that prevent their intermingling. The molecular mechanism of this cell sorting has been shown to be dependent on the differential expression of Eph receptors and ephrins (Gale et al., 1996). Eph receptors are expressed in r3 and r5 while r2, r4 and r6 display high levels of ephrins (Xu et al., 2000). Consequently, cells can intermingle when placing even or uneven rhombomeres next to each other (Guthrie et al., 1993). Thus, r2, r4 and r6 as well as r3 and r5 share common properties indicating that the hindbrain is patterned in a two-segment periodicity. The segmentation of the hindbrain is relevant for the formation of distinct structures as it enables every rhombomere to respond to environmental stimuli in a unique manner. Individual rhombomeres also act as signaling centers that influence their neighboring rhombomeres. Finally, the proper development of other structures like cranial neural crest cells, which are relevant for head development, are critically dependent on rhombomere formation (Tumpel et al., 2009).

Hox PGI-4 genes are expressed during the segmentation phase of the hindbrain. Each of them has a sharp anterior expression boundary, which precisely corresponds to boundaries between different rhombomeres. r1 is the only Hox negative rhombomere in the hindbrain and from r2 onwards Hox genes are expressed in various combinations. *Hoxa1* is the first Hox gene expressed in the presumptive r4 territory and subsequently induces *Hoxb1*

expression. Both genes have been shown to be essential for the identity of r4/r5 and also sufficient to infer the r4 identity to more anterior rhombomeres (Carpenter et al., 1993; Studer et al., 1996; Zhang et al., 1994). *Hoxa2* is the only Hox gene found in r2 and is required for the proper development of this segment. *Hoxa2* mutants show an enlargement of r1 at the expense of r2 (Gavalas et al., 1997). Further, *Hoxa2* expression influences the size of r3 (Davenne et al., 1999). Besides *Hoxa1*, *Hoxb2* is added in r3. *Hoxb2* knockouts show r4 defects, indicating its importance in the maintenance of this segments identity (Gavalas et al., 2003). Each following Hox class is added in a two-segment periodicity, meaning *Hox PG3* genes are expressed up to the r4/r5 boundary and *Hox PG4* genes up to the r6/r7 one. Finally, *Hox PG5* genes are added in the pseudo-rhombomere r8 at late stages (Oosterveen et al., 2003). While there are mild defects detectable in *Hox PG3* mutants (Gaufo et al., 2003; Manley and Capecchi, 1997), *Hox PG4* and *PG5* genes do not seem to have a significant role in hindbrain segmentation (Horan et al., 1995). The expression of Hox genes in the hindbrain is regulated by signaling molecules, auto- and cross-regulatory mechanism as well as other transcription factors as explained earlier (Alexander et al., 2009). Precise Hox expression patterns depend particularly on RA during early induction and on Krox20 and Kreisler during r3/r5 and r5/r6 specification. The regional expression of anterior Hox genes is often modulated or even lost within the hindbrain upon initial activation (Tumpel et al., 2009).

1.4.2. Function of Hox genes during circuit formation

Neural circuits underlying basic behavior are thought to be largely hard-wired. Their precise connectivity with pre- and postsynaptic targets must thus be established by specific combinations of transcription factors that confer identity to each neuronal subset found in the CNS. Those transcription factors are likely to control all aspects of circuit formation by defining migratory pathways, axonal projections and synaptic specificity. The transcription factor expression domains are mostly set in neuronal progenitors. Patterning of neuronal progenitors occurs predominantly along the D-V and A-P axis. Different D-V progenitor populations give rise to different classes of neurons such as inhibitory vs. excitatory or sensory vs. motor. The A-P axis instead specifies the neuronal subtype identity as evidenced by differential migratory or axonal pathfinding behaviour of progenies arising from different segments (e.g. different motor neuron pools in the spinal cord).

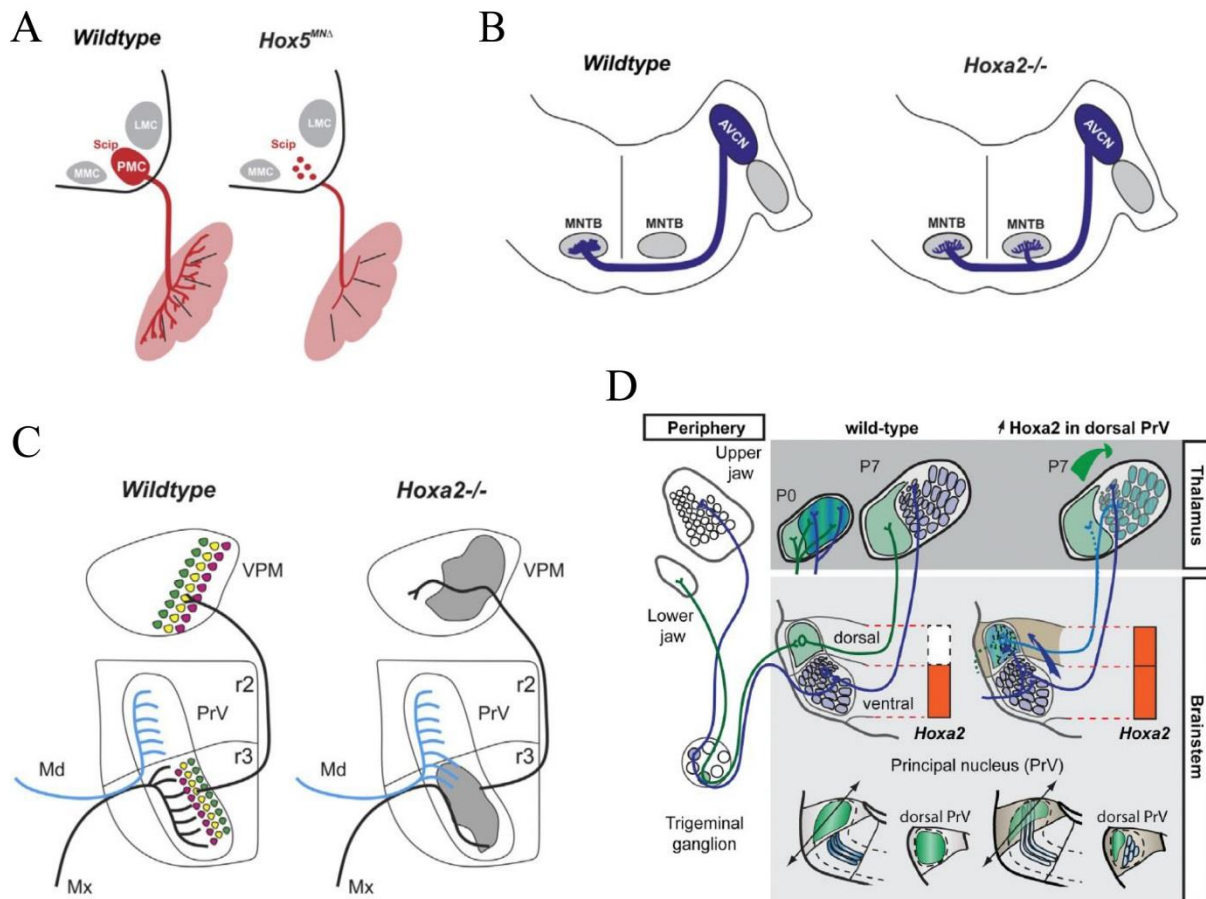


Figure 10: Role of Hox genes during neuronal circuit assembly. (A) *Hox PG5* deleted phrenic motor neurons fail to arborize in the diaphragm leading to respiratory failure. (B) *Hoxa2* inactivation affects the axonal pathfinding of antero-ventral cochlear nucleus (AVCN) neurons leading to ectopic ipsilateral innervation of the medial nucleus of the trapezoid body. (C, D) *Hoxa2* is required for topographic map formation of the whisker system. (C) Absence of *Hoxa2* inhibits arborisation of the maxillary branch of the trigeminal nerve and a mistargets the ventral principal trigeminal nucleus (PrV) derived projection in the thalamus. (D) Maintenance of *Hoxa2* expression in the dorsal PrV leads to ectopic barrelette formation and aberrant innervation of the ventral posteromedial nucleus in the thalamus. Adapted from (Bechara et al., 2015; Philippidou and Dasen, 2013)

Besides their roles in early development, Hox genes are also more and more considered to be major determinant of neuronal circuit formation during late development. Early evidence for such an involvement came from Hox mutants that showed defects in cranial nerve development. Herein, the manipulation of *Hox PG1* and *PG2* genes in r1 to r3 territories lead to misspecification and circuit formation defects of trigeminal and facial motor neurons (Gavalas et al., 1997; Jungbluth et al., 1999; Studer et al., 1996). The r5 and r6 derived motor neurons instead require *Hox PG3* activity for correct specification and pathfinding (Gaufo et al., 2003; Manley and Capecchi, 1997). Hox genes confer identity and thus connectivity principles to motor neurons also in the spinal cord, where motor neurons are organized in

longitudinal array of columns that span multiple segments. *Hoxc9* mutants have a brachial like thoracic motor column and *Hox PG5* mutants show defects in the organization and target innervation of the phrenic motor column (Figure 10A) (Jung et al., 2010; Philippidou and Dasen, 2013). Besides, a functional relevance of Hox genes in late stages of locomotor circuit assembly in the spinal cord is suggested by experiments in conditional *Foxp1* knockout animals, a major Hox co-factor. These knockouts display motor discoordination as a consequence of disturbed input-output connectivity of motor neurons (Surmeli et al., 2011). Other circuits that critically depend on Hox gene activity in the hindbrain belong to the respiratory network, auditory and somatosensory maps as well as the precerebellar system. Respiration is controlled by the parafacial respiratory group and pre-Bötzing complex derived from r3-4 and r6-8 respectively. *Hoxa1* mutations consequently leave the pre-Bötzing complex unaffected but disrupt normal function of the parafacial respiratory group (del Toro et al., 2001). In the auditory system, the different subdivisions of the cochlear nucleus are derived from r2-5 and show differential expression of *Hoxa2* and *Hoxb2*. While *Hoxa2* is mainly present in the r2-3 derived antero-ventral cochlear nucleus (AVCN), *Hoxb2* expression can be detected in the AVCN as well as the r4 derived posterior-ventral cochlear nucleus (PVCN) and the r3-5 derived granule cells. Accordingly, knockout of *Hoxa2* affects the normal AVCN circuit formation while *Hoxb2* knockout animals display projection defects of the PVCN (Figure 10B) (Di Bonito et al., 2013). Furthermore, the use of a conditional approach allowed for the late inactivation of these genes, bypassing early patterning defects and revealing novel roles for Hox transcription factors in the late aspects of auditory nuclei development. The role of Hox genes in the somatosensory system has been best exemplified for the point-to-point connectivity of individual whiskers through the hindbrain trigeminal circuit. The ventral principal trigeminal nucleus (vPrV) plays a central role in the whisker circuit while its dorsal part (dPrV) is dedicated to the mandibular region of the face (Erzurumlu et al., 2010). *Hoxa2* turned out to be a major determinant of PrV connectivity at various stages of development. It is selectively expressed in vPrV neurons and its early expression in the hindbrain is required to guide sensory afferents to their appropriate target (Oury et al., 2006). Late expression of *Hoxa2* is crucial for correct arborisation of the maxillary branch of the somatosensory ganglion into the vPrV (Figure 10C). Finally, the ectopic maintenance of *Hoxa2* expression in dPrV is sufficient to impose a vPrV like identity in which both input and output connectivity is significantly altered (Figure 10D) (Bechara et al., 2015). The role of Hox genes in the hindbrain precerebellar system was highlighted in

recent publications (Di Meglio et al., 2013; Geisen et al., 2008). These studies indicated a direct involvement of Hox genes in topographic circuit formation between cortex and pontine nuclei (PN).

1.5. The rhombic lip

The rhombic lip (RL) was first described by His as a territory of germinative neuroepithelium in the hindbrain (His, 1891). The RL spans the entire A-P axis of the hindbrain and resides along the fourth ventricle at the interface of the roof plate and the dorsal alar plate (Figure 11A). Besides its particular rhombical morphology, the RL is characterized by a sustained mitotic activity through late stages of embryonic development. The cells emanating from the RL migrate tangentially in superficial streams. Already His suggested that these neurons form the ventrally located pontine and olivary nuclei. This was confirmed later on and also the cerebellum, the cochlear nuclei, other precerebellar nuclei as well as non-neuronal structures were identified to be RL derivatives (Hunter and Dymecki, 2007; Rodriguez and Dymecki, 2000; Wingate and Hatten, 1999).

Genetic fate mapping studies gave first insight into the molecular mechanisms and transcription factor networks that specify the RL territory. These studies identified that all RL progenies, neuronal as well as non-neuronal, can be identified by *Wnt1* expression at the progenitor stage (Rodriguez and Dymecki, 2000). *Wnt1* expression turned out to be graded with high levels found dorsally and lowers levels ventrally. This suggests that the RL is further subdivided along the D-V axis and that different neuronal populations have distinct progenitor compartments within the RL. Subsequent experiments revealed that these subdomains are specified by the expression of basic helix-loop-helix (bHLH) transcription factors such as *Lmx1a*, *Math1*, *Ngn1*, *Mash1* and *Ptf1a* (Figure 11B) (Landsberg et al., 2005; Storm et al., 2009; Wang et al., 2005; Yamada et al., 2007). The dorsal most *Lmx1a* positive domain defines the non-neuronal RL zone that gives rise to cells contributing to the roof plate and choroid plexus (CPe). Immediately adjacent, *Math1* expression characterizes precerebellar mossy fiber neurons. The remaining domains marked by *Ngn1*, *Mash1* and *Ptf1a* expression contribute to the climbing fiber system of the inferior olive nuclei. Most of these bHLH transcription factors are necessary for the development of their respective RL subdomain (Wang et al., 2005; Yamada et al., 2007). In addition, the homeodomain containing protein Pax6 and the bHLH transcription factor Olig3 are essential for patterning

the overall RL rather than specific progenitor subsets (Landsberg et al., 2005; Storm et al., 2009). Besides *Wnt1*, BMPs and *Shh* have been shown to be key morphogens relevant for RL patterning (Alder et al., 1999; Huang et al., 2009; Liu et al., 2004). BMPs secreted from the roof plate and choroid plexus cells are particularly important for the induction of *Math1* and thus the generation of mossy fiber neurons. BMP activity is mediated through *Pax6*. Thus, the absence of either BMP signaling or *Pax6* expression leads to comparable phenotypes characterized by an expansion of the *Ngn1* positive domain at the expense of *Math1* positive progenitors.

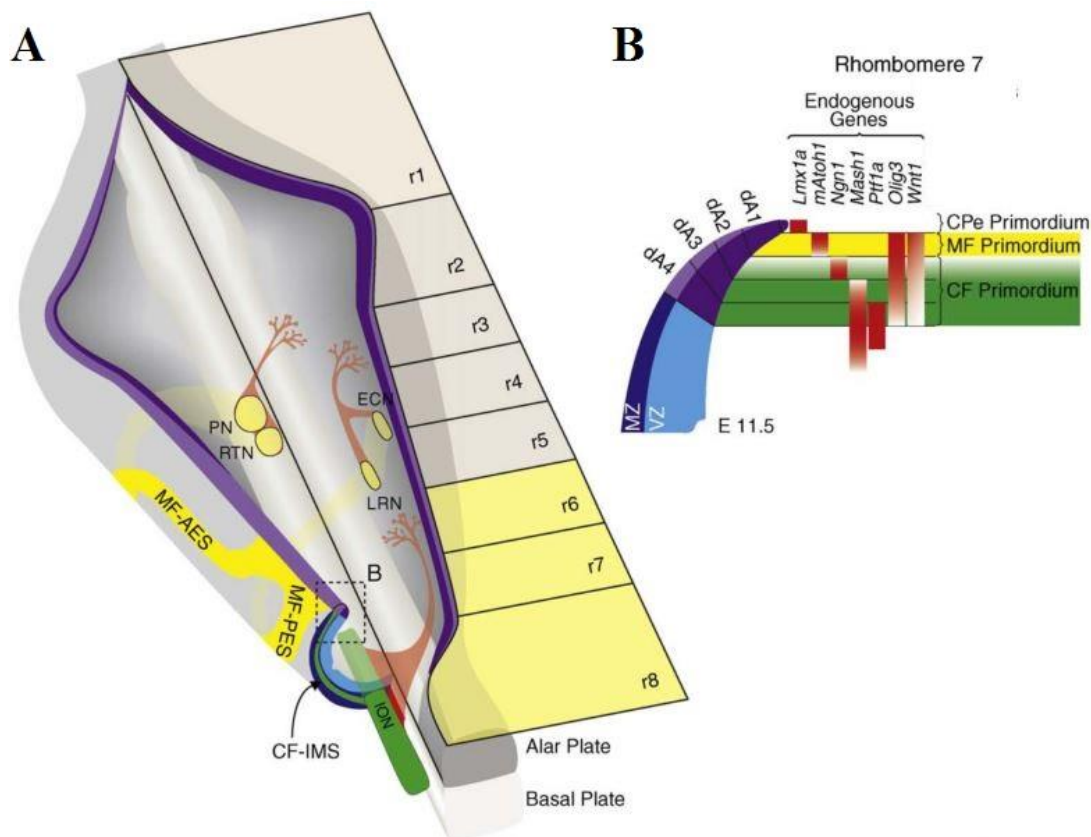


Figure 11: The precerebellar rhombic lip (RL) derivatives and the D-V axis of the RL. (A) Schematic representation of the developing mouse hindbrain. The RL (purple) frames the 4th ventricle along the entire antero-posterior (A-P) axis. At different time points RL derivatives from rhombomere (r) 6-8 engage into the posterior extramural stream (PES) or anterior extramural stream (AES), or migrate intramurally to form the precerebellar nuclei including pontine gray nuclei (PGN), reticulotegmental nuclei (RTN), lateral reticular nuclei (LRN), external cuneate nuclei (ECN) and inferior olivary complex (IO). All precerebellar nuclei project to the cerebellum. (B) A schematic cross-section through the precerebellar RL. The progenitor domains in the ventricular zone (VZ) for the choroid plexus (CPe), the mossy fiber (MF) and climbing fiber (CF) neurons along the D-V axis can be distinguished from each other according to the expression of key transcription factors including *Wnt1*, *Lmx1a*, *mAtoh1* (*Math1*), *Mash1*, *Ptf1a*, and *Olig3*. Adapted from (Ray and Dymecki, 2009)

By intersecting the D-V axis of the RL with the A-P axis, three main domains can be identified. The entirely Hox negative r1 domain generates cerebellar neurons such as granule and purkinje cells (Wingate and Hatten, 1999). The r2-5 derivatives contribute to the auditory system (Di Bonito et al., 2013) and the precerebellar system with its mossy and climbing fiber nuclei originates from the most posterior r6-8 part of the RL (Di Meglio et al., 2013; Okada et al., 2007). Furthermore, within the precerebellar system complexity is increased through the differential effect of certain factors. *Tcf4*, for instance, is selectively required for PN development but no other mossy fiber or climbing fiber nuclei despite being co-expressed throughout (Flora et al., 2007). *Nscl-1* and *Nscl-2* are further examples for genes specifically required for PN development (Schmid et al., 2007).

1.6. The precerebellar system

Besides its classical role in motor learning and coordination of movements, the cerebellum is more and more shown to be involved in cognition and emotion (D'Angelo and Casali, 2012). For these purposes, extensive reciprocal communication between different parts of the CNS, especially the cerebral cortex and the cerebellum, has to be realized. Communication between the cerebellum and the cortex is mediated through cerebello-thalamo-cerebro-cortical circuits. Most efferent projections from the cerebellum to the cortex pass through thalamic nuclei while the majority of afferent information from the cortex to the cerebellum is relayed in the PN (Schwarz and Thier, 1999). The PN is part of a large system of precerebellar nuclei that resides within the hindbrain and is entirely derived from the RL as indicated earlier (Altman and Bayer, 1987a). One common feature of these precerebellar nuclei is their postmitotic long-range circumferential tangential migration from the RL to their final position. The precerebellar system is comprised of climbing fiber and mossy fiber nuclei. Climbing fiber nuclei synapse on cerebellar purkinje cells and are of inhibitory nature. All climbing fibers are organized in the inferior olivary complex (IO) (Altman and Bayer, 1987b). The IO receives input equally from the cortex, mid- as well as hindbrain regions (Berkley and Hand, 1978; Berkley and Worden, 1978; Saint-Cyr, 1983). Mossy fiber nuclei provide excitatory input to granule neurons in the cerebellum. Mossy fiber neurons are distributed over a number of nuclei including the pontine gray nuclei (PGN), reticulotegmental nuclei (RTN), lateral reticular nuclei (LRN), external cuneate nuclei (ECN) as well as the recently identified interfascicular trigeminal nucleus (IFV) and linear nucleus (LI) (Altman and Bayer, 1987c, d; Fu et al., 2013; Fu et al., 2009). The PGN and the RTN are located adjacent to each other in

the rostral parts on the ventral hindbrain. They are usually referred to as PN as they have a very similar development, connectivity and function. Mossy fiber nuclei tend to be biased to certain sources of input. As mentioned, most of the cortical information is processed in the PN. The LRN on the contrary receives limited amount of input from cortical areas but conveys mostly peripheral input arriving from the spinal cord to the cerebellum (Pivetta et al., 2014).

1.6.1. Specification of the different components of the precerebellar system

The climbing fiber system of the IO can be easily distinguished from the mossy fiber nuclei by their origin from different progenitor compartments of the RL. The neurons contributing to the IO arise mostly from the *Ptf1a* positive domain and migrate ventrally through the intramural olivary migratory stream. All neurons contributing to the mossy fiber system originate from a single progenitor compartment in the RL defined through the expression of *Math1*. Some specificity might still be generated within this *Math1* positive domain as suggested by the differential effects of *Tcf4*, *Nscl-1* and *Nscl-2* (Flora et al., 2007; Schmid et al., 2007). However, the presence of entirely separated progenitor populations for each nucleus is unlikely. With respect to the A-P axis, mossy fiber projecting neurons derive only from the posterior aspects of the RL comprising r6-8. Thereby, it has been shown that all mossy fiber nuclei contain neurons from the r7 and r8 compartment while r6 mostly contributes to the PN. How is the allocation of neurons to distinct nuclei achieved if the different components of the mossy fiber system do arise from the same D-V and A-P axis? Altman and Bayer attempted to answer this question and found that the generation of neurons contributing to different nuclei is a process that is separated by time (Altman and Bayer, 1987a). IO neurons are the first ones to be generated. Next, ECN and subsequently LRN neurons emanate and migrate to their contralateral target position through the posterior extramural stream (PES). Finally, RTN and shortly afterwards PGN neurons originate from the RL, undertake their long-distance tangential migration via the anterior extramural stream (AES) and settle ipsilateral at the ventral midline of r4. In mice, the first PN neurons start migrating at around E12.5 and the development of the nucleus is completed only at the end of gestation making these neurons some of the latest born in the vertebrate hindbrain.

1.6.2. Migration and nucleation of pontine nuclei neurons

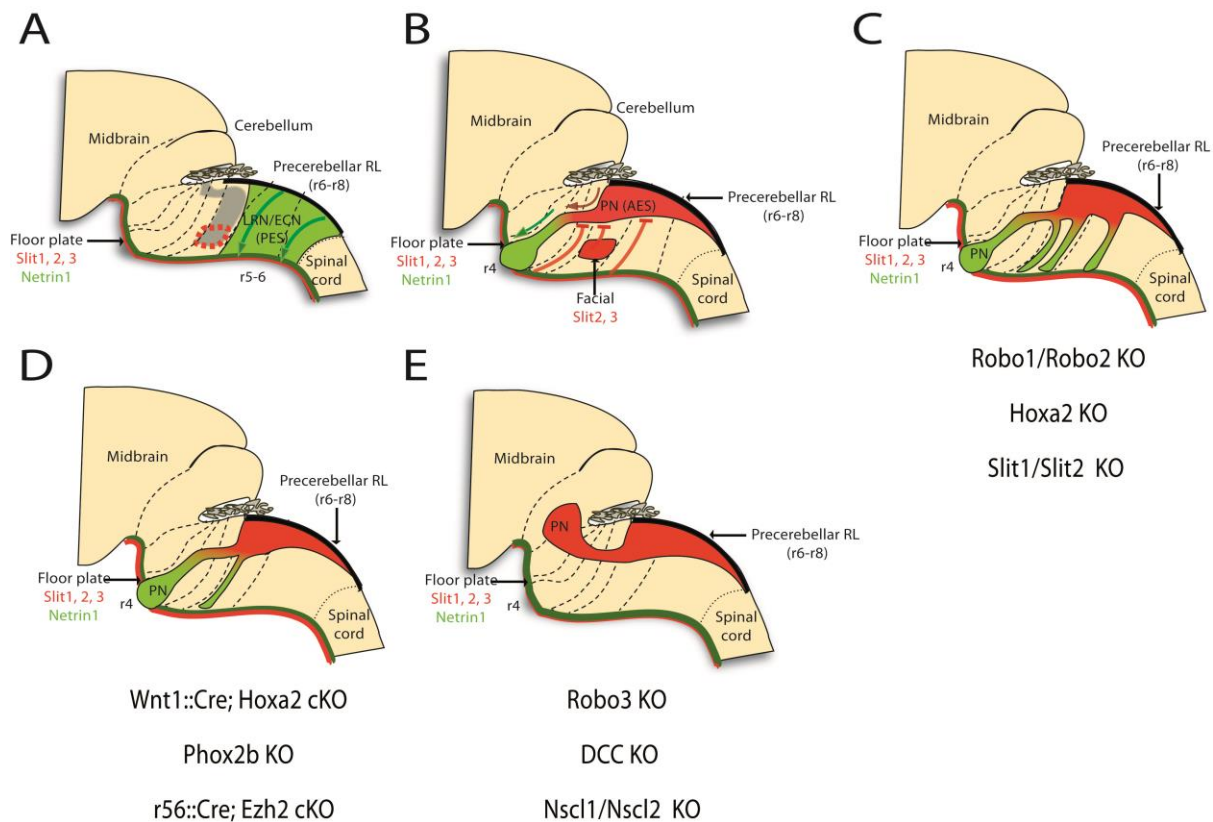


Figure 12: Molecular mechanisms of pontine nuclei (PN) neuron tangential migration. (A) Until E13.5 rhombic lip (RL) derivatives engage into the posterior extramural stream (PES) due to strong attraction by Netrin1. (B) Upon formation, the facial motor nucleus (FMN) secretes Slit2 and Slit3 and thus creates a repulsive cue for precerebellar neurons. Consequently, PN neurons are forced to migrate anteriorly and can only turn to the midline after passing the FMN in r4. (C-E) PN migratory defects as observed in a number of mutants. (C) By disrupting Slit/Robo repulsive signaling, either through direct knockout or *Hoxa2* knockout, PN neurons are prematurely attracted to the ventral midline at various places along the A-P axis. (D) PN neuron specific *Hoxa2* conditional knockout (cKO), interference with FMN formation through *Phox2b* knockout and an increase in environmental Netrin1 after r5-6 specific *Ezh2* cKO leads to the formation of an additional ectopic PN. (E) Silencing of Slit/Robo repulsive signaling through *Robo3* and Netrin1 insensitivity due to absence of DCC renders PN neurons unable to turn ventrally in r4. *Nsc1-1* and *Nsc1-2* positively regulates DCC and represses *Unc5c* expression. Thus, in *Nsc1* and 2 knockouts Netrin prematurely repels PN neurons. Adopted from (Di Meglio and Rijli, 2013)

The final position of precerebellar neurons is distant to their place of origin in the RL. This is especially true for PN neurons, which undergo a long-distance tangential migration from the dorsal posterior to the ventral anterior hindbrain. To achieve such a directed and precise movement over long distances, neurons scan their environment for appropriate cues that determine their further path, much as already described for neuronal circuit formation.

Precerebellar neurons adopt a unipolar morphology once exiting the RL (Marin et al., 2006). The leading process of precerebellar neurons which can extend to hundreds of micron, probes the environment for signaling cues. After committing to a certain direction the nucleus moves along through cytokinesis (Kawauchi et al., 2006). The homeodomain transcription factor *Barhl1* is a marker for the migratory fate of precerebellar neurons and is essential for correct migration (Li et al., 2004). All posterior RL derived neurons are attracted by the ventral midline through Netrin1 (de Diego et al., 2002). The respective receptor allowing for this attraction is DCC. Despite this mutual attraction being present in all precerebellar neurons, the mossy fiber neurons adopt two different migratory pathways. The earlier born LRN and ECN neurons are migrating in the PES directly towards the midline and cross it once to the contralateral side (Figure 12A) (Di Meglio et al., 2008). Subsequently, LRN and ECN neurons start expressing Robo1 and Robo2 receptors, which leads to a repulsion from the midline due to increased sensitivity towards Slit signaling (Stein and Tessier-Lavigne, 2001). Together with the silencing of the Netrin1 – DCC mediated attraction, this allows the LRN and ECN neurons to reach their final target in the lateral and dorsal aspects of the posterior hindbrain respectively. The later born mossy fiber population of the PN adopts a caudo-rostral migratory route after a short initial D-V migration forming the AES (Figure 12B) (Geisen et al., 2008). Only after reaching the r4 territory these neurons turn ventrally and settle ipsilateral at the ventral midline, two days after they started their journey from the RL. Both attractive and repulsive cues have been described to account for this anterior migration. PN neurons migrate superficially just below the meninges, which secrete chemokines essential for proper PN neuron migration. Interaction between the secreted chemokine Cxcl12 and its receptor Cxcr4 in PN neurons is needed for anterior migration (Zhu et al., 2009). Another significant reason for PN neurons to migrate along the AES but not PES was discovered in 2008 by Geisen et al. Here, the authors observed a temporal correlation between the formation of the facial motor nucleus (FMN) and the switch of precerebellar neurons from the PES to the AES (Figure 12B) (Geisen et al., 2008). Due to the position of the FMN and the expression of high levels of *Slits* in FMN neurons, the authors hypothesized that the FMN is the source of repulsion needed to force PN neurons to migrate anteriorly. Indeed, manipulation of *Slit* expression or interference with the formation of the FMN leads to migratory defects of PN neurons with premature attraction to the ventral midline (Figure 12C). In accordance to this finding, *Robo1* and *Robo2* knockout in PN neurons show a similar phenotype (Geisen et al., 2008). Contrary, *Netrin1*, *DCC* or *Robo3* knockout PN

neurons never manage to commit themselves to the ventrally oriented migration towards the ventral midline (Figure 12E) (Bloch-Gallego et al., 1999; Marcos et al., 2009; Marillat et al., 2004). An increase in *Netrin1* expression upon *Ezh2* knockout in territory r5-6 leads to a split of the AES with some neurons forming an ectopic PN in a more posterior position (Figure 12D) (Di Meglio et al., 2013). This shows how crucial the balance between the Netrin1 mediated attraction and the Slit mediated repulsion is to allow for appropriate PN neuron migration.

Hox genes are an important class of transcription factors for PN neuron migration. Postmitotic PN neurons express *Hox PG2-5* genes, according to their A-P origin throughout migration and nucleation (Geisen et al., 2008). In *Hox PG2* mutants, PN neurons prematurely turn to the ventral midline (Figure 12 C, D). As these phenocopies the *Slit*, *Robo1* and *Robo2* mutants, it is assumed that *Hox PG2* genes are involved in the regulation of either of these genes. In fact, *Robo2* was confirmed to be a direct target of *Hoxa2* in PN neurons (Geisen et al., 2008). It was recently demonstrated that PN neurons keep their relative A-P organization during migration (Di Meglio et al., 2013). Meaning that r6 derived neurons migrate most dorsally in the AES and r8 derived neurons most ventrally. The maintenance of this relative position was attributed to differential *Unc5b* expression in PN subsets. The level of *Unc5b* expression in PN neurons correlates with a distinct responsiveness towards environmental Netrin1 and thus keeps the different PN neuron subsets largely segregated. A link between *Hox PG5* genes and *Unc5b* levels has been described suggesting that *Hox PG5* genes are fundamentally important for the maintenance of this topographic migration (Di Meglio et al., 2013). However, direct prove for the role of Hox genes in positioning individual neurons in the PN is still lacking.

Two general principles of neuronal organization exist in the mammalian CNS. First, the cerebral and cerebellar cortices are laminar structures. The development of such structures has been studied extensively. For instance the cortex is assembled in an inside-out manner in which late born neurons migrate through the existing laminae and settle on the cerebral surface (Nadarajah and Parnavelas, 2002). On the contrary, subcortical regions are primarily organized in nuclei such as the thalamus or the PN (Romanes, 1949). The process of forming such condensed structures, which can be easily delineated from its surrounding, has been termed nucleogenesis. It is less understood how neurons find their precise position within a certain nucleus as the final position of the nucleus tends to be tangentially displaced from the

progenitor domain. Studies on the PN have shown that during nucleogenesis neurons switch from tangential migration to radial migration to penetrate into the tissue of the hindbrain (Okada et al., 2007). Also the migration of neurons along the A-P axis has been reported within the PN (Shinohara et al., 2013). PN neurons settle in their final position in an orderly manner and nucleate in concentric rings (Altman and Bayer, 1987d). Early born neurons form an inner core next to the future cortico-spinal tract (CST). Later born neurons successively add layers around the already present ones forming the nucleus in an inside-out sequence (Figure 13). Thus, birth dating plays a pivotal role in determining the final position of PN neurons. Besides this inside-out organization, the PN is further patterned along the A-P axis. PN neurons not only keep their relative A-P organization during migration but also during nucleation (Di Meglio et al., 2013). Consequently, r6 derived neurons settle most anteriorly and r8 derived neurons most posteriorly in the PN (Figure 13). It is unclear if this segregation entirely depends on the maintenance of segregation during migration or also on the above mentioned A-P migration of neurons in the PN.

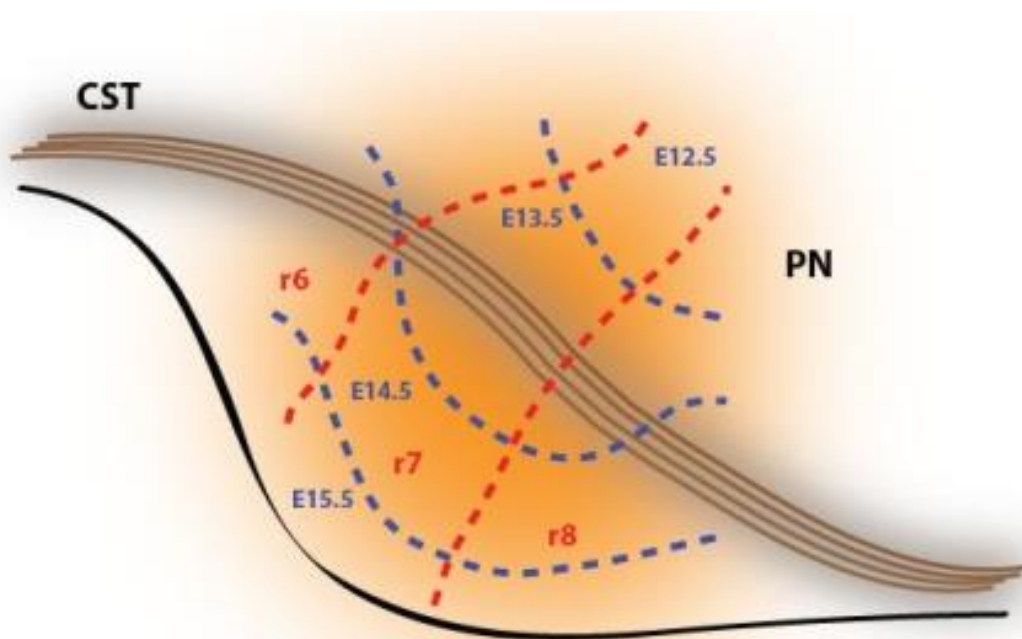


Figure 13: The anatomy of the pontine nuclei (PN). PN neurons are patterned along the inside-out and A-P axis according to their birthdays and origin in the rhombic lip respectively. Figure by D. Kraus based on (Altman and Bayer, 1987d; Di Meglio et al., 2013)

1.6.3. Circuitry of the pontine nuclei: Input connectivity

The PN connects the cortex and the cerebellum (Figure 14A). PN neurons receive their major input from ipsilateral cortical layer 5 neurons and project to cerebellar granule cells

(Tomasch, 1969; Wiesendanger and Wiesendanger, 1982). The fiber system that connects cortex and PN is one of the largest ones in the mammalian CNS. It has been estimated that in humans up to 40 million fibers in the CST send collaterals into the PN (Tomasch, 1969). Studies have revealed that all regions of the cortex are projecting to the PN, though with different intensities across species (Glickstein et al., 1985; Wiesendanger and Wiesendanger, 1982). Despite regions, which developed the most from rodents to primates, having only sparse inputs to the PN, recent findings concerning the importance of the cerebellum in higher brain functions, strongly supports involvement of the PN in such functions (D'Angelo and Casali, 2012).

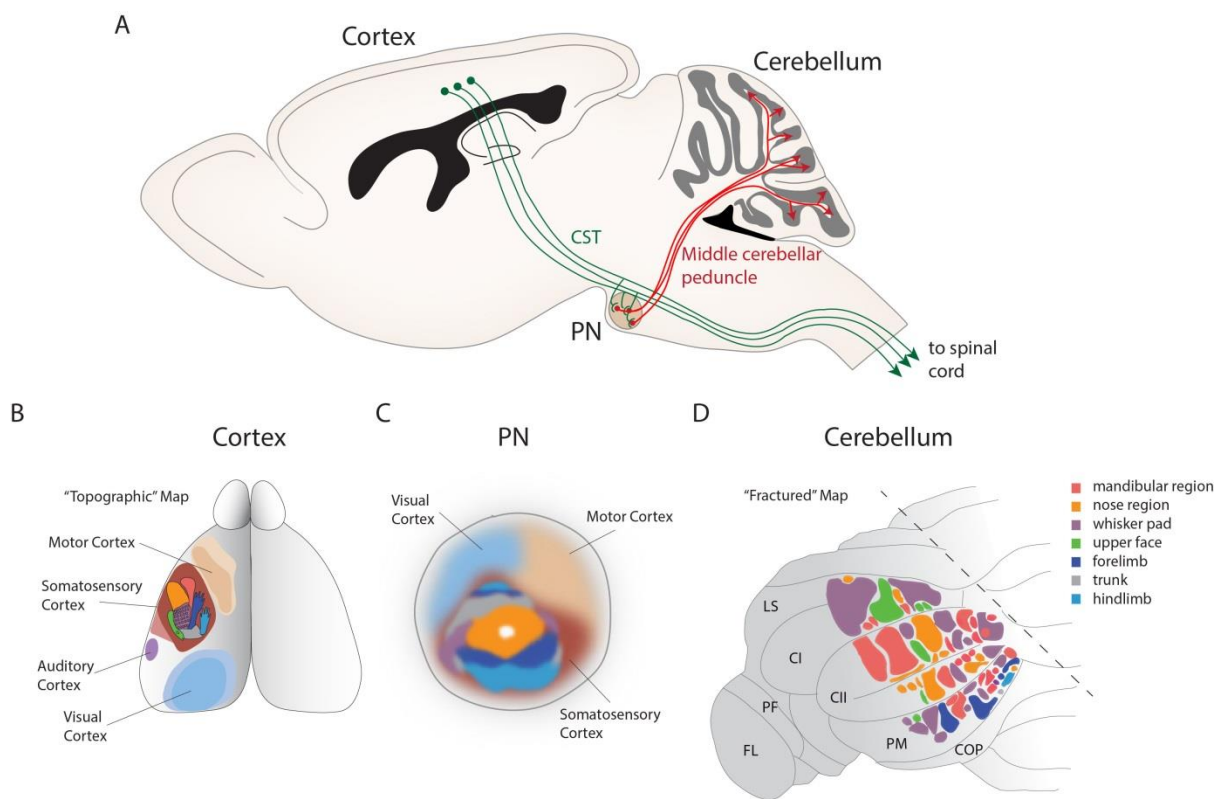


Figure 14: Pontine nuclei (PN) circuitry. (A) The PN is the main connection between cortex and cerebellum. It receives input from layer 5 cortical neurons via the cortico-spinal tract (CST) and projects exclusively to the granule neurons of the cerebellum. (B-D) Topographic maps present in the cortex are fractured during the PN relay and represented in patches in the cerebellum. (B) In the cortex different modalities are processed in separate areas. These areas are topographically organized as exemplified by the somatosensory homunculus. (C) In the PN these topographic maps are largely maintained. (D) While projecting to the cerebellum, PN neurons fracture the cortical information into a fractured representation in the cerebellum. Adapted from (Kratochwil, 2013)

The cortex is topologically organized (Chapin and Lin, 1984). For instance, information in primary cortices, including visual, auditory and somatosensory is organized in a way that the

relative spatial relationships are maintained from the periphery (Figure 14B). The organization of the projections from the cortex to the PN has been highly debated until the early 2000s (Bjaalie and Leergaard, 2000; Schwarz and Thier, 1999; Schwarz and Thier, 2000). Seminal work from Leergaard et al. finally revealed and established the existence of an orderly topographic relationship allowing a continuous mapping of cortical representations in the PN (Leergaard and Bjaalie, 2007; Leergaard et al., 2006). Thus, neighboring relationships are maintained and different cortical regions project to segregated domains in the PN (Figure 14C). This is particularly evident when assessing the somatosensory representation in the PN. However, the transformation of the 2D cortical map into a 3D PN map creates neighboring relationships that are initially not present. In general, temporal and occipital regions, including the visual cortex, project antero-laterally, frontal motor areas antero-medially and parietal somatosensory regions centro-caudally. Substantial efforts were made to understand the principles underlying the circuit formation between cortex and PN. As a result, the notion emerged that the A-P axis of the cortex is roughly projected onto the medio-lateral (M-L) axis of the PN. Further, by mapping of the antero-lateral to medio-posterior axis, a pattern of concentric organization is revealed in the PN. As organizing principles, neurogenesis and patterned expression of transcription factors such as *Pax6* and *Emx2* have been discussed but any functional prove is lacking (Leergaard and Bjaalie, 2007). It is interesting to note that the A-P to M-L transformation is already present in the CST and might simply be a consequence of the arrangements of fibers in the tract (Coleman et al., 1997). The concentric or lamellar organization of cortical input matches the neurogenetic gradient in the cortex with the already mentioned inside-out organization of the PN according to the birthdate of neurons (Leergaard et al., 1995). However, functional evidence is entirely lacking for this correlation. Finally, the A-P patterning of the PN through the differential expression of Hox genes might have some relevance for organizing cortical input. Not only do major regions of the cortex tend to segregate along the A-P axis (e.g. visual and somatosensory cortices) but also ectopic nuclei, displaced from the normal position along the A-P axis, attract cortical input according to their molecular composition (Di Meglio et al., 2013). This further argues for the existence and importance of chemotrophic cues secreted by PN neurons as suggested by a number of *in vivo* and *in vitro* experiments (O'Leary et al., 1991). Together, different modalities seem to be processed largely in parallel by discrete functional units in the PN. This is further substantiated by the finding that PN neurons tend to organize their axons by respecting the borders of cortical input (Schwarz and Thier, 1995).

Convergence of input to single PN neurons is consequently also a function of distance between the cortical neurons (Oka et al., 1975; Ruegg and Wiesendanger, 1975).

Subcortical input to the PN has been described in various species including primates (Aas, 1989; Glickstein et al., 1990; Mihailoff et al., 1989). Nuclei projecting to the PN can be classified into two main groups according to their pattern of projections. Spatially non-specific projections arise from neuromodulatory systems such as the raphe nuclei and the locus coeruleus. According to the function of such neuromodulatory systems, this input globally affects the function of the PN. Spatially restricted input arises from a large set of nuclei. Precisely mapped structures include visual nuclei (e.g. superior colliculus and pretectal nuclei), somatosensory nuclei (e.g. dorsal column and trigeminal nuclei), deep-cerebellar nuclei and the hypothalamus. For a number of these inputs, convergence with the respective cortical input has been suggested. For instance, fibers from the dorsal column nuclei segregate in PN areas that also receive input from somatosensory cortex (Kosinski et al., 1986). However, there are exceptions like the colliculo-pontine projections that terminate in different zones in the PN rather than projecting to visual and somatosensory areas (Schwarz et al., 2005).

1.6.4. Circuitry of the pontine nuclei: Output connectivity

The entire PN projects as mossy fibers through the middle cerebellar peduncle to different parts of the cerebellum (Figure 14A). PN mossy fibers largely target the granule cells in the cerebellar cortex but also supply deep cerebellar nuclei with excitatory input, though to a much lower extent. Projections of the PN cross mostly contralaterally but also ipsilateral projections can be identified which originate from segregated pools (Herrero et al., 2002). However, retrograde double labelling studies showed that some neurons send collaterals to both hemispheres (Rosina and Provini, 1984). Mossy fiber input from PN, LRN, ECN, vestibular nucleus and spinal cord synapse in largely segregated but partially overlapping regions of the cerebellum. Only recently an integration of PN and ECN input on single granule cells has been demonstrated (Huang et al., 2013). PN mossy fibers are mostly present in the hemispheres of the posterior cerebellum including the simple lobule (SL), the paramedian lobule (PML), Crus1, Crus2 and the paraflocculus (PFL). PN neurons can send collaterals to different lobules within one hemisphere as well as to different folia within one single lobule (Bjaalie and Brodal, 1997; Mihailoff, 1983). Still, the inter-lobule divergence of

PN neuron projections seems to follow some logic as double labelling is only observed for certain combinations of lobules. Thus, the same information is transferred from the PN to specific parts of the cerebellum. This notion is supported by electrophysiological data which revealed a fractured somatotopy in the cerebellum (Shambes et al., 1978). Different body parts are thus represented in several discrete spots in the cerebellum and the spatial relation between different body parts is not necessarily faithfully recapitulated (Figure 14D).

The complexity of fracturing the continuous maps in the cortex to the patchy representation in the cerebellum through the PN is underlined by the fact that until today no rules have been described that would explain an overall topography between PN and cerebellum. Retrograde tracings from even small areas in the cerebellum label neurons which are spread over large areas of the PN arguing for convergence of unrelated PN inputs (Mihailoff et al., 1981). Solely tracings from different folia of the paraflocculus result in a lamellar like pattern of labelled cells in the PN (Bjaalie et al., 1991; Nikundiwe et al., 1994). No apparent patterns along the A-P, D-V or M-L axis in the PN have ever been identified despite numerous experiments in different species (Brodal and Bjaalie, 1992). Accordingly, trans-synaptic rabies tracings from the cerebellum label widespread regions in the cortex (Suzuki et al., 2012). However, when tracing from physiologically defined regions from the cerebellum, neurons are reliably labelled in the termination zones of the corresponding cortico-pontine projections (Leergaard et al., 2006). Also the trans-synaptic rabies tracings revealed distinct sets of cortical neurons dependent on the initiation site in the cerebellum (Suzuki et al., 2012). So, each cerebellar patch gets the respective cortical input from the PN. Furthermore, sensorimotor convergence has been demonstrated recently in single Golgi cells (Proville et al., 2014).

Mossy fiber input to the cerebellum has also been studied in relation to the climbing fiber system. Climbing fibers from sub-nuclei in the IO synapse onto Purkinje cells in one or two longitudinal zones in the cerebellum (Apps and Hawkes, 2009). Anterograde tracings from the PN would occasionally also reveal a stripe like pattern (Mihailoff, 1993). However, defined mossy fiber inputs diverge to multiple longitudinal zones. Still, mossy fibers seem to respect the Purkinje cells stripe boundaries while potentially forming sub-stripes (Ji and Hawkes, 1994). Tracings from different longitudinal zones (either zebrin-positive or negative) labels distinct populations in the PN (Cerminara et al., 2013). Recent data suggest that mossy and climbing fiber somatosensory information is matched in the cerebellum (Odeh

et al., 2005; Pijpers et al., 2006). Moreover, PN mossy fibers initially contact Purkinje cells (Kalinovsky et al., 2011). Since these connections are removed subsequently, this might indicate that Purkinje cells are directly involved in regulating mossy fiber targeting in the cerebellum.

Overall, the ponto-cerebellar connectivity is characterized by both convergence and divergence. The potential topography of PN mossy fiber projections is complex and a relation to the climbing fiber system needs further investigations. Together with the cortico-pontine connectivity it is likely that the fracturing of the map between cortex and cerebellum occurs at the ponto-cerebellar level. However, a molecular or cellular framework for such a transformation is entirely lacking.

1.6.5. Function of the pontine nuclei

Initially the PN was assumed to be a simple relay station that faithfully transmits information between the computational units in the cortex and the cerebellum (Schwarz and Thier, 1999). However, a number of findings over the past decades have challenged this traditional view. First, PN neurons display complex electrophysiological properties (Mock et al., 1997; Schwarz et al., 1997). Second, PN neurons receive inhibitory input (Border and Mihailoff, 1990). Third, the PN is under the influence of feedback from deep cerebellar nuclei (Mihailoff et al., 1989). Fourth, despite still not being proven, the sheer amount and the substantial overlap of cortical and sub-cortical input arriving to the PN strongly suggests that information from different areas is integrated in single cells. Evidence for an integration at least multi-synaptically is already present (Oka et al., 1975). Together, this strongly suggests that PN neurons have major filter and integrator capacities and argues against a simple relay of information. It seems more likely that basic computations are already executed in the PN and adapted signals are then transmitted into the cerebellum. Another function of the PN might be to combine relevant information for various sources through their convergent and divergent projections to the cerebellum.

Hypotheses concerning the physiological relevance of the PN have been made based on its circuitry. As motor, sensory as well as multimodal areas of the cortex send abundant projections to the PN, roles in the execution of motor plans (Allen and Tsukahara, 1974), the sensory guidance of movements (Stein and Glickstein, 1992) and potentially higher cognitive functions have been postulated (Schwarz and Thier, 1999). Actual data have been generated

by lesion experiments of the middle cerebellar peduncle and the PN. Persistent impairments involved the execution of visually coordinated movements (Turner and German, 1941). Also smooth pursuit eye movements and visually guided saccades have been associated with the PN (Suzuki et al., 1990; Thier et al., 1991). Finally, peripheral vestibulopathy, ataxia and hemiparesis are symptoms in humans with PN defects as underlying cause (Magrotti et al., 1990; Thomke and Hopf, 1999). Altogether, the described symptoms are in agreement with the expected function of the PN. However, considering the prominence of the cortico-ponto-cerebellar pathway in the CNS the resulting symptoms were rather mild and mostly transitory (Brodal and Bjaalie, 1992).

1.7. Aim of this thesis

The lab of Filippo M. Rijli focuses on the transcriptional mechanisms underlying topographic circuit formation in the mouse hindbrain. Much of the work addresses the functional role of Hox transcription factors and their regulation during late phases of neuronal development. A major focus of the lab is thereby on the developmental of the precerebellar system. Within this system the PN takes a prominent role as it relays most of the cortical information present in the cerebellum. Previous work showed that the PN is patterned through the differential expression of a specific paralogous group of Hox factors: the *Hox PG5* genes.

The first main object of this thesis was to understand how PN neuron subsets become specified during development by the induction of *Hox PG5* genes. We found that *Hox PG5* genes are selectively induced in a specific subset of postmitotic PN neurons, whereas the domain of mitotic progenitors is devoid of *Hox PG5* expression. We particularly focused on the interactions between environmental signaling and epigenetic remodeling at *Hox PG5* loci. To achieve this goal it was important to precisely map the expression pattern of *Hox PG5* genes in the precerebellar system and identify signaling pathways as well as epigenetic modifiers that show a dynamic regulation at the onset of *Hox PG5* expression. The relevance of such signaling pathways and epigenetic modifiers were subsequently confirmed through a variety of molecular biological and mouse genetic tools. Furthermore, we aimed at characterizing how the interplay of environmental signaling and epigenetic remodeling impacts on higher order chromatin organization *in vivo*.

The second main aim of this thesis was to assess the functional significance of *Hox PG5* expression on the nucleation and circuit formation of the PN. Our main hypothesis was hereby that *Hox PG5* genes are key players in organizing the projections to the cerebellum and to select specific input from cortical and subcortical regions. To this end, we generated mouse genetic tools to manipulate the Hox expression of PN neurons and adapted trans-synaptic viral tracing tools for assessing PN connectivity. Using these tools we aimed at setting out experiments to address the role of *Hox PG5* genes during PN nucleation, their effect on transcriptional programs on PN neurons and the resulting consequences on cortico-ponto-cerebellar sub-circuit diversification. Our results further suggest that *Hoxa5* expression in a specific subset of PN postmitotic neurons may underlie transformation of cortical somatotopic maps into fractured cerebellar maps.

2. Material and Methods

2.1. Animals

All animal procedures were performed in accordance with institutional guidelines and were approved by the Veterinary Department of the Kanton Basel-Stadt

2.1.1. Generation of the *Math1::Cre* line

The original goal was to generate a *Math1::CreERT2* line. In these transgenic mice, CreERT2 is driven by a 1.7 kb enhancer of *Math1* (Helms et al., 2000). The enhancer was subcloned into the vector pKS- β -globin-CreERT2-SV40pA, created by replacing the *LacZ* gene of the pKS- β -globin-lacZ vector (BGZ40) (Studer et al., 1996) with a CreERT2 cassette (Santagati et al., 2005) using homologous recombination. The enhancer was amplified by PCR from genomic DNA using the following primers: 5'AGT TGT GCC TGT CTA AGG TC 3' and 5'ATC TAC TAG TGC TCT GGC TTC TGT AAA CTC 3'. The PCR band was purified and inserted 5' of the β -globin promoter using restriction sites SacII and SpeI, thus generating construct consisting of the enhancer, a β -globin minimal promoter and CreERT2 encoding sequence. The construct was linearized, purified and microinjected into the pronuclei of mouse zygotes. Founders were identified by PCR (907bp fragment) using the following primers: 5'AGT GGA GAA TGG GTT AAA TCC 3' and 5'ATC AGT GCG TTC GAA CGC TA 3'. Due to some Cre activity even in absence of tamoxifen-dependent induction for one of the founders (#45), this line was therefore renamed *Math1::Cre* and used as a standard Cre-expressing line (#ER45).

2.1.2. Generation of the *Jmjd3* knock-in line

The knock-in mouse strain *Jmjd3lacZ* was created from ES cell clone (EPD0330_7_F03, *Kdm6btm1(KOMP)Wtsi*) obtained from the NCRRI-NIH supported KOMP Repository (www.komp.org) and generated by the CSD consortium for the NIH funded Knockout Mouse Project (KOMP). Methods used on the CSD targeted alleles have been published by (Testa et al., 2004). The ES cells were aggregated with morula-stage embryos obtained from inbred (C57BL/6 x DBA/2) F1 mice. Germline transmission of the *Kdm6btm1(KOMP)Wtsi* allele was obtained and heterozygous mice were viable and fertile. The mice were genotyped by PCR (359bp wild type and 572bp mutant fragments) with the following primers: wild type forward, 5' CCT TAG AGA GAG CAG AGT TC 3'; wild type reverse, 5' TGG TTT CCG

ACT GCT GTG TG 3'; mutant reverse, 5' CTG TCC CTC TCA CCT TCT AC 3'. The in-frame LacZ expression cassette was flanked by two flip sites which allowed its Flippase mediated removal.

2.1.3. Generation of the *ROSA26::CAG(lox-stop-lox)3xFlag-Hoxa5-IRES-GFP* knock-in line

The conditional *Hoxa5* overexpression mouse line was generated by homologous recombination in the *ROSA26* locus using the targeting vector pR26-CAG-lsl-3xflagHoxa5-IRES-GFP, consisting of a CAG promoter, a lox-stop-lox cassette, a codon optimized *Hoxa5* tagged with a 3xFlag, an IRES-GFP, a WPRE element, a bGH poly(A) and a PGK-Neo cassette. To generate this vector, we used the vector pR26-CAG-lsl-Kir (kind gift from Guillermina López-Bendito and derived from the plasmid Ai27 (Madisen et al., 2012); Addgene Plasmid #34630) in which we replaced the insert located between the two FseI restriction sites by the cassette 3xflagHoxa5-IRES-GFP (PCR amplified from the BAC *ROSA26::(lox-stop-lox)Hoxa5-IRES-GFP* and cloned into the TOPO vector pCRII (Invitrogen) with insertion of a 3xFlag tag). The final targeting vector pR26-CAG-lsl-3xflagHoxa5-IRES-GFP was linearized with PvuI and electroporated into the E14 ES cell line. The positive ES cell clones selected by G418 resistance and screened by PCR were aggregated with morula-stage embryos obtained from inbred (C57BL/6 x DBA/2) F1 mice. Germline transmission of the *ROSA26::CAG(lox-stop-lox)3xFlag-Hoxa5-IRES-GFP* allele was obtained. Heterozygous and homozygous mice were viable and fertile. The mice were genotyped by PCR (603-bp wild type and 325-bp mutant fragments) with the following primers: wild type forward, 5' AAA GTC GCT CTG AGT TGT TAT 3'; wild type reverse, 5' GGA GCG GGA GAA ATG GAT ATG 3'; mutant reverse, 5' GGC CAT TTA CCG TAA GTT ATG 3'.

2.1.4. Generation of the *ROSA26::(lox-stop-lox)Hoxa5-IRES-GFP* BAC transgenic line

The generation of the conditional *Hoxa5* overexpression bacterial artificial chromosome (BAC) transgenic line was a two-step process. First we generated a BAC *ROSA26::(lox-stop-lox)galK-IRES-GFP* used as an entry for further constructs and allowing us the introduction of different cDNAs between the lox-stop-lox sequence and the IRES-GFP by using BAC recombineering and galK negative selection (Warming et al.). Then we used this strategy to

replace the *galK* gene by a codon optimized DNA sequence encoding for the Hoxa5 protein. The original BAC clone RP23-401D9 containing the ROSA26 locus was obtained from BACPAC Resources Center (Children's Hospital Oakland Research Institute, Oakland, Calif., USA) and was used as a template for bacterial recombination. To prevent any further interactions, the LoxP511 and the LoxP sites located in the backbone vector of this BAC were removed respectively by recombination of an ampicillin resistance gene and by using the *galK* positive/negative selection (Warming et al., 2005) (see table for the primer sequences). The final BAC ROSA26::(*lox-stop-lox*)Hoxa5-IRES-GFP (consisting of a splice acceptor, a *lox*-PGK-Neo-3xpA(*stop*)-*lox* cassette, a codon optimized Hoxa5, an IRES-GFP-pA) and all the intermediate constructs were tested by PCR, restriction enzyme digestion and sequencing for correct recombination and removals of the *lox/galK* sequences. The purified BAC was linearized by PI-SceI digestion prior to microinjection into pronuclei of mouse zygotes. Founders were identified by PCR (220bp fragment) using the following primers: 5' TGC AGC CCA AGC TAG CTT AT 3' and 5' TCT CTG AAC TGC TCG GAC AC 3'.

2.1.5. Generation of the *Tau::(lox-stop-lox)Rabies-glycoprotein-IRES-nls-LacZ* line

The *Tau::(lox-stop-lox)Rabies-glycoprotein-IRES-nls-LacZ* mouse line was generated by inserting a cassette encoding (*lox-stop-lox*)Rabies-glycoprotein-IRES-nls-LacZ into exon 2 of the Tau locus using a strategy described previously (Hippenmeyer et al., 2005).

2.1.6. Other mouse lines used in this study

RARE::lacZ (Rossant et al., 1991), *ACTB::Flip* (Rodriguez et al., 2000), *Wnt1::Cre* (Danielian et al., 1998), *r5-6::Cre*, *Hoxa5::Cre*, *MafB::CreERT2* (Di Meglio et al., 2013), *Krox20::cre* (Voiculescu et al., 2000), *Ezh2^{fl/fl}* (Puschendorf et al., 2008), *Hoxa5*, *Hoxb5*, *Hoxc5* knockout mice (McIntyre et al., 2007), and *ROSA26::(lox-stop-lox)TVA-IRES-LacZ* (Seidler et al., 2008) lines were as described. *ROSA26::(lox-stop-lox)tdTomato* (Madisen et al., 2010) mice were obtained from The Jackson Laboratory, USA.

2.1.7. Retinoic acid and tamoxifen treatment

Tamoxifen was dissolved in corn oil (SIGMA: T-5648) at 37°C. Animals were injected by gavage at appropriate time points. Trans retinoic acid (Sigma) was dissolved in DMSO.

Pregnant mice were treated with RA by intraperitoneal injection (60 mg/kg) at appropriate time points.

2.2. In utero electroporation

In utero electroporation was performed on embryos at E13.5 or E14.5 as described previously (Taniguchi et al., 2006). Plasmids used for electroporation were diluted to 1mg/ml in 1x phosphate buffer (PBS). Plasmids used in this study were as follows: pCX-eGFP (Okada et al., 2007), pCX-rabies-glycoprotein-WPRE, pCAG-mGFP-2a-Cyp26b1, pCAG-dnRAR-GFP (Damm et al., 1993), pCAG-Tcf3vp16 (Kim et al., 2000), pCAG-iCRE, pAAV-EF1a-TVA-WPRE (kind gift from B. Roska).

2.3. Histological analysis, immunostaining, and in situ hybridization

Prenatal brains were dissected if necessary and fixed in 4% PFA diluted in 1xPBS from 30 minutes at room temperature to overnight at 4°C. Postnatal animals were perfused with 4% PFA diluted in 1xPBS for 10 minutes and post fixed in 4% PFA diluted in 1xPBS overnight at 4°C. For cryostat sections, tissues were cryoprotected in 10% sucrose (Fluka) / 1xPBS and embedded in gelatin 7.5% (Sigma) / 10% sucrose / 1xPBS before being frozen at -80°C. Cryostat sections (25-30 µm) were cut (Microm HM560) in coronal and sagittal orientations, respectively. Vibratome sections (50-80 µm) were prepared from postnatal brains after embedding in 4% agarose (Promega) / 0.1 M phosphate buffer (pH7.4). Immunohistochemistry was performed as described before (Geisen et al., 2008) using primary antibodies rabbit anti-mouse Pax6 (Millipore; AB2237; 1/1000), anti-Hoxa5 (Sigma; HPA029319; 1/200), anti-RFP (Rockland, 600-401-379, 1/1000), anti-Raldh2 (Abcam, ab96060, 1/500) rat anti-Hoxb4 (developed by A. Gould and R. Krumlauf; obtained from the Developmental Studies Hybridoma Bank developed under the auspices of the NICHD and maintained by The University of Iowa, Department of Biology, Iowa City, IA 52242; 1/100) and chicken anti-GFP (Invitrogen, A10262, 1/1000) followed by species-specific fluorochrome-coupled secondary antibody staining (Alexa Fluor 488, 546, or 647, Invitrogen, 1/1000). Nuclei were stained with DAPI (Invitrogen, 1/10000). Simple and double in situ hybridisations were performed as described previously (Geisen et al., 2008). The following probes were used: Barhl1, Math1, Wnt1, Axin2, Hoxb2, Hoxb3, Hoxb4, Hoxb5, Hoxa5,

Ezh2, Cyp26b1, Raldh2, Chl1, Alcam1, Nrp1, and Nrp2. X-Galactosidase staining were performed as previously described (Geisen et al., 2008).

2.4. Fluorescent activated Cell Sorting (FACS)

Regions of interested were micro-dissected in 1xPBS at the desired stage and incubated for 5 – 10 minutes in activated dissociation solution (HBSS, 2.5mM Cystein, 0.5mM EDTA, 10mM HEPES, 1mg/ml Papain (Roche)) at 37°C. Samples were rinsed five times in HBSS / 10% FBS. Single cell suspension was achieved through mechanical dissociation of tissue with Pasteur pipettes. Fluorescent cells were collected by FACS (FACSCalibur, Becton Dickson) in appropriate solutions for ongoing analysis.

2.5. Quantitative PCR (qPCR)

100 cells isolated by FACS were directly sorted into the reverse transcription (RT) buffer (1x CellsDirect One-Step qPCR Kit (Invitrogen, 11753-100), SuperScript III RT Platinum Taq Mix, Primer mix (50nM final concentration)). RT was done for 15 minutes at 50°C followed by inactivation of the reverse transcriptase and activation of the Taq at 95°C for 2 minutes. 18 cycles (95°C 15 seconds, 60°C 4 minutes) of pre-amplification of specific targets were done on a standard thermal cycler. Unincorporated primers were removed by Exonuclease I treatment (NEB, M0293S, 1U/μl) for 30 minutes at 37°C. The final product was diluted 10-fold with DNA Suspension Buffer (TEKnova, T0221). qPCR was carried out with StepOne Real Time PCR System (Applied Biosystems) with the primers described below. Calculations were done using the delta delta cycle threshold (ddCt) model using Ssu72 as endogenous control.

Hoxb3_F: GGCCTCAATCACCTTTCCCA
Hoxb3_R: CAGGGTCCATGATGCTGGTT
Hoxb4_F: GCAAAGAGCCCGTCGTCTA
Hoxb4_R: GGCGTAATTGGGGTTTACCG
Hoxa5_F: CCCCAGATCTACCCCTGGATG
Hoxa5_R: TGGGCCACCTATATTGTCGTG
Ssu72_F: GGTGTGCTCGAGTAACCAGAA
Ssu72_R: CAAAGGAGCGGACACTGAAAC

2.6. Chromatin immunoprecipitation (ChIP)

Micro-dissected tissue samples were dissociated to single cells. Cells were cross-linked for 15 min in 1% PFA/1xPBS solution and subsequently lysed in cell lysis buffer (5mM PIPES pH8.0, 85mM KCl, 0.5% NP40, and protease inhibitors) for 10 min on ice. Nuclei were spun down at 2500g for 5 min at 4°C and finally lysed in nuclei lysis buffer (50mM Tris-HCl pH8.0, 10mM EDTA, 1% SDS and protease inhibitors). Following 15 min of lysis on a tube shaker at 4°C, samples were sonicated on Covaris and centrifuged at 22000g for 15 min at 4°C. Chromatin preparation was diluted 10x with IP Dilution Buffer (0.01% SDS, 1.1% Triton-X 100, 1.2mM EDTA, 16.7mM Tris-HCl pH8.0, 167 mM NaCl, and protease inhibitors) and used for IP. For IP, chromatin preparations were incubated overnight with primary antibodies against H3K27me3 (Millipore, 17-622, 1µg), H3K4me3 (Millipore, 17-614, 1µg), RAR (Santa Cruz, sc-773, 1µg), or Jmjd3 (Abcam, ab38113, 1µg) on a tube roller at 4°C. 50 µl of protein G magnetic beads was added and the incubation continued for 2 h. Beads were washed 3 times with 1ml of 0.02% Tween20/TBS solution. Precipitated material was eluted twice for 15min with 100µl of 1% SDS/ 100 mM sodium hydrogencarbonate (NaHCO₃) solution at 65°C on a thermal shaker. 20µl of 5M NaCl was added to the elute and the cross-links reversed by incubating for 6 h at 65°C. DNA was purified using Min-elute PCR purification kit (Qiagen). qPCR for amplification of genomic regions of interest was described as above with the following primer pairs.

Hoxa2_promoter_F: CGCCTGCAGTCATTAACAAA
Hoxa2_promoter_R: TCCCCTCTGCTCCTTTCTC
Hoxa5_promoter_F: CACCCAAATATGGGGTACGA
Hoxa5_promoter_R: CCCCATTAGTGCACGAGTTT
Hoxb5_promoter_F: CAGCCACGGTAATTCTCCAT
Hoxb5_promoter_R: TATTTGAGGCAAAGCCAAGC
Hoxa9_promoter_F: TCACCTCGCCTAGTTTCTGG
Hoxa9_promoter_R: GGAGGGAGGGGAGTAACAAA
Hoxa5_RARE_F: ATTGCATTTCCCTCGCAGTTCC
Hoxa5_RARE_R: GCTGACGGCCTCACAATTGG
NCR_F: ATGCCCTCAGCTATCACAC
NCR_R: GGACAGACATCTGCCAAGGT

2.7. 4C sequencing

2.7.1. 4C template preparation

4C template was prepared as described in (van de Werken et al., 2012) with modifications. Briefly, cells were dissociated (30' @ 37°C in 0.25% trypsin; 1mg/ml collagenase type II; 5mM EDTA). Cells were fixed using 2% formaldehyde/10%FCS/PBS for 10' at RT. Cells were lysed for 10' on ice (50mM Tris-HCl pH 7.5, 150mM NaCl, 5mM EDTA, 0.5% NP40 substitute, 1% Triton-X100, 1X proteinase inhibitors). Chromatin was digested in the context of the nucleus using the restriction enzymes NlaIII, followed by ligation. Ligated chromatin was de-crosslinked in the presence of proteinase K at 65°C O/N and subsequently treated with RNase A. Genomic DNA was extracted by beads purification and subsequently digested O/N using the restriction enzymes Csp6I and ligated under diluted conditions (16°C, O/N) favoring intra-molecular ligations. Genomic DNA was cleaned up using bead purification.

2.7.2. 4C PCR, mapping and analysis of 4C data

The 4C PCR was performed as described in (van de Werken et al., 2012) using the primers below and sequencing was done on the Illumina HiSeq. Reads were mapped, allowing no mismatches, to a database of 4C-seq fragment-ends generated from the mm10/NCBI m38 version of the mouse genome. Interaction profiles shown are produced using all fragments (blind and non-blind) calculating a running mean with a window of 31 fragments. The profiles are normalized to the total amount of reads in cis.

| Primer Name | Primer sequence | Tissue |
|--------------|---------------------------------|-----------|
| Hoxa5_Fw | AAGGATCGAAATAGCTCATG | Cortex WT |
| Hoxa5_Fw_TTG | TTG AAGGATCGAAATAGCTCATG | Cortex RA |
| Hoxa5_Fw_TCA | TCA AAGGATCGAAATAGCTCATG | r8 WT |
| Hoxa5_Fw_GAC | GAC AAGGATCGAAATAGCTCATG | r8 RA |
| Hoxa5_Fw_CTT | CTT AAGGATCGAAATAGCTCATG | r5-6 WT |
| Hoxa5_Fw_AGT | AGT AAGGATCGAAATAGCTCATG | r5-6 RA |
| Hoxa5_Rev | AAACGCACTGAAGCACTACT | |

| | | |
|--------------|---------------------------------|-----------|
| Hoxb5_Fw | AAAGACATTGAAGGAACATG | Cortex WT |
| Hoxb5_Fw_GTA | GT AAAGACATTGAAGGAACATG | Cortex RA |
| Hoxb5_Fw_GAC | GAC AAAGACATTGAAGGAACATG | r8 WT |
| Hoxb5_Fw_CTT | CTT AAAGACATTGAAGGAACATG | r8 RA |
| Hoxb5_Fw_AGT | AGT AAAGACATTGAAGGAACATG | r5-6 WT |
| Hoxb5_Fw_AAG | AAG AAAGACATTGAAGGAACATG | r5-6 RA |
| Hoxb5_Rev | TAGATCCCCAAAGAGACTCA | |

2.8. RNA sequencing

All samples were run in triplicates with three embryos per replicate. 2000 cells per sample were isolated by FACS, directly sorted into lysis buffer and snap frozen to -80°C. RNA was extracted using the PicoPure RNA Isolation Kit (Applied Biosystems) and retro-transcribed. cDNA was amplified from total RNA using the Ovation RNA Amplification System (NuGEN). Libraries were prepared using the Total RNA Sequencing TotalScript Kit (Epicenter) and sequencing was performed using Hi-Seq 2500 Illumina solid sequencer. Data analysis was performed using the Bioconductor QuasR Package (Gaidatzis et al., 2015). The cut-off for low abundant transcripts was set to 1 count per million reads in control samples. Gene Ontology analysis was performed using the GO Enrichment Analysis tool powered by PANTHER (<http://geneontology.org/page/go-enrichment-analysis>).

2.9. Virus and retrograde tracing experiments

EnvA-Rabies-ΔG-mCherry 8 (a kind gift of E. Callaway) viruses were produced in B19G2 and BHK-EnvA2 cells stably expressing the rabies-glycoprotein and viral titers were determined as described elsewhere (Wickersham et al., 2010). Multiple injections per animal were targeted to the cerebellar hemisphere contralateral to the electroporated PN at P2. Mice were sacrificed 5 days later and processed as described.

2.10. Imaging and picture processing

Chromogenic staining was examined by classical wide-field or binocular microscopy (Nikon). Imaging of fluorescent signals was performed using an Axio imager Z2 upright microscope coupled to a LSM700 Zeiss laser scanning confocal 5x (NA 0.25), 10x (NA

0.45), 20x (NA 0.8) or 40x (NA 1.3) lens. Stitching of whole-mounts was performed using Zen software or Xuvtools (<http://www.xuvtools.org>). For 3D reconstructions the whole brain was sliced in 50 μ m sections and imaged with an Axio Scan.Z1 using a 10x (NA 0.45) lens. Regions of interest in consecutive images were aligned using TrakEM2 as incorporated into the Fiji software (<http://fiji.sc/wiki/index.php/Fiji>). Reconstructions were visualized using Bitplane Imaris v8.1. Counting of mossy fiber terminals in the cerebellum and neuronal cell bodies in different regions of the CNS was done with Imaris Spot detection.

2.11. Statistical analysis

Graphs were generated and statistical analysis was done with GraphPad Prism 6 software. All results are presented as the mean \pm S.D. Statistical significance was accepted at the $p < 0.05$ level ($p < 0.05 = *$, $p < 0.01 = **$, $p < 0.001 = ***$). Statistical significance was assessed by nonpaired, two-tailed Student's t test for the comparison of two unmatched groups, ordinary one-way ANOVA followed by Bonferroni's multiple comparisons test for more than two unmatched groups, and by ordinary two-way ANOVA followed by Bonferroni's multiple comparisons test

3. Results

3.1. Antagonistic Wnt and RA signaling results in postmitotic induction of *Hox PG5* in a specific subset of PN neurons

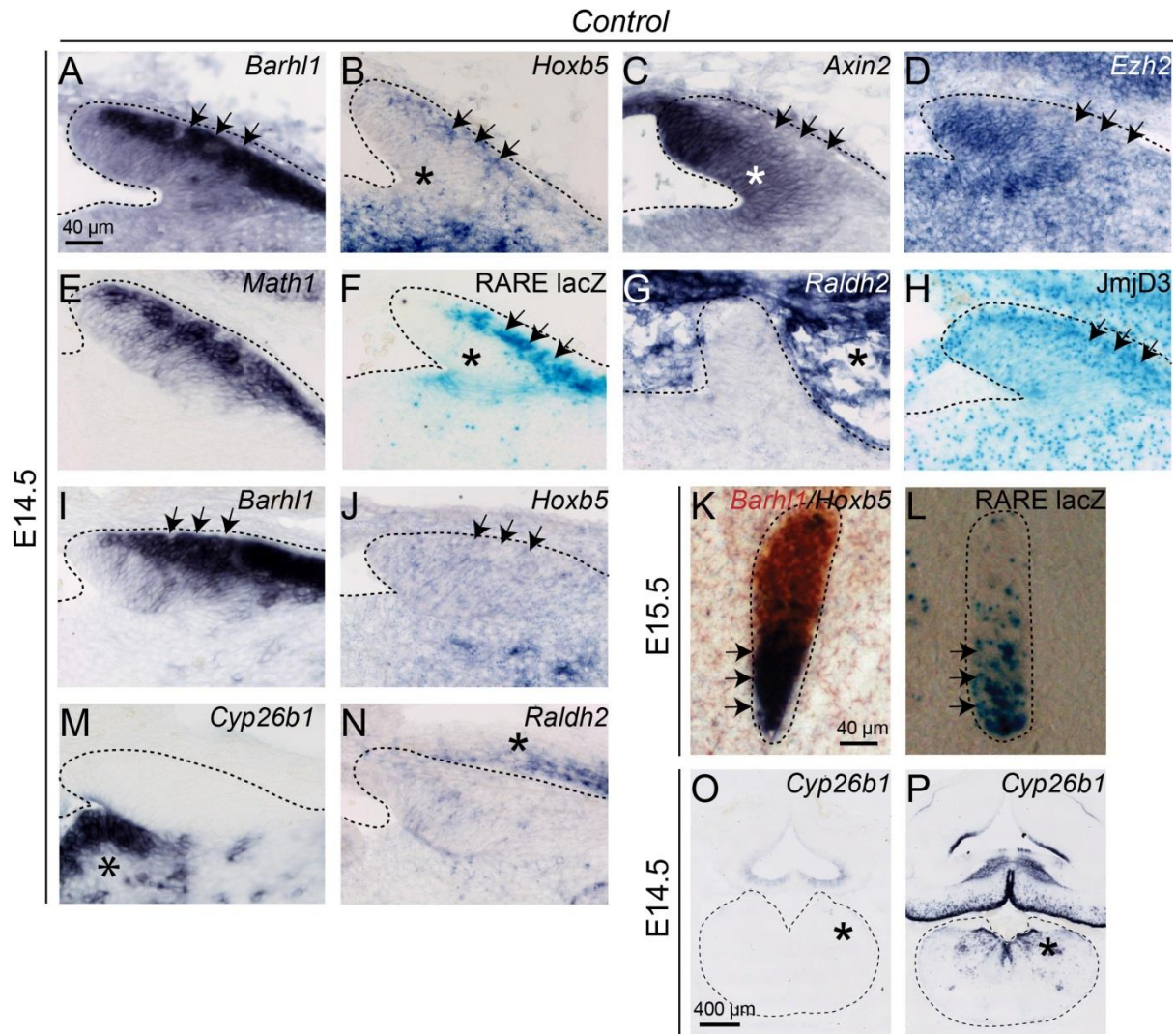


Figure 15: *Hox PG5* genes are induced postmitotically in posterior IRL derived PN neurons

(A-P) E14.5 coronal sections with *in situ* hybridizations using *Barhl1* (A, K), *Hoxb5* (B, J, K), *Axin2* (C), *Ezh2* (D), *Math1* (E), *Raldh2* (G, N), and *Cyp26b1* (M, O, P) probes or β-Gal staining in RARE lacZ (F) and *Jmjd3*^{lacZ/+} embryos. Arrows indicate the induction of *Hoxb5* (B) in *Barhl1*⁺ migrating neurons (A) that coincides with a response to RA signaling (F), upregulation of *Jmjd3* expression (H), diminished Wnt signaling (C), and downregulation of *Ezh2* (D). Asterisk indicated the absence of *Hoxb5* (B) expression and RA signaling (F) from the *Axin2*⁺ (C) progenitor domain. Arrows in I and J show the absence of *Hoxb5* expression in more anterior derived IRL progenies. Arrows in K and L show the correlation between *Hoxb5* expression and RA response in migrating neurons. Asterisks in G and N show the difference in *Raldh2* and M, O and P show the difference in *Cyp26b1* expression along the A-P axis in the hindbrain.

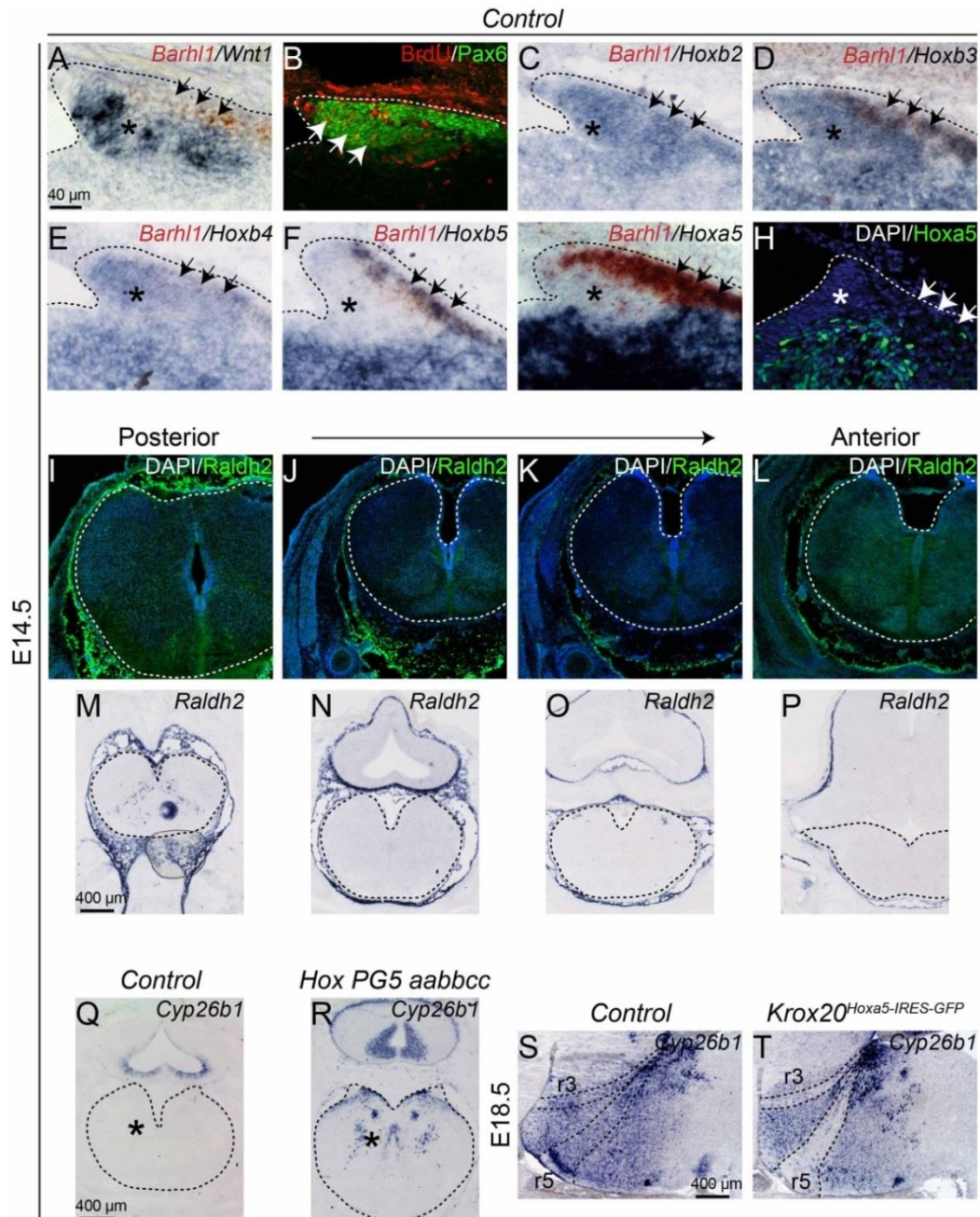


Figure 16: Hox PG2-5 expression pattern in the IRL and expression of RA signaling pathway members in the developing hindbrain

(A-R) E14.5 coronal sections with *in situ* hybridizations using *Barhl1* (A, C, D, E, F, G), *Wnt1* (A), *Hoxb2* (C), *Hoxb3* (D), *Hoxb4* (C), *Hoxb5* (F), *Hoxa5* (G), *Raldh2* (M-P), and *Cyp26b1* (Q-R) probes or immunohistochemistry stainings for BrdU/Pax6 (B), Hoxa5 (H) and Raldh2 (I-L) in wild type embryos. Asterisks indicate the mitotically active Wnt1+ progenitor domain and arrows indicate the onset of migration (A, C-H). *Hoxb2*, *b3* and *b4* (C-E) genes are expressed in both compartments while *Hoxb5* (F) and *a5* (G) as well as Hoxa5 protein (H) are only found in migrating neurons. *Raldh2* expression (M-P) and protein levels (I-L) are graded with high levels in posterior and lower levels in anterior rhombomers. *Cyp26b1* expression is present in r8 only upon *Hox PG5* triple knockout (Q, R). (S, T) E18.5 sagittal sections with *in situ* hybridizations using *Cyp26b1* probes in control and *Krox20^{Hoxa5-IRES-GFP}* embryos. *Cyp26b1* expression is lost in the *Krox20⁺* r3 and r5 domain upon *Hoxa5* overexpression (T).

To assess the spatial and temporal expression pattern of *Hox* genes within the precerebellar system, we carried out *in situ* hybridization on coronal sections through the E14.5 RL. Co-staining for *Wnt1*, a marker for mitotically active IRL progenitors (Rodriguez and Dymecki, 2000) and *Barhl1*, a marker for onset of migration in precerebellar neurons (Bulfone et al., 2000) was performed to distinguish between mitotic and post-mitotic neurons, respectively. *Barhl1* and *Wnt1* showed a mutually exclusive expression pattern in the IRL. Mitotic cells were confined to the *Wnt1*⁺ compartment as shown by BrdU staining (Figure 16A, B). *Hox PG2-4* genes showed an expression pattern with similar levels of expression in both populations (Figures 16C-E). However, *Hox PG5* genes were absent in the *Wnt1*⁺ mitotic cells, and only expressed in the *Barhl1*⁺ migratory cells (Figure 15A, B and 16F-H). The induction of *Hox PG5* expression was confined to the most posterior aspects of the IRL, since no expression could be detected in anterior IRL *Barhl1*⁺ neurons as previously shown (Di Meglio et al., 2013). This indicates a highly specific spatial and temporal regulation of *Hox PG5* expression in a subset of postmitotic PN neurons (Figure 15I, J).

RA dependent signaling pathways are critical for the establishment of *Hox* expression in the hindbrain (Gavalas and Krumlauf, 2000; Vitobello et al., 2011). Therefore we asked whether the expression pattern of *Hox PG5* genes correlates with RA responsiveness. Indeed, endogenous retinoid activity, as visualized by β -gal staining in reporter mice for RA activity (RARE::lacZ) (Rossant et al., 1991), overlaps with the expression of *Hox PG5* genes in the IRL (Figure 15F). Moreover, in the AES we observed a graded response of PN neurons to RA, with high responsiveness to RA in *Hox PG5* positive neurons (ventral AES) and lower responsiveness in *Hox PG5* negative neurons (dorsal AES) (Figure 15K, L). In accordance to the RARE::lacZ pattern in the AES, we found a graded posterior-high to anterior-low expression of *Raldh2* in meninges as detected by *in situ* hybridization and immunohistochemistry (Figure 15G, N and Figure 16I-P) (Zhang et al., 2003). Additionally, the expression of *Cyp26b1*, a RA degrading enzyme (MacLean et al., 2001) was entirely absent from the caudal hindbrain, while high levels were detected in more anterior regions just adjacent to the IRL (Figure 15M, O, P). Interestingly, *Cyp26b1* expression was observed in r8-derived territory of *Hox aabbcc PG5* triple knockout animals (Figure 16Q, R) and was downregulated in anterior rhombomere-derived territories of ectopically expressing *Hoxa5* mice (Figure 16S, T). Thus, *Cyp26b1* is under negative control of *Hox PG5* genes in the hindbrain, suggesting that environmental *Hox PG5* expression contributes to ensuring high levels of RA in caudal hindbrain linking yet another member of the RA pathway to *Hox*

expression (Vitobello et al., 2011). These findings indicate that the postmitotic induction of *Hox PG5* genes critically depend on high local levels of RA. Sufficient levels of RA are only present in the posterior but not anterior parts of the IRL due to differential expression of *Cyp26b1* and *Raldh2*, with *Cyp26b1* expression being negatively regulated by *Hox PG5* genes.

The functional relationship between RA signaling and *Hox PG5* genes was analysed by assessing by the consequences of increased or decreased RA availability. First, by providing exogenous RA through intraperitoneal injections during gestation (60mg/kg at E11.5), we expanded the expression domain of *Hox PG5* to more dorsal parts of the AES as shown by *in situ* hybridization (Figure 17A-F). To quantify the expression of *Hox PG5* genes, we crossed the *Math1::Cre* line (see Methods; Figure 19) with *ROSA26::(lox-stop-lox)tdTomato* (referred to as *Math1^{td-tomato}*) to fluorescently label PN neurons and isolated them by fluorescence activated cell sorting (FACS). A significant increase in the expression levels of *Hox PG5* genes in PN neurons upon RA treatment could be demonstrated by qPCR (Figure 17K). Secondly, *in utero* co-electroporation of GFP together with either a dominant negative retinoic acid receptor (dnRAR) (Damm et al., 1993) or *Cyp26b1* in IRL progenitor cells of E13.5 *RARE::lacZ* embryos decreased RA responsiveness (Figure 18D, E). In accordance, we found a significantly diminished *Hox PG5* expression in electroporated GFP⁺ neurons as shown by *in situ* hybridization at E15.5 (Figures 17G-J) as well as by qPCR on electroporated GFP⁺ neurons isolated by FACS at E18.5 (Figure 17L). Thus, the data strongly suggest that levels of *Hox PG5* genes in PN neurons directly depend on RA availability at the moment they undergo their final division and start tangential migration towards the PN.

The absence of *Hox PG5* expression in the mitotic cells of the IRL led us to hypothesize that Wnt signaling might play an active role in preventing their induction. To test this hypothesis, we globally assessed Wnt signaling by *in situ* hybridization on E14.5 coronal sections for *Axin2*, which is a universal marker for Wnt activity (Jho et al., 2002). *Axin2* expression overlapped with the Wnt1 domain suggesting a strong Wnt activity in progenitor cells, which was greatly reduced as soon as the neurons start to migrate (Figure 15C). Dorsally migrating *Hox PG5* negative cells however maintained low levels of *Axin2* expression suggesting a potential role in keeping *Hox PG5* genes repressed in more anteriorly derived PN subsets (Figure 18F). To understand if active Wnt signaling might prevent *Hox PG5* induction, we did *in utero* co-electroporation to target IRL progenitors with GFP and the chimeric Tcf3vp16

construct, expressing a transcriptional activator of Wnt signaling (Kim et al., 2000). We found high levels of *Axin2* expression in electroporated GFP⁺ neurons in the AES (Figure 18G). However, proliferation was still confined to the IRL progenitor domain with no mitosis detectable in GFP⁺ neurons upon onset of migration (Figure 18H, I). As hypothesized, electroporated GFP⁺ neurons failed to induce significant expression of *Hox PG5* genes as shown by *in situ* hybridization at E15.5 as well as qPCR at E18.5 (Figure 17G, J, M).

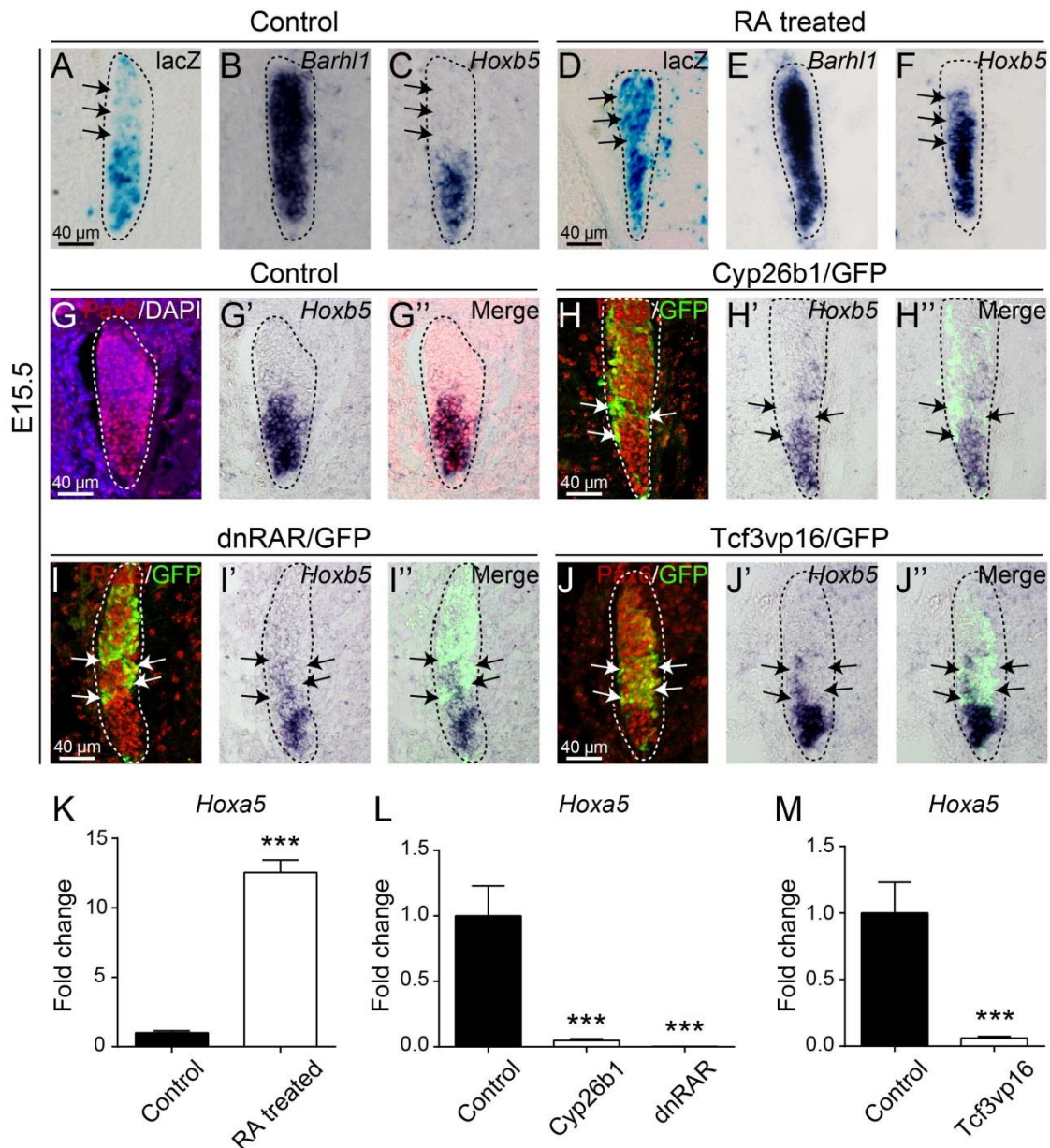


Figure 17: RA and Wnt signaling have antagonistic roles in PN neuron specification (A-F) E15.5 coronal sections of RARE lacZ embryos with β -Gal staining (A,D) or *in situ* hybridizations using *Barhl1* (B,E), and *Hoxb5* (C, F) probes in control (A-C) and RA treated (E11.5, 60 mg/kg) embryos (D-F). Exogenous amounts of RA increase the response of PN neurons in the dorsal aspect of the AES (compare A and D) and induce *Hoxb5* expression (compare C and F). (G-J) E15.5 coronal sections of control (G-G'') and *In utero*

electroporated embryos with Cyp26b1 and GFP (H-H''), dnRAR and GFP (I-I''), and Tcf3vp16 and GFP (J-J'') showing immunohistochemistry for Pax6 and GFP (G-J), *in situ* hybridizations using *Hoxb5* probes (G'-J'), and Merged pictures (G''-J''). Note the absence of *Hoxb5* staining in GFP⁺ neurons in the ventral part of the AES in all three conditions. (K-M) qPCR on PN neurons isolated by FACS from E18.5 control or RA treated *Math1^{tdTomato}* embryos (K) or *in utero* electroporated embryos (L, M). RA treatment significantly increased *Hoxa5* expression (K, n = 3, p < 0.0001) while interference with RA signaling (L, n = 3, p < 0.001) or maintenance of Wnt signaling (M, n = 3, p = 0.0021) significantly decreased *Hoxa5* expression in PN neurons. Data are presented as mean + SD.

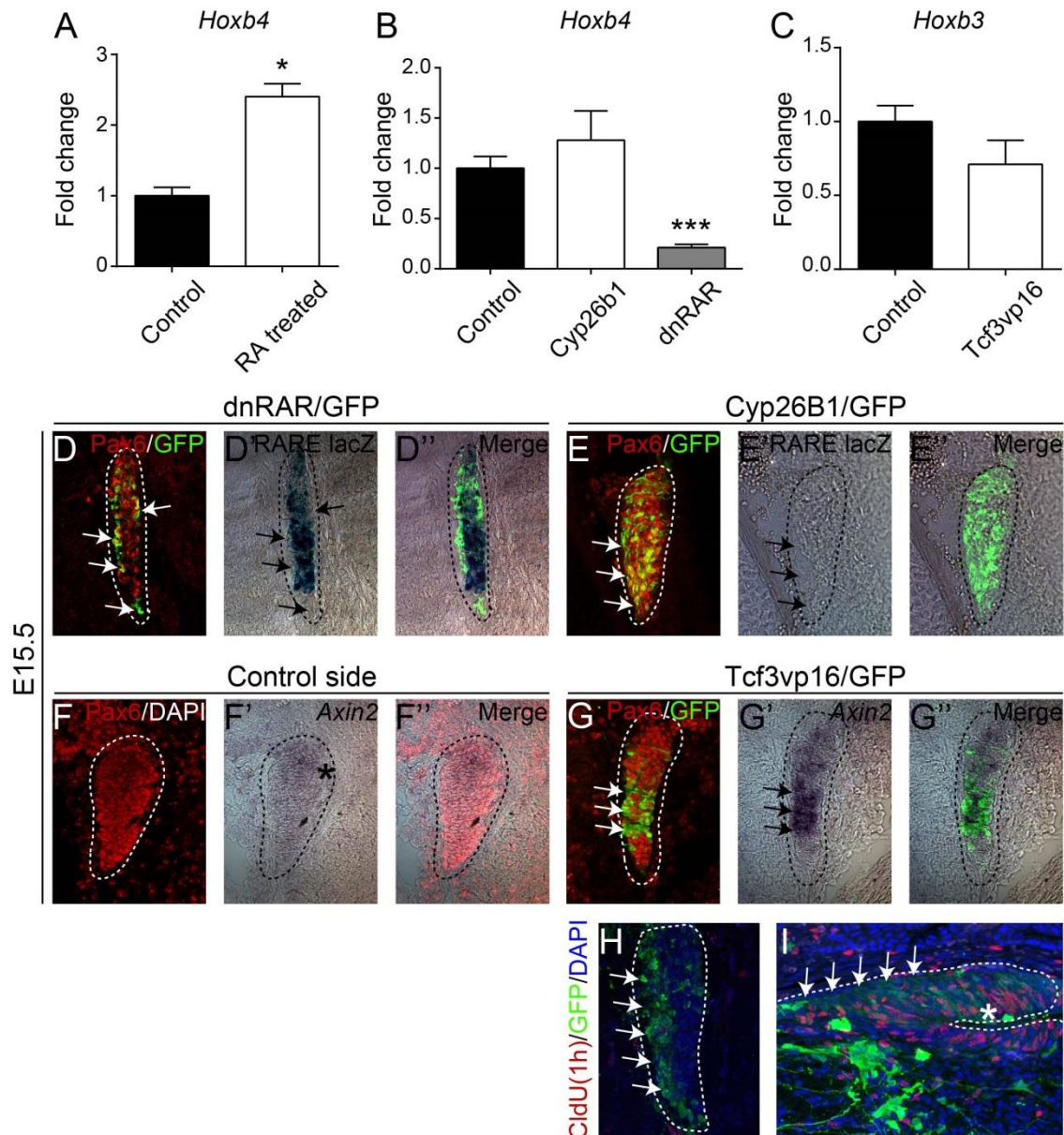


Figure 18: Effects of RA or Wnt signaling manipulation in IRL derived PN neurons by *in utero* electroporation

(A-C) qPCR on PN neurons isolated by FACS from E18.5 control or RA treated *Math1^{tdTomato}* embryos (A) or *in utero* electroporated embryos (B, C). RA treatment (E11.5, 60 mg/kg) significantly increased *Hoxb4* expression (A, n = 3, p = 0.0004). Interference with RA signaling through dnRAR but not Cyp26b1 overexpression leads to a change in *Hoxb4*

expression (B, $n = 3$, $p = 0.2183$ (Cyp26b1); $p = 0.0037$ (dnRAR)). Maintenance of Wnt signaling through Tcf3vp16 overexpression leaves *Hoxb3* expression unaffected in PN neurons (C, $n = 3$, $p = 0.0612$). Data are presented as mean + SD. (D, E) E15.5 coronal sections of *in utero* electroporated *RARE-lacZ* embryos with dnRAR and GFP (D-D'') and Cyp26b1 and GFP (E-E'') showing immunohistochemistry for Pax6 and GFP (D, E), or β -Gal staining (D', E'), and Merged pictures (D'', E''). Note the absence of β -Gal staining in GFP⁺ neurons in the ventral part of the AES in both conditions. (F-I) E15.5 coronal sections of *in utero* electroporated control embryos with Tcf3vp16 and GFP showing immunohistochemistry for Pax6 (F, G), GFP (G, H, I) and CldU (, H, I), or *in situ* hybridization using *Axin2* probes (F', G'), and Merged pictures (F'', G''). Note the absence low level of *Axin2* expression in dorsally migrating PN neurons (Asterisks in F'). Maintenance of Wnt signaling through Tcf3vp16 overexpression leads to high levels of *Axin2* expression in the AES (Arrows in G-G'') but no proliferation in migrating neurons (Arrows in H, I). Data are presented as mean + SD.

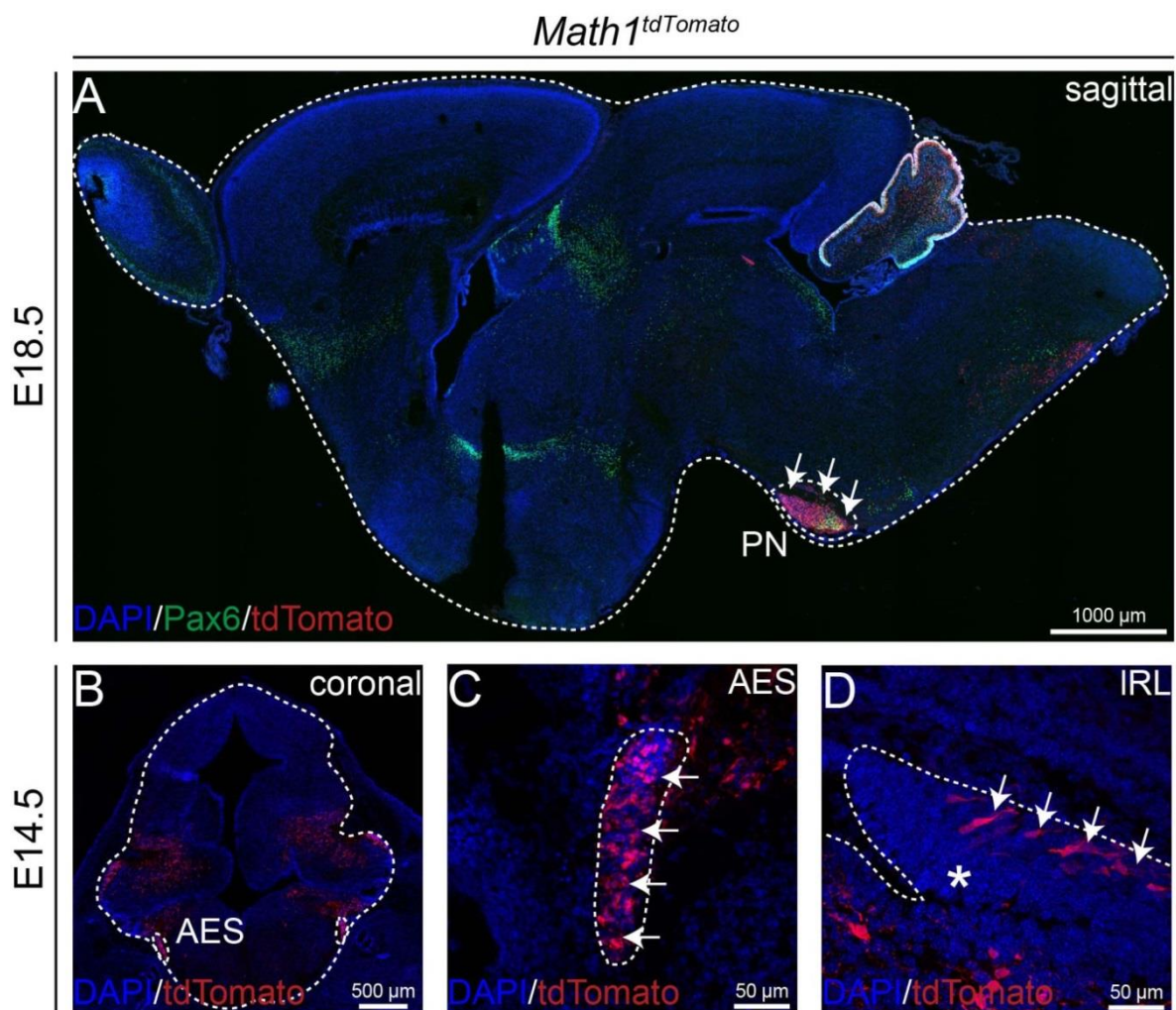


Figure 19: Generation and characterization of *Math1::Cre* transgenic mouse line

(A) Sagittal section through an E18.5 *Math1*^{tdTomato} embryo with immunohistochemistry for Pax6 showing specific labeling of RL derived neuronal populations including PN, cerebellum and other precerebellar nuclei. (B-D) Coronal section through an E14.5 *Math1*^{tdTomato} embryo showing specific labeling of RL derived neuronal populations (B), tdTomato positive cells in the AES (C) and Cre activity selectively in postmitotic migratory PN neurons (D).

In summary, we show that Wnt signaling maintains repression of *Hox PG5* genes in mitotically active IRL progenitors and it is likely to contribute to the repression in dorsally migrating PN neurons. RA signaling, on the other hand, is required to induce *Hox PG5* expression at the onset of migration in a specific subset of caudal PN postmitotic neurons. Only high levels of RA are capable of overcoming the repression, which is only given in the posterior IRL. Consequently, the antagonistic effect of Wnt and RA induce cellular heterogeneity within the migratory stream of PN neurons by regulating *Hox PG5* induction in postmitotic PN cells.

3.2. Depletion of Polycomb-dependent H3K27me3 repressive mark is necessary but not sufficient for *Hox PG5* expression in the precerebellar system

Hox PG5 genes show spatially and temporally restricted expression patterns in PN neurons. PRC2 has already been shown to be fundamental for maintaining *Hox PG5* genes silent in the anteriorly derived IRL postmitotic progenies (Di Meglio et al., 2013). Hence, we hypothesized a similar role for PRC2 in keeping the balance between maintenance of the repression in IRL progenitors and the RA mediated onset of expression in posteriorly derived PN neurons. High levels of H3K27me3 are thought to be associated with silent gene loci (Margueron and Reinberg, 2011). To test if H3K27me3 levels are similarly correlated to Hox gene expression in the developing hindbrain we performed ChIP-qPCR for H3K27me3 on *Hox PG5* negative (r5-6-derived) and positive domains (r8-derived). We found high levels of H3K27me3 in *Hox PG5* negative domains and markedly reduced levels in *Hox PG5* positive regions at the *Hoxa5* and *Hoxb5* promoters (Figure 21A,C). Enrichment of H3K4me3, a mark generally correlated with active gene expression (Heintzman et al., 2009), was distributed complementary to H3K27me3 (Figure 21D). Control genes which are expressed or repressed in both domains showed no regulation of H3K27me3 and H3K4me4 levels. We then asked, if RA treatment would reverse the H3K27me3/H3K4me3 ratio in the r5-6 domain as suggested by experiments done in ES cells (De Kumar et al., 2015; Kashyap et al., 2011). Indeed, RA treatment (60 mg/kg at E9.5) not only induced *Hox PG5* expression within the r5-6 domain but also led to a depletion of H3K27me3 and a gain of H3K4me3 at the *Hox PG5* promoter regions (Figure 21B-D). These findings further indicate that induction of *Hox PG5* genes through RA is tightly linked to depletion of H3K27me3, as previously suggested (Kashyap et al., 2011). As a consequence, we reasoned that we could induce premature expression of *Hox*

PG5 genes by removal of H3K27me3 in IRL progenitor cells through the conditional inactivation of *Ezh2*, the catalytic subunit of the PRC2 complex (Margueron and Reinberg, 2011). Expression analysis of *Ezh2* in the E14.5 IRL further supported this idea as the levels of *Ezh2* were high in the progenitors and reduced at the onset of migration (Figure 15D). To generate conditional *Ezh2* knockouts (cKO) in the IRL, we crossed *Wnt1::Cre* mice with a floxed *Ezh2* allele (referred to as *Wnt1^{Ezh2cKO}*) (Puschendorf et al., 2008), resulting in a specific depletion of *Ezh2* and thus the H3K27me3 mark from early stages on throughout the IRL (Di Meglio et al., 2013). Surprisingly, *Ezh2* deletion did not result in the anticipated upregulation of *Hox PG5* genes in the *Axin2*⁺ progenitor domain (Figure 20A-C, F-H). Yet, the levels of *Hox PG5* genes at the onset of migration appeared upregulated, as compared to control animals indicating an increased sensitivity of *Ezh2* depleted neurons to endogenous RA. Furthermore, *Hox PG5* expression was observed at the onset of migration throughout the antero-posterior axis in *Wnt1^{Ezh2cKO}* animals, though still maintaining higher levels of expression in the posterior IRL derivatives (Figure 20D, E, I, J) (Di Meglio et al., 2013).

To further support that indeed H3K27me3 depletion is a key prerequisite for high levels of *Hox PG5* expression, we assessed *Hox PG5* expression in a *Jmjd3* knockout line. To generate this line we used a construct carrying an in-frame knock-in of the lacZ reporter gene substituting large parts of *Jmjd3* (referred to as *Jmjd3^{lacZ/lacZ}*) (Figure 22A-C). *Jmjd3* is one of two described H3K27 specific demethylases (Agger et al., 2007; De Santa et al., 2007; Lan et al., 2007; Lee et al., 2007). Loss of *Jmjd3* results in perinatal lethality (Burgold et al., 2012). Transcriptional activation of the *Jmjd3* locus (visualized by β -gal staining) in heterozygote mice (*Jmjd3^{+lacZ}*) was elevated at the onset of migration in the IRL coinciding with the RA mediated *Hox PG5* induction (Figure 15H). The targeted deletion of *Jmjd3* did not affect overall PN formation (Figure 22D, I, N, O). Nonetheless, as hypothesized, *in situ* hybridization for *Hoxa5* and *Hoxb5* in *Jmjd3^{lacZ/lacZ}* mice did not show any signal in postmitotic (*Barhl1*⁺) precerebellar neurons in the posterior IRL, suggesting that *Jmjd3* is indeed necessary for postmitotic *Hox PG5* upregulation (Figure 20K, L and Figure 22M, H). Furthermore, we observed a prolonged *Axin2* expression in the IRL with substantial overlap between *Barhl1* and *Axin2* staining in the initial phase of migration (Figure 20M). Flippase-mediated removal of the lacZ expression cassette in *Jmjd3^{+lacZ}* mice (referred to as *Jmjd3^{+/-}*; see Material and Methods, Figure 22B) and crossing to *RARE::lacZ* allowed for monitoring of the endogenous response of PN neurons to RA. Strikingly, in *Jmjd3^{-/-} RARE::lacZ* mice, the RA response was markedly diminished in the early phase of migration and increased RA

response was observed only after the downregulation of *Axin2* in PN neurons as visualized by β -gal staining (Figure 20N, O). Normal expression of *Raldh2* and *Cyp26b1* ruled out the possibility of changes in the levels of RA synthesis or degradation in *Jmjd3^{lacZ/lacZ}* mice (Figure 22E-G, J-L). This indicates that differentiation of IRL neurons is delayed upon *Jmjd3* knockout and a strong response to RA signaling can only be achieved upon completion of cell fate transition.

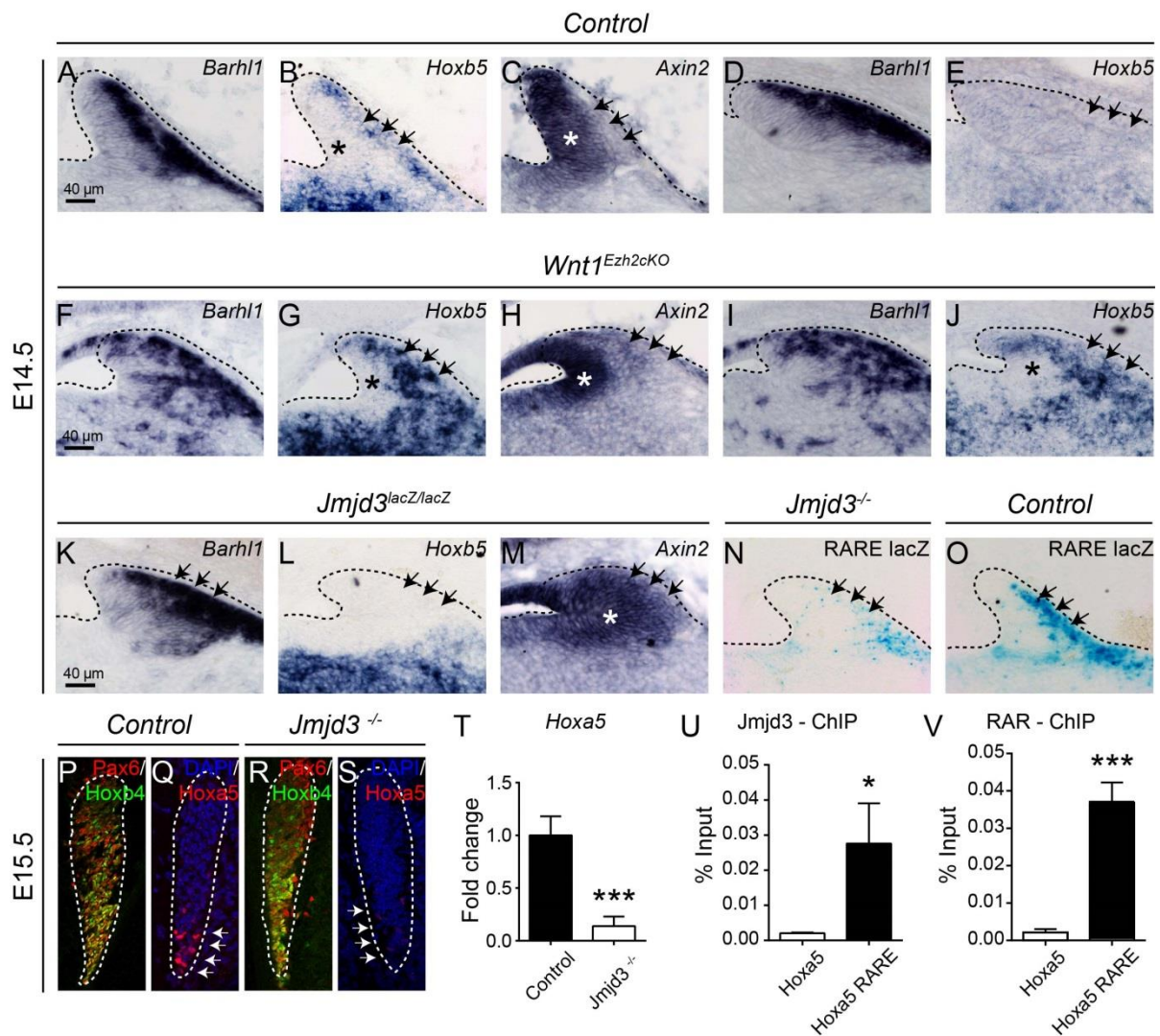


Figure 20: Roles of Ezh2 and Jmjd3 in the regulation of Hox PG5 expression (A-O) E14.5 coronal sections of control (A-E, O), *Wnt1^{Ezh2cKO}* (F-J), *Jmjd3^{lacZ/lacZ}* (K-M), or *Jmjd3^{-/-}* (N) embryos. Shown are *in situ* hybridizations using *Barhl1* (A, D, F, I, K), *Hoxb5* (B, E, G, J, L), and *Axin2* (C, H, M) probes or β -Gal staining for RARE lacZ (N, O). Note the absence of *Hoxb5* expression in the *Axin2*⁺ domain in *Wnt1^{Ezh2cKO}* embryos (Asterisks in G, H, J) as well as in *Barhl1*⁺ neurons in the *Jmjd3^{lacZ/lacZ}* embryos (arrows in K, L) but presence of *Hoxb5* expression in more anterior derived IRL progenies in *Wnt1^{Ezh2cKO}* embryos (Arrows in E, J). *Axin2* expression is prolonged in the IRL of *Jmjd3^{lacZ/lacZ}* embryos (arrows in C, M) and RA response is absent in initial phase of migration in *Jmjd3^{-/-}* embryos (compare N and O). (P-S) Immunohistochemistry for Pax6 and Hoxb4 (P, R) or Hoxa5 (Q, S) on E15.5 coronal sections of control (P, Q) or *Jmjd3^{-/-}* (R, S) embryos showing decreased levels of Hoxa5 protein in the AES of *Jmjd3^{-/-}* embryos (arrows in Q, S). (T) qPCR on PN neurons

isolated by FACS from E18.5 *Math1^{tdTomato} Jmjd3^{-/-}* embryos showing significantly reduced levels of *Hoxa5* ($n = 3$, $p < 0.001$). (U, V) ChIP analysis of *Jmjd3* (U) and retinoic acid receptor (RAR, V) binding to a *Hoxa5* associated RARE and the *Hoxa5* promoter carried out on micro-dissected E14.5 hindbrain tissue. *Jmjd3* (U, $n = 3$, $p = 0.0184$) and RAR (V, $n = 3$, $p = 0.0005$) bind specifically to the *Hoxa5* RARE but not *Hoxa5* promoter. Data are presented as mean + SD.

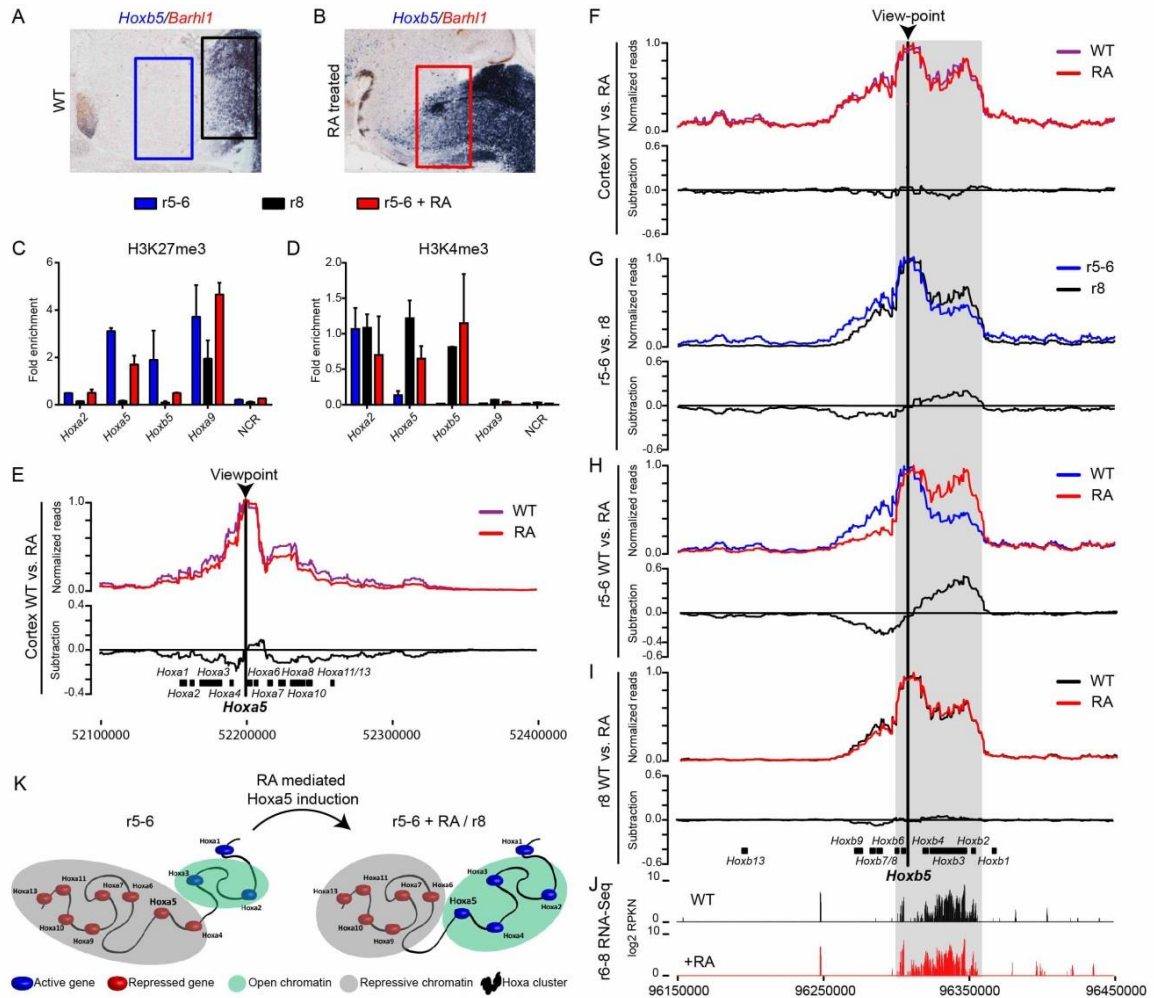


Figure 21: Epigenetic and higher order chromatin conformational changes upon RA induced onset of *Hox PG5* expression *in vivo*

(A, B) E18.5 sagittal sections with *in situ* hybridizations using *Barhl1* and *Hoxb5* probes in control (A) and RA treated embryos (B, E9.5, 60 mg/kg). Exogenous amounts of RA induce *Hoxb5* expression in previously *Hoxb5* negative rhombomers (compare blue box in A to red box in B). (C, D) ChIP analysis of H3K27me3 (C) and H3K4me3 (D) levels at different *Hox* promoter and a NCR carried out on micro-dissected E14.5 r5-6, r8, and r5-6 with RA treatment (E9.5, 60 mg/kg) hindbrain tissue. High levels of H3K27me3 and low levels of H3K4me3 are associated with transcriptionally repressed genes (*Hoxa5*, *Hoxb5* and *Hoxa9*) and vice versa (*Hoxa2*) in r5-6. Expression of *Hoxa5* and *Hoxb5* in r8 is correlated with a strong decrease in H3K27me3 and increase in H3K4me3 levels at the respective promoters in r8 as compared to r5-6. RA treatment photocopies these changes in H3K27me3 and H3K4me3 levels at *Hoxa5* and *Hoxb5* but not *Hoxa9* genes in r5-6 as compared to the control situation. Data are presented as mean + SD. (E-I) Contact profiles of cc, r5-6 and r8 populations looking from the *Hoxa5* promoter as a viewpoint (arrow head) within a 400kB window spanning the *Hoxa* (E) and *Hoxb* (F) cluster at E14.5 with or without RA treatment

(E9.5, 60 mg/kg). The subtractions of the respective comparisons are depicted below the traces with the normalized reads. *Hoxa* as well as the *Hoxb* clusters are organized as one large association domain, correlating with the silent state of all the genes in the cluster (E, F). The change in frequencies of associations of the *Hoxb5* promoter with the active or passive domains between r5-6 and r8 derived samples shows the bimodal state of the *Hoxb* cluster in the hindbrain (C). Exogenous amounts of RA leads to a reorganization of the chromatin conformation *in vivo* at the *Hoxb5* locus in r5-6 (H) but not in cc or r8 derived samples (F, I) and *Hoxa5* locus in cc (E). (J) RNA-seq profile of the *Hoxb* cluster in r6-8 derived neurons with or without RA treatment (E11.5, 60 mg/kg). The gray box shows the active domain found in r8 derived neurons. (K) Model of the RA mediated chromatin reorganisation of the *Hoxa* cluster *in vivo*.

Based on these results we could not rule out whether the lack of *Hox PG5* expression is due to a direct effect of *Jmjd3* at the *Hoxa5* and *Hoxb5* loci or due to a delay in cell fate transition. Therefore, we analyzed the expression levels of *Hox PG5* genes in *Jmjd3*^{-/-} mice during migration and nucleation in the PN. Notably, a strongly reduced level of *Hoxa5* protein was observed in the AES by immunohistochemistry while *Hoxb4* protein levels appeared unchanged (Figure 20M-P and Figure 22Q). Moreover, qPCR on PN neurons isolated by FACS from E18.5 *Math1*^{tdTomato} *Jmjd3*^{-/-} mice showed significantly reduced *Hoxa5* expression levels while *Hoxb4* and *Hoxb3* levels were unchanged (Figure 20Q and Figure 22P-Q). To demonstrate that *Jmjd3* mediates such transcriptional effects on *Hox PG5* genes directly, we examined *Jmjd3* binding to a *Hoxa5* associated RARE *in vivo* by ChIP-qPCR (Mahony et al., 2011a). We confirmed co-binding of *Jmjd3* and RA receptors at a *Hoxa5* associated RARE indicating a direct involvement of *Jmjd3* in H3K27me3 demethylation at the *Hoxa5* locus (Figure 20R, S).

Taken together, these results demonstrate the necessity of *Jmjd3* for efficient transcription of *Hox PG5* genes, most likely due to its H3K27me3 demethylase capability to overcome H3K27me3 mediated repression. However, the removal of the H3K27me3 mark alone does not result in *Hox PG5* expression, which still requires appropriate environmental conditions (i.e. reduction of Wnt signaling and increased response to presence of RA signaling).

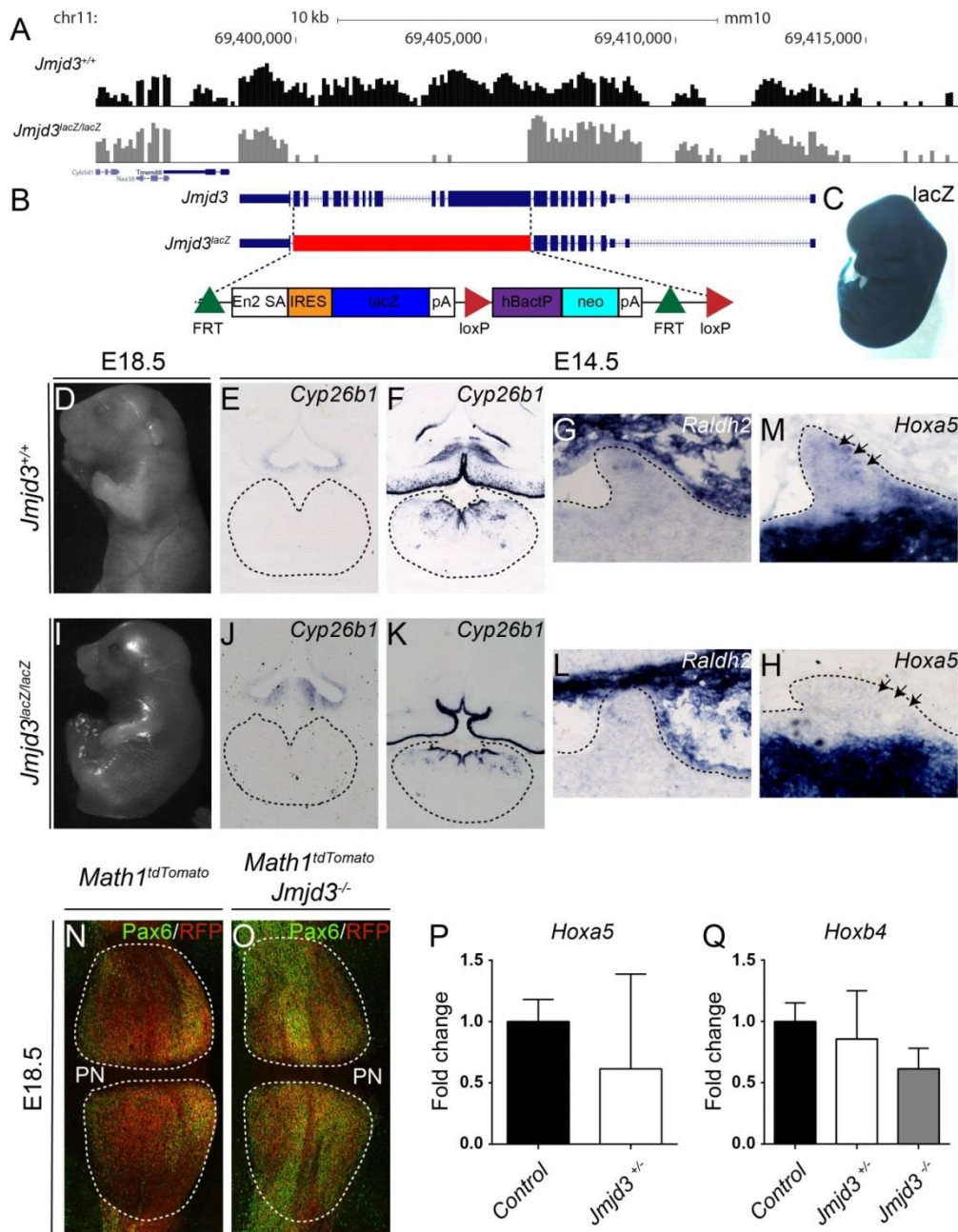


Figure 22: Generation and characterization of *Jmjd3* knock-in mice

(A) RNA-seq profiles of the *Jmjd3* gene in control and *Jmjd3*^{lacZ/lacZ} embryos confirming the deletion of Exons 2-13. (B) Schematic drawing of the construct used for generation of *Jmjd3*^{lacZ} mice. (D, I) Whole mount images of E18.5 control and *Jmjd3*^{lacZ/lacZ} embryos. (E-M, J-H) E14.5 coronal sections with *in situ* hybridizations using *Cyp26b1* (E, F, J, K), *Raldh2* (G, L) and *Hoxa5* (M, H) probes in control and *Jmjd3*^{lacZ/lacZ} embryos. No change in *Cyp26b1* (E, F, J, K) or *Raldh2* (G, L) expression was observed upon *Jmjd3* KO but no *Hoxa5* (Arrows in M, H) expression was evident at the onset of migration. (N, O) Whole mount images of E18.5 *Math1*^{tdTomato} and *Math1*^{tdTomato} *Jmjd3*^{-/-} embryos with immunohistochemistry for Pax6 showing normal PN neuron migration and nucleation. (P, Q) qPCR on PN neurons isolated by FACS from E18.5 *Math1*^{tdTomato}, *Math1*^{tdTomato} *Jmjd3*^{+/+} or *Math1*^{tdTomato} *Jmjd3*^{-/-} embryos. *Hoxa5* levels were unchanged in *Math1*^{tdTomato} *Jmjd3*^{+/+} embryos (P, n = 3, p = 0.4286) and *Hoxb4* levels were unchanged in both *Math1*^{tdTomato} *Jmjd3*^{+/+} and *Math1*^{tdTomato} *Jmjd3*^{-/-} embryos (O, n = 3, p = 0.999 (*Jmjd3*^{+/+}), p = 0.3002 (*Jmjd3*^{-/-})). Data are presented as mean + SD.

3.3. Three Dimensional (3D) conformational change of chromatin organization upon RA mediated *Hox PG5* induction

Changes in the transcriptional status of developmentally regulated genes, including Hox genes, go along with changes in the chromatin organisation as shown in cultured cells as well as in the developing embryo (Chambeyron and Bickmore, 2004; Ferraiuolo et al., 2010; Noordermeer et al., 2011; Palstra et al., 2003; Patel et al., 2013). The signals that affect the 3D structure of the genome are less understood. The tight regulation of *Hox PG5* genes by RA might be accompanied by the physical separation of active and inactive Hox genes in the r5-6-derived and r8-derived domains in the hindbrain. To examine the role of RA on higher order chromatin conformation, we employed 4C-Seq (van de Werken et al., 2012). We performed 4C-seq on *Hox PG5* negative (r5-6-derived) and positive domains (r8-derived) at E14.5, using the *Hoxa5* (Figure 23) and *Hoxb5* (Figure 21) promoters as view-points. 4C-seq was also performed with cerebral cortex (CC), used as an entirely Hox negative control tissue. In the CC both the *Hoxa* and the *Hoxb* clusters organized as one large association domain (Figure 21E, F), correlating with the silent state of the gene clusters. In contrast, a bimodal transcriptional state correlated with the segregation of both Hox clusters into distinct 3D domains (Figure 23A, D and Figure 21G, J). Depending on their transcriptional state, *Hox PG5* genes were included either in an inactive (r5-6-derived) or active association domain (r8-derived). We reasoned that the endogenous source of RA could be responsible for setting the bimodal state of the *Hox PG5* genes comparing the r5-6- to the r8-derived domain. To test this, we used exogenous RA treatment (60mg/kg at E9.5) to induce *Hox PG5* genes in the *Hox PG5* negative r5-6-derived domain. Indeed, upon induction of *Hox PG5* gene expression by RA, the *Hoxa5* gene was included in an active chromatin domain encompassing *Hox PG2-5* (Figure 23B and Figure 21H). In contrast, RA treatment did not result in topological changes in the Hox negative CC, nor in the *Hox PG2-5* positive r8-derived domain (Figure 23C and Figure 21E, F, I). Thus, RA is capable of reorganizing chromatin conformation in vivo at *Hox PG5* loci in a context dependent manner (Figure 21K).

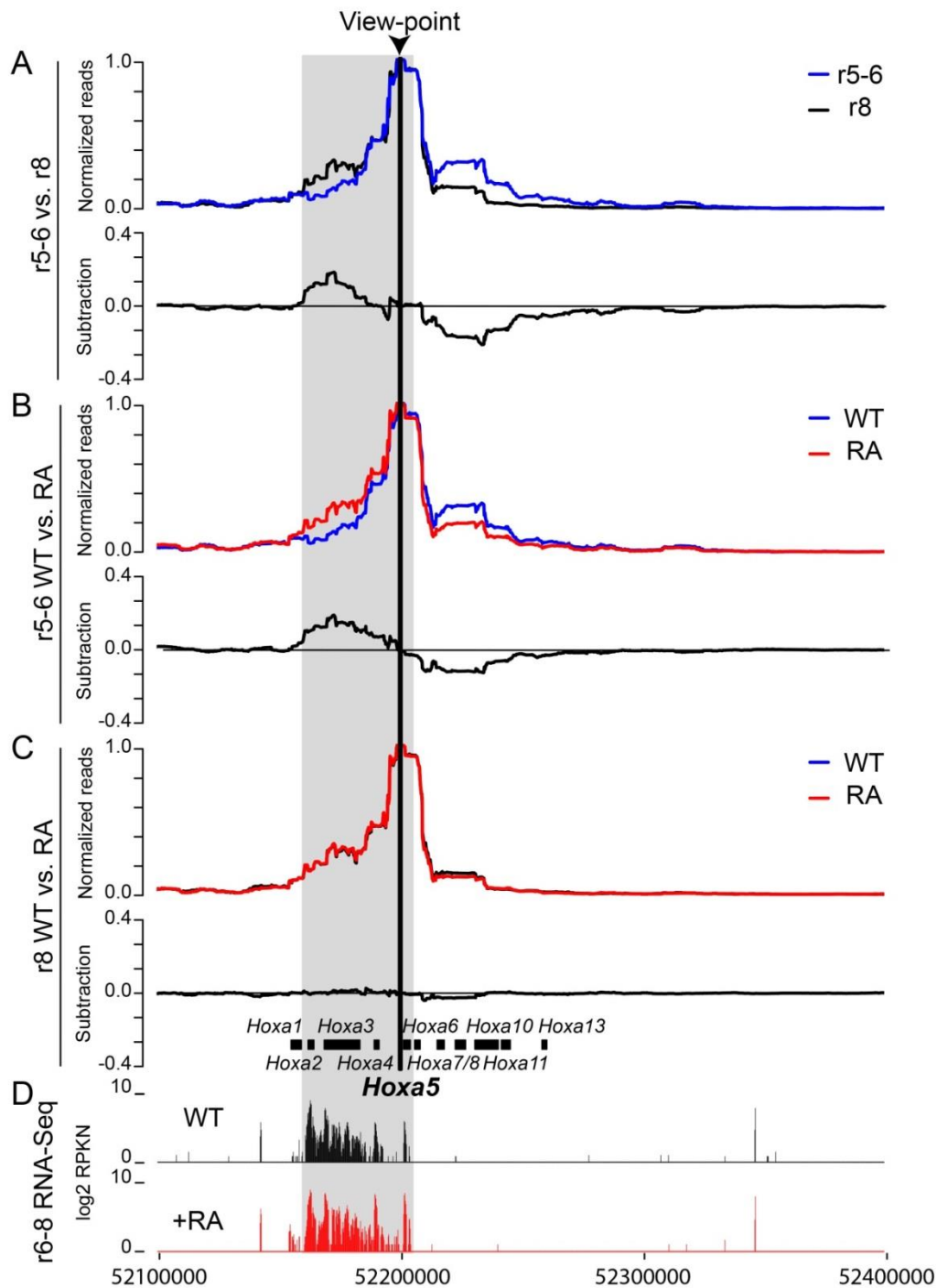


Figure 23: 4C-seq profiles reveal that RA signaling is instructive for inactive and active domain association of *Hox PG5* genes

(A-C) Contact profiles of r5-6 and r8 populations looking from the *Hoxa5* promoter as a viewpoint (arrow head) within a 400kB window spanning the *Hoxa* cluster at E14.5 with or without RA treatment (E9.5, 60 mg/kg). The subtractions of the respective comparisons are depicted below the traces with the normalized reads. The change in frequencies of associations of the *Hoxa5* promoter with the active or passive domains between r5-6 and r8 derived samples shows the bimodal state of the *Hoxa* cluster in the hindbrain (A). Exogenous amounts of RA leads to a reorganization of the chromatin conformation *in vivo* at the *Hoxa5* locus in r5-6 (B) but not r8 derived samples (C). (D) RNA-seq profile of the *Hoxa* cluster in r6-8 derived neurons with or without RA treatment (E11.5, 60 mg/kg). The gray box shows the active domain found in r8 derived neurons.

3.4. *Hoxa5* expression is sufficient to drive neurons into a posterior position in the PN

So far, the presented experiments show that the spatial expression pattern of *Hox PG5* genes in a subset of PN postmitotic neurons is tightly regulated through complex interactions between signaling pathways and chromatin modifying enzymes. In an effort to understand the implications for the developing PN and its circuitry, we attempted to address the functional role of *Hox PG5* expression in PN neurons subsets. Due to the maintenance of relative rostro-caudal position of PN neurons throughout migration and in the target nuclei it has been suggested that the expression of *Hox PG5* genes influences the migration pattern of PN neurons (Figure 24H) (Di Meglio et al., 2013). However, direct evidence of whether positioning in the PN is dependent on Hox expression is still lacking. To assess the direct role of *Hox PG5* genes in positioning neurons in the PN, we generated a conditional *Hoxa5* overexpression mouse line by the knock-in of a CAG(lox-stop-lox)3xFlag-Hoxa5-internal ribosome entry site (IRES)-GFP expression cassette into the ROSA26 locus (*ROSA26::CAG(lox-stop-lox)3xFlag-Hoxa5-IRES-GFP*). When crossing this transgenic line to the *Math1::Cre* driver (together referred to as *Math1^{Hoxa5-IRES-GFP}*), we observed both GFP and Hoxa5 protein in PN neurons (Figure 24C-E). Levels of ectopic Hoxa5 protein detected by immunohistochemistry in PN neurons were comparable to endogenous Hoxa5 levels (Figure 24E). Notably, no fluorescently labeled cells were found at any stage in the IRL progenitor domain showing selective Cre expression in postmitotic precerebellar neurons (Figure 19D). In control *Math1^{tdTomato}* mice at postnatal day 0 (P0), PN were homogenously labeled by tdTomato⁺ cells throughout (Figure 24A, B). In contrast, *Math1^{Hoxa5-IRES-GFP}* PN lacked GFP⁺ neurons in the most anterior aspects in lateral sections and a more pronounced bias to the posterior parts in medial sections (Figure 24C, D). The number of *Hoxa5* overexpressing neurons was significantly higher in the posterior half of the PN, while in control new-borns neurons were found equally distributed (Figure 24C,D,G,H) without affecting overall cell number (Figure 24F). We can therefore directly link *Hoxa5* expression to positioning of cells in the PN.

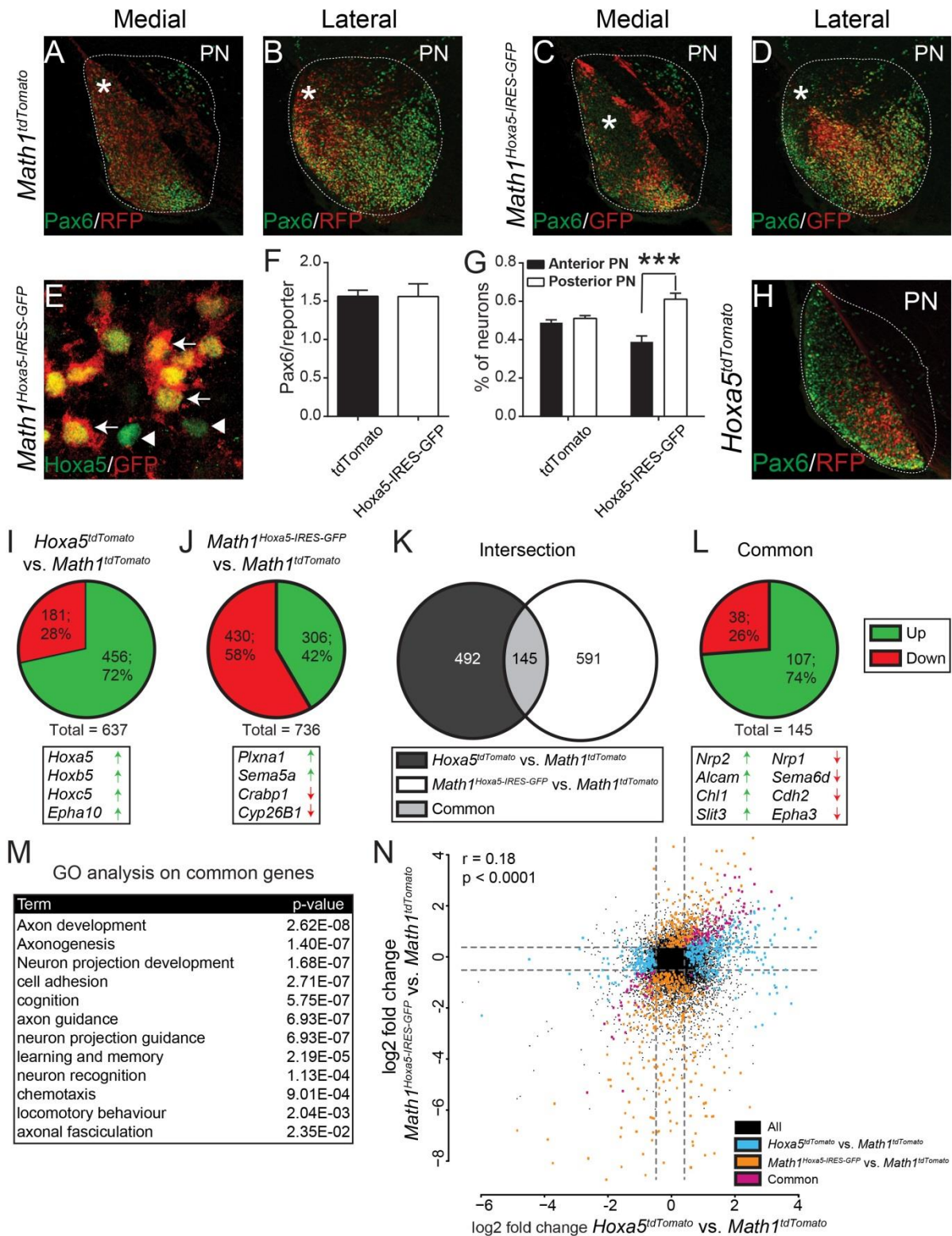


Figure 24: Posterior positioning and transcriptional program of *Hoxa5* expressing PN neurons

(A-E) PN with Pax6/RFP signals from *Math1^{tdTomato}* embryos (A, B) and Pax6/GFP (C, D) or *Hoxa5*/GFP (E) signals from *Math1^{Hoxa5-IRES-GFP}* embryos at P0. Pax6, *Hoxa5* and GFP are detected by immunostaining, RFP by direct fluorescence. Note the homogenous distribution of RFP⁺ PN neurons in *Math1^{tdTomato}* embryos and the lack of GFP⁺ PN neurons in the anterior aspects in *Math1^{Hoxa5-IRES-GFP}* embryos (Asterisks in A-D). Protein levels between

ectopically *Hoxa5* overexpressing and endogenously expressing PN neurons are comparable (Arrows and arrowheads in E). (F, G) Quantification of fluorescently labeled neurons showing no difference in overall cell number (F, $n = 4$) but a significant bias of GFP⁺ PN neurons in *Math1*^{*Hoxa5*-IRES-GFP} embryos at E18.5 to the posterior which is not observed in RFP⁺ PN neurons of *Math1*^{*tdTomato*} embryos (G, $n = 4$, $p < 0.0001$). (H) *Hoxa5*^{*tdTomato*} Pax6/RFP signals showing the bias of HoxPG5 positive PN neurons to the posterior at P0. (H, I & L) Pie charts showing genes regulated in *Hox PG5* positive PN neurons (I), *Hoxa5* overexpressing PN neurons (J), as well as commonly regulated genes (L) as assessed by RNA-seq at E18.5 after isolation of PN neurons from *Math1*^{*tdTomato*}, *Hoxa5*^{*tdTomato*}, and *Math1*^{*Hoxa5*-IRES-GFP} embryos by FACS (FC > 1.5; FDR < 0.07). Examples of genes and their regulation are in the boxes below the respective pie charts. (K) Venn diagram showing the intersection between the *Hoxa5*^{*tdTomato*} vs. *Math1*^{*tdTomato*} and *Math1*^{*Hoxa5*-IRES-GFP} vs. *Math1*^{*tdTomato*} comparisons. (M) Gene Ontology analysis of commonly regulated genes showing enrichment of genes important for processes involved in topographic circuit formation. (N) Scatter plot showing a significant correlation between the *Hoxa5*^{*tdTomato*} vs. *Math1*^{*tdTomato*} and *Math1*^{*Hoxa5*-IRES-GFP} vs. *Math1*^{*tdTomato*} comparisons ($r = 0.19$; R squared = 0.036; $p < 0.0001$). Data are presented as mean + SD.

3.5. PN neuron subpopulations have distinct, Hox dependent transcriptional programs

Topographic circuit formation requires patterned expression of chemotropically active molecules as well as differential expression of axon guidance molecules. We carried out RNA-sequencing experiments on different subsets of PN neurons followed by comparative transcriptome analysis to identify genes potentially involved in controlling PN circuit formation and regulated by *Hox PG5* genes. We did this by micro-dissection of PN from *Math1*^{*tdTomato*} mice followed by FACS. Similar isolation of PN neurons from *Hoxa5::Cre* mice (Di Meglio et al., 2013) crossed to *ROSA26::(lox-stop-lox)tdTomato* (referred to as *Hoxa5*^{*tdTomato*}) mice provided neurons enriched in the *Hox PG5* positive subset. PN dissection and FACS was carried out at E18.5, a stage when migration and nucleation of the PN is largely completed. We extracted RNA from the isolated neurons and compared the sequencing data from both data sets. We identified 637 differentially expressed genes (FC > 1.5; FDR < 0.07) amongst which 456 (72%) were up- and 181 (28%) were downregulated in *Hoxa5*^{*tdTomato*} positive PN neurons (Figure 24I). As expected, *Hoxa5*, *Hoxb5* and *Hoxc5* were enriched in the *Hoxa5*^{*tdTomato*} samples. Additionally, we found significant differences in the expression of a broad range of axon guidance molecules or their receptors and other molecules potentially used by growth cones to navigate properly such as NGFs, FGFs and Wnts (Kolodkin and Tessier-Lavigne, 2011). To validate our approach, we performed *in situ* hybridization on selected target genes (Figure 25A-P) as well as screened the Allen Mouse Brain Atlas (Lein et al., 2007) (<http://mouse.brain-map.org>) and Allen Developing Mouse

Brain Atlas (<http://developingmouse.brain-map.org>) (Figure 25F-J). Most genes examined, including *Nrp2*, *Nrp1*, *Robo3*, *Chl1*, *Alcam*, *Clb1*, *Cdhr1*, *Ephb1*, *Sox11*, *Epha3*, *Pcdh19*, *Cdh23*, *Robo2*, *Peg10* and *Lmo3* showed a rostro-caudally graded expression strongly supporting our experimental approach to uncover molecular gradients within the PN.

Even though the observed differences between *Math1*^{tdTomato} and *Hoxa5*^{tdTomato} correlate with the differential expression of *Hox PG5* genes, the above experiment does not allow the assessment of their direct or indirect involvement in gene regulation with PN. To gain insight in their possible role for specifying the transcriptional identity of PN neurons, we extracted RNA from isolated *Math1*^{Hoxa5-IRES-GFP} PN neurons at E18.5 and compared it to the RNA extracted from *Math1*^{tdTomato} neurons. Using the same cut-off criteria (FC > 1.5; FDR < 0.07) we found 736 genes to be differentially expressed with 306 (42 %) being up- and 430 (58 %) being down-regulated in the *Math1*^{Hoxa5-IRES-GFP} samples (Figure 24J). Interestingly, none of the *Hox PG5* genes showed a significant change indicating that *Hoxa5* does not auto- or cross-regulate other PG Hox genes in PN neurons. At the same time, we could determine genes specifically controlled by *Hoxa5*. Notably, two members of the RA signaling pathway, *Cyb26b1* and *Crabp1*, were significantly decreased upon *Hoxa5* overexpression.

We next combined the datasets and asked which genes are commonly regulated in *Math1*^{tdTomato} vs. *Hoxa5*^{tdTomato} and *Math1*^{tdTomato} vs. *Math1*^{Hoxa5-IRES-GFP}. We found 107 (74%) genes to be up- and 38 (26%) to be down-regulated in both *Hoxa5*^{tdTomato} and *Math1*^{Hoxa5-IRES-GFP} (Figure 24K-L). Many molecules known to be important for axon guidance were significantly changed in both comparisons. Subsequent Gene Ontology (GO) analysis confirmed a substantial accumulation of genes critical for biological processes involved in topographic circuit formation like cell adhesion ($p = 2.71^{-07}$), axon guidance ($p = 6.93^{-06}$) as well as chemotaxis ($p = 9.01^{-04}$) (Figure 24M) but also showed an enrichment of genes relevant for higher order brain functions like cognition ($p = 5.75^{-07}$), learning and memory (2.19^{-05}) and locomotory behavior ($p = 2.04^{-03}$). Finally, we found a highly significant genome-wide correlation ($r = 0.18$; $p < 0.0001$) between *Hoxa5* overexpressing PN neurons and the *Hox PG5* positive part of the PN (Figure 24N).

Together, our comparative transcriptome analysis revealed the existence of complex molecular gradients within the PN, which in part are established by Hox transcription factors such as *Hoxa5*.

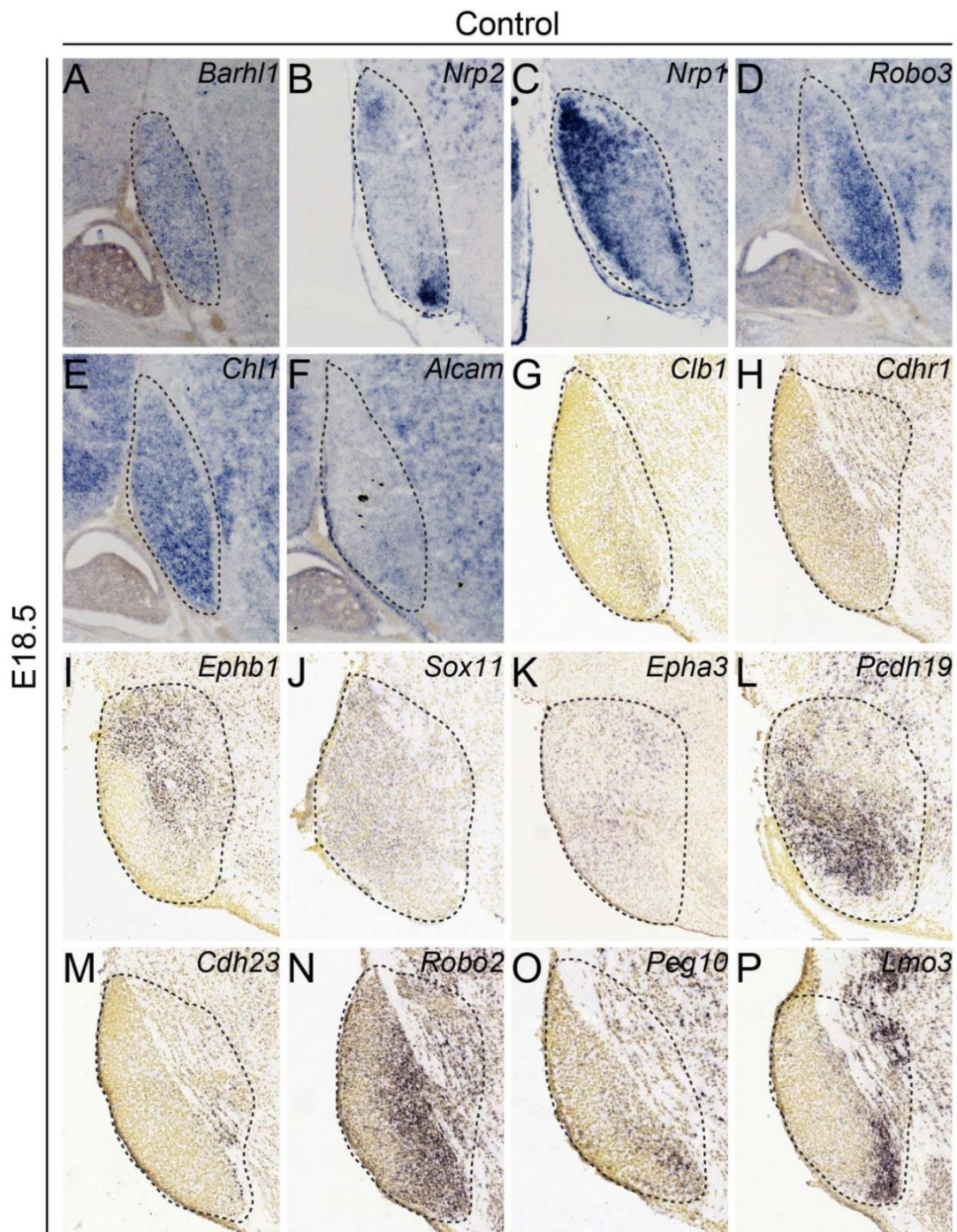


Figure 25: Validation of RNA-seq candidate genes

(A-F) E18.5 sagittal sections with *in situ* hybridizations using *Barhl1* (A), *Nrp2* (B), *Nrp1* (C), *Robo3* (D), *Chl1* (E), and *Alcam* (F) probes in control animals showing differential expression of candidate genes along the A-P axis. (G-H) E18.5 sagittal sections with *in situ* hybridizations using *Clb1* (G), *Cdhr1* (H), *Ephb1* (I), *Sox11* (J), *Epha3* (K), *Pcdh19* (L), *Cdh23* (M), *Robo2* (N), *Peg10* (O) and *Lmo3* (P) showing differential expression of candidate genes along the A-P axis. Image credit: Allen Institute for Brain Science. © 2015 Allen Institute for Brain Science. Allen Developing Mouse Brain Atlas [Internet]. Available from: <http://developingmouse.brain-map.org> and © 2015 Allen Institute for Brain Science. Allen Mouse Brain Atlas [Internet]. Available from: <http://mouse.brain-map.org>.

3.6. Ectopic expression of *Hoxa5* rearranges PN neuron output connectivity

The above results strongly indicate an important role for *Hoxa5* in the establishment of cortico-ponto-cerebellar sub-circuit formation, thus directing us to further analysis of PN neuron input and output connectivity. To map the projection pattern of an identified subset of PN neurons, we crossed *MafB::CreERT2* mice, whose *Cre* expression pattern is restricted to the r6-derived *Hox PG5* negative PN neurons (Figure 27A) (Di Meglio et al., 2013), to *ROSA26::(lox-stop-lox)tdTomato* mice (referred to as *MafB^{tdTomato}*) and analyzed the positioning and projection pattern of the labeled neurons at P21. Recombined cells strictly localized to the anterior and antero-lateral parts of the PN as predicted from the previous data (Figure 27B and 26A). Interestingly, mossy fiber terminals in the cerebellum were largely restricted to a specific lobule, showing a strong and localized innervation of the paraflocculus (PF) with only few terminals arriving in other lobes of the cerebellar hemispheres (Figure 27C, D and 26B-E). We next assessed the effect of ectopic *Hoxa5* overexpression on the specificity of this sub-circuit. *MafB^{tdTomato}* mice were crossed to *ROSA26::(lox-stop-lox)Hoxa5-IRES-GFP* BAC transgenic mice (referred to as *MafB^{Hoxa5-IRES-GFP;tdTomato}*) and analyzed at P21 (Figure 26E). *MafB^{Hoxa5-IRES-GFP;tdTomato}* r6-derived cells lost their rostral spatial segregation and were found in more posterior-medial aspects of the PN (Figure 27F and 26F, n = 3), thus further supporting the effect of *Hoxa5* overexpression on PN neuron positioning. Moreover, distribution of mossy fiber terminals in the cerebellum was not restricted to PF anymore but significantly more mossy fiber terminals were identified in other lobules including Crus1, Crus2 and the SL of the cerebellar hemispheres (Figure 27G, H and 26G-J, n = 3). Retrograde tracing experiments confirmed the presents of posterior PN neuron mossy fiber terminals in Crus1 and simple lobule of the cerebellum (Figure 26K-P).

In summary, these findings reveal that a topographic organization of connectivity between genetically identified PN neuron subsets and specific cerebellar lobules exists and this topography is dependent on *Hox* expression in PN neuron subsets.

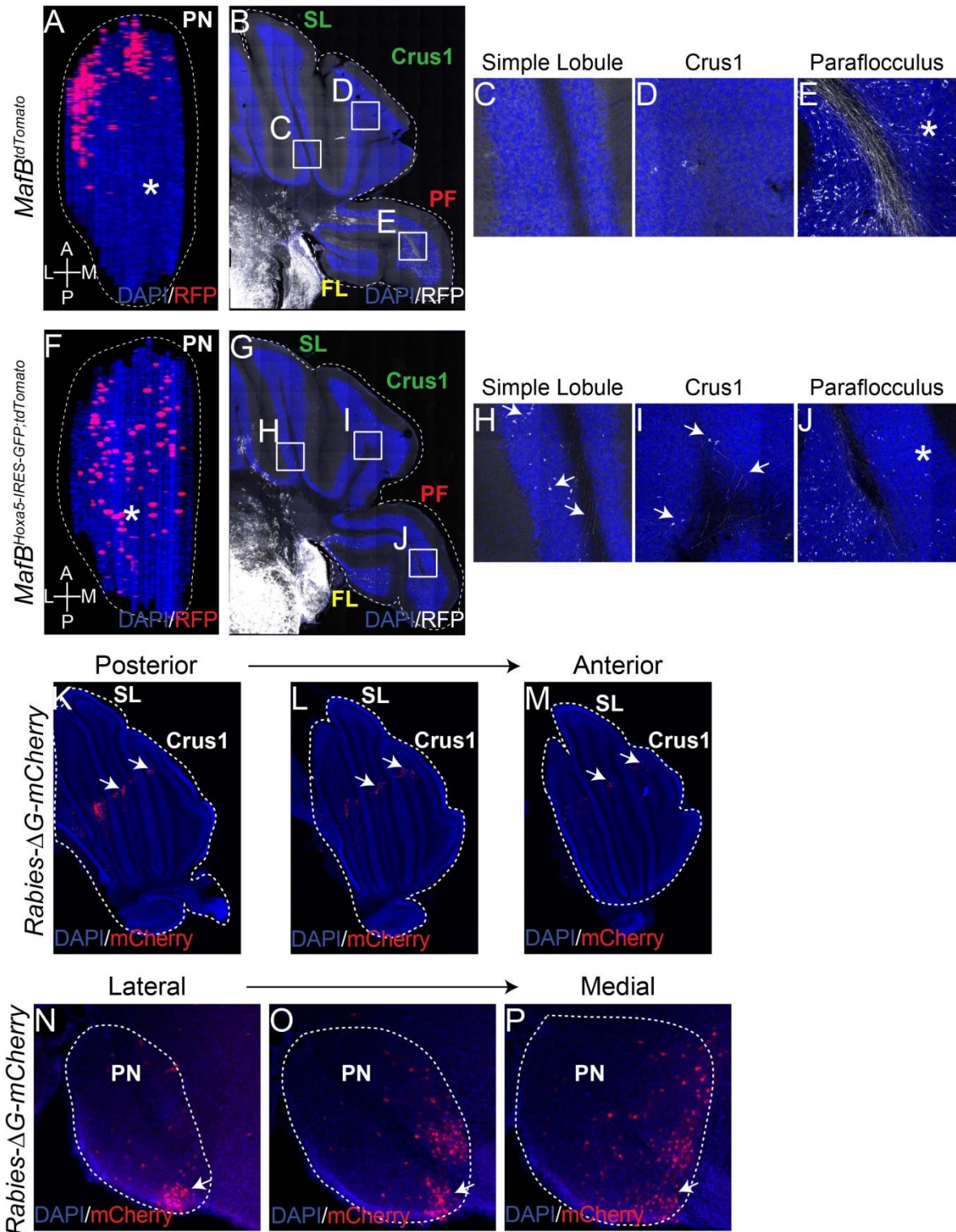


Figure 26: Projection pattern of ectopically *Hoxa5* expressing r-6 derived and posteriorly located PN neuron

(A, E) 3-D reconstruction of sagittal sections at P21, showing the distribution of r6 IRL derived neurons in the PN. In control embryos *Hox PG5* negative neurons are restricted to antero-lateral parts (B) while upon *Hoxa5* overexpression neurons are ectopically positioned

in the posterior-medial aspects of the nucleus (Asterisks in B and F). **(B-E, G-J)** Coronal section showing the distribution of mossy fiber terminals within the cerebellum of *MafB^{tdTomato}* (B-E) and *MafB^{Hoxa5-IRES-GFP;tdTomato}* (G-J) embryos at P21. Note the selective innervation of the paraflocculus in control (B, E) and the spread of mossy fiber terminals over several lobes in *Hoxa5* overexpressing embryos (arrows in G, H, I, J). **(K-P)** *Rabies-ΔG-mCherry* mediated retrograde tracing of PN neurons (N-P) by injections into the cerebellum hemispheres including SL and Crus1 (arrows in K-M). Note the high number of labelled neurons in the posterior most aspect of the PN (arrows in N-P).

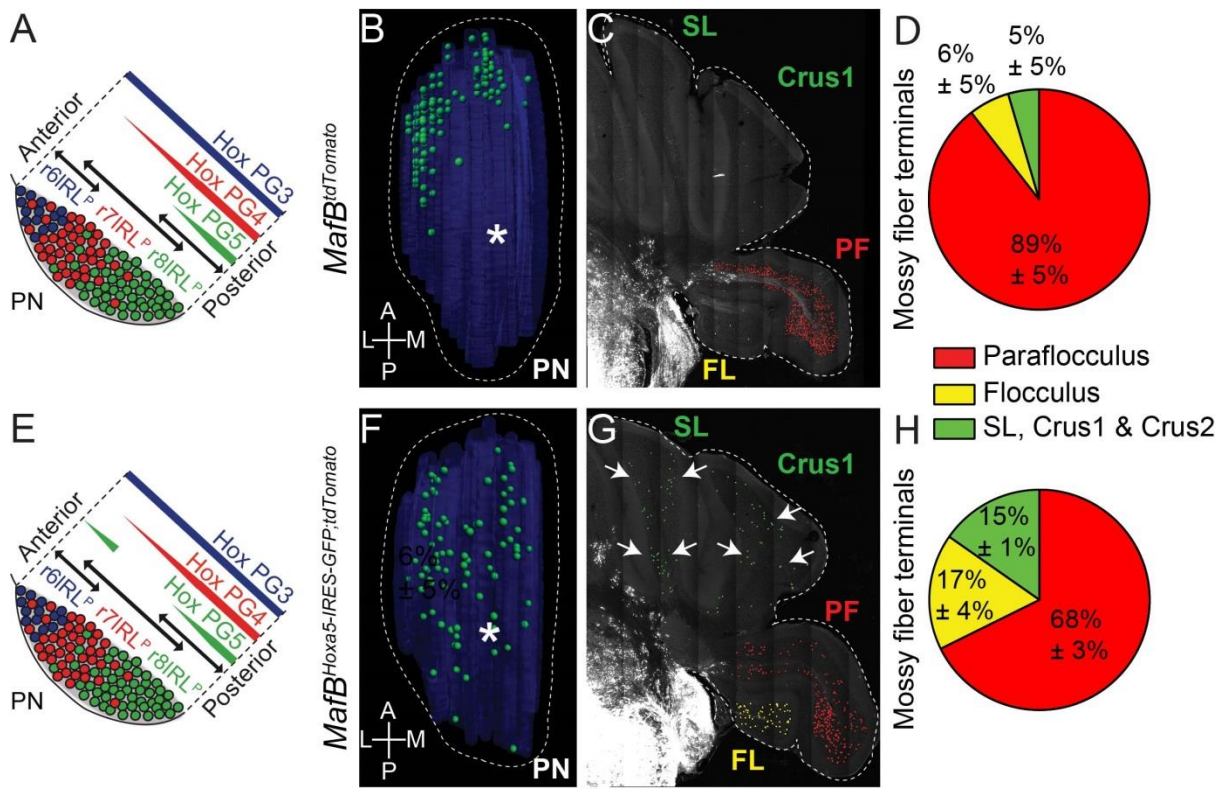


Figure 27: Ectopic expression of *Hoxa5* rearranges PN neuron output connectivity
(A, E) Models of the cellular composition of the PN with respect to rhombomeric origin and combinatorial Hox code along the A-P axis in *MafB^{tdTomato}* (A) and *MafB^{Hoxa5-IRES-GFP;tdTomato}* (E). **(B, F)** 3-D reconstruction of sagittal sections at P21, showing the distribution of r6 IRL derived neurons in the PN. In control embryos *Hox PG5* negative neurons are restricted to antero-lateral parts (B) while upon *Hoxa5* overexpression neurons are ectopically positioned in the posterior-medial aspects of the nucleus (Asterisks in B and F). **(C, G)** Coronal section showing the distribution of mossy fiber terminals within the cerebellum of *MafB^{tdTomato}* (C) and *MafB^{Hoxa5-IRES-GFP;tdTomato}* (G) embryos at P21. Note the selective innervation of the paraflocculus in control (C) and the spread of mossy fiber terminals over several lobes in *Hoxa5* overexpressing embryos (arrows in G). **(D, H)** Quantification of mossy fiber terminals in *MafB^{tdTomato}* (D) and *MafB^{Hoxa5-IRES-GFP;tdTomato}* (H) embryos (n = 3; Paraflocculus: p < 0.0001; Flocculus: p = 0.0175; Hemispheres: p = 0.0211). Data are presented as mean ± SD.

3.7. Relative A-P position of neurons within the PN is predictive for their cortical input connectivity

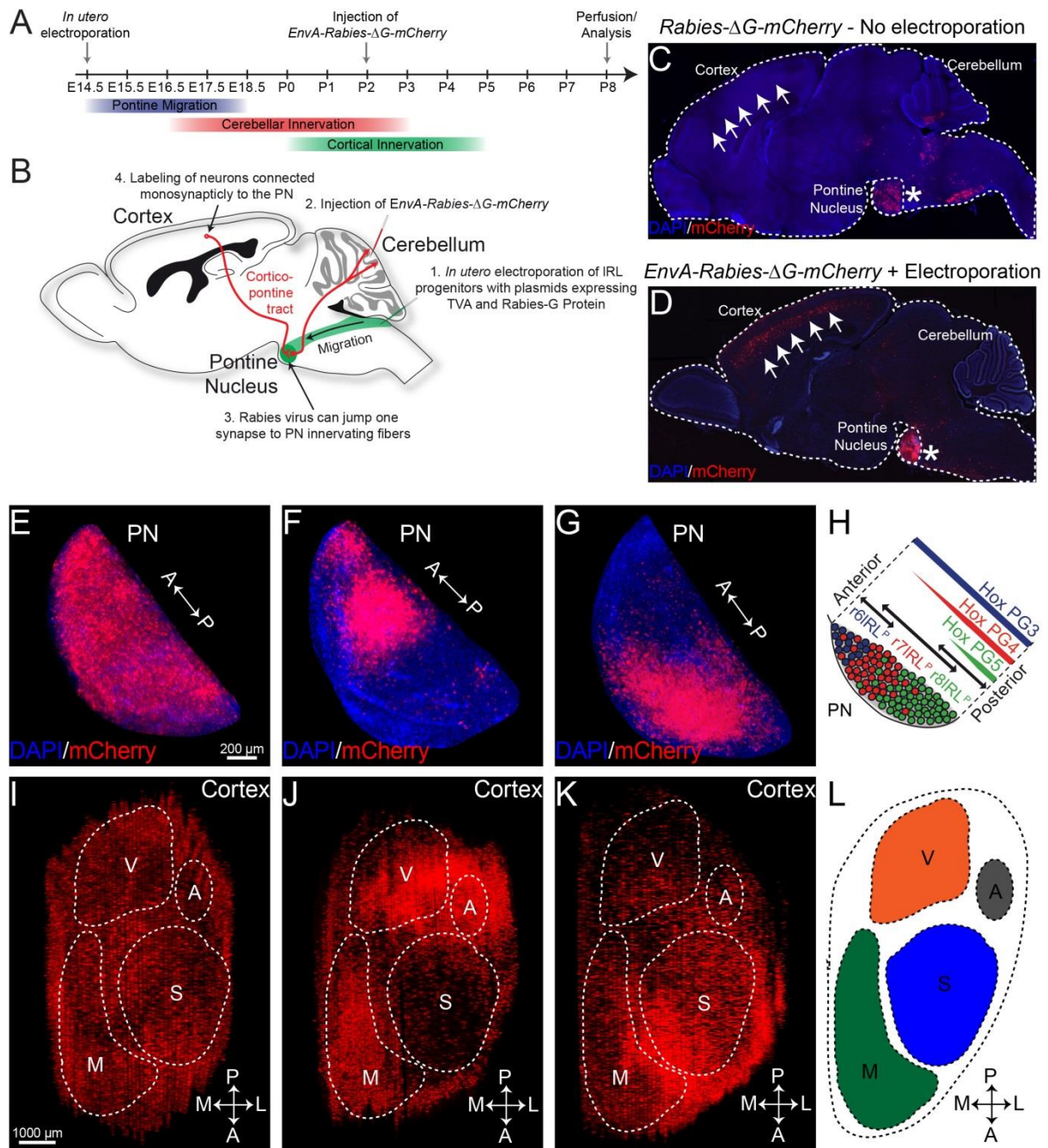


Figure 28: Relative A-P position of neurons within the PN is predictive for their cortical input connectivity

(A, B) Schematic illustration of the experimental design to initiate trans-synaptic rabies spread from PN neurons. (C) Sagittal section at P8 showing the distribution of mCherry⁺ neurons upon a cerebellar injection of *Rabies-ΔG-mCherry* in a non electroporated animal. (D) Sagittal section at P8 showing the distribution of mCherry⁺ neurons upon a cerebellar injection of *EnvA-Rabies-ΔG-mCherry* in an electroporated animal. Note the labelling of PN neurons by the cerebellar injection (Asterisks in C, D) and appearance of mCherry⁺ neurons in layer 5 of the ipsilateral cortex upon complementation of the Rabies virus (Arrows in C, D). (E-G) 3-D reconstructions of sagittal sections at P8, showing the distribution of mCherry⁺ neurons in the PN upon cerebellar injections of *EnvA-Rabies-ΔG-mCherry* in electroporated animals. (H) Model of the cellular composition of the PN with respect to rhombomeric origin and combinatorial Hox code along the A-P axis. (I-K) Ipsilateral cortices

of respective PN upon cerebellar injections of *EnvA-Rabies-ΔG-mCherry* in electroporated animals. Changing distributions of mCherry⁺ neurons in the PN (E-G) result in changes of distributions of mCherry⁺ neurons in the respective cortices (I-K). (L) Schematic illustration of a ventral view onto the mouse cortex with different areas being depicted. Panels A and B adapted from (Kratochwil, 2013), H from (Di Meglio et al., 2013)

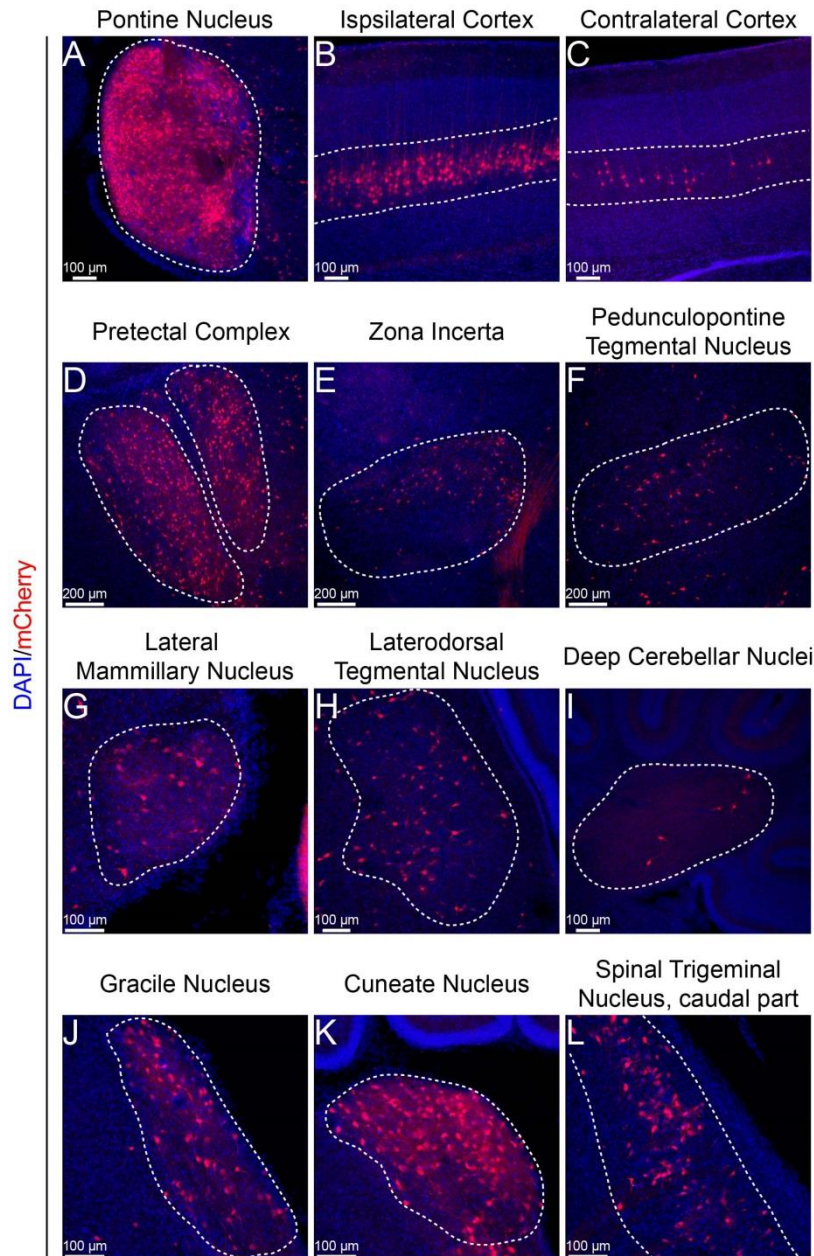


Figure 29: Input connectivity of PN neurons as revealed by trans-synaptic Rabies tracings

(A-L) Sagittal sections through a P8 mouse brain after *in utero* electroporation of the IRL with plasmids expressing rabies-glycoprotein and TVA at E14.5 and injections of *EnvA-Rabies-ΔG-mCherry* into the contralateral cerebellar hemisphere at P2. PN neurons (A) are initially labelled by the *EnvA-Rabies-ΔG-mCherry* injection and mono-synaptically restricted jumping of the virus from PN neurons allows to label the presynaptic inputs of the PN in the cortex (B, C), midbrain (D-H), cerebellum (I), hindbrain (J, K) and spinal cord (L).

Cortico-pontine projections arrive in an orderly fashion in the PN, largely preserving the neighbouring relationships present in the cortex (Leergaard, 2003). Moreover, patterning of PN neurons along the rostro-caudal axis may correlate with the establishment of cortico-pontine topographic connectivity (Di Meglio et al., 2013). To achieve a further understanding of relation between the physical location of PN neurons and their respective input-connectivity, we designed an experimental approach that allows trans-synaptic labelling of cortical cells from PN neurons (Wickersham et al., 2007). We combined *in utero* electroporation of the rabies-glycoprotein and the TVA receptor at E14.5 specifically into IRL progenitors with injections of an EnvA pseudotyped glycoprotein-deleted rabies viruses carrying mCherry (*EnvA-Rabies-ΔG-mCherry*) into the contralateral cerebellar hemisphere at P2 (Figure 28A, B). TVA/EnvA cell-type specific viral infection system as well as the complementation of the Rabies virus with the glycoprotein, achieved through the *in utero* electroporation of PN neuron progenitors, allowed the selective identification of cells mono-synaptically connected to electroporated PN neurons. In P8 specimen that were both electroporated with the rabies-glycoprotein and the TVA receptor and infected on their cerebellar terminals with the *EnvA-Rabies-ΔG-mCherry* the majority of labelled cells outside the PN were located in the cortical layer 5, ipsilateral to the electroporated PN, which were absent in control animals without electroporation but with cerebellar injections of a non-pseudotyped *Rabies-ΔG-mCherry* (Figure 28C, D). A variety of structures in the CNS exhibited labelled cells including contralateral cortical layer 5 neurons, pretectal complex, zona incerta as well as cuneate and gracile nuclei (Figure 29A-L). Even though most of these regions are in accordance to the literature on PN connectivity (Kolmac et al., 1998; Mihailoff et al., 1989; Swenson et al., 1984; Terenzi et al., 1995), our trans-synaptic virus approach shows that neurons within these structures do not just send axons to the PN but they are also mono-synaptically connected to PN neurons. We focused our attention on the ipsilateral cortex and screened the retrieved samples for either homogenous distribution of labelled cells or we took advantage of some variability within the experimental procedure resulting into infecting either anteriorly or posteriorly biased PN neuron subsets. The vast majority of brains (8 out of 10) showed a homogenous distribution of infected cells in the PN (Figure 28E). By 3D reconstruction of the cortex from serial sections in one of these specimens, we were able to show that layer 5 neurons throughout the cortex are mono-synaptically connected to PN neurons (Figure 28I). Additionally, we identified one sample each out of 10 with a strong anterior or posterior bias of infected neurons in the PN (Figure 28F-H). 3D

reconstruction of the respective cortical areas trans-synaptically labeled from such subsets revealed labelling of distinct mCherry⁺ cortical areas (Figure 28J-K). Monosynaptic tracing from anteriorly located PN neurons showed many marked neurons in the posterior-lateral and antero-medial regions of the cortex comprising visual, auditory and motor cortex (Figure 28J, D). Conversely, posteriorly located PN neurons were most heavily connected to the antero-lateral cortex comprising somatosensory regions and parts of the motor cortex (Figure 28K, D).

Thus, broad topographic input-connectivity of PN neurons from cortical areas correlates with rostrocaudal position within the PN. These findings underlie the importance of the PN A-P axis in terms of cortico-pontine circuit formation.

3.8. *Hoxa5* overexpression is sufficient to reorganize input connectivity of PN neurons

Since *Hoxa5* overexpression in randomly selected PN neuron subsets is sufficient to confer them a posterior position bias, we reasoned that it might also be sufficient to allow specific cortical afferent input normally targeting the posterior PN (i.e. mostly from somatosensory cortex). This hypothesis was tested by a modified trans-synaptic rabies tracing protocol (Figure 30A, B). Instead of plasmids encoding the rabies-glycoprotein and TVA, we electroporated a plasmid overexpressing a Cre recombinase under the CAG promoter in embryos of females homozygote for the *ROSA26::(lox-stop-lox)TVA-IRES-LacZ* (Seidler et al., 2008) and *Tau::(lox-stop-lox)Rabies-glycoprotein-IRES-LacZ* knock-in mated with heterozygote *ROSA26::CAG(lox-stop-lox)Hoxa5-IRES-GFP* males at E14.5. Thus, electroporated PN neurons would always express the rabies-glycoprotein and the TVA receptor (referred to as $WT^{TVA/Rabies-glycoprotein}$) but only half of the litter would additionally overexpress *Hoxa5* (referred to as $Hoxa5^{TVA/Rabies-glycoprotein}$). In accordance to the above findings, mCherry⁺ cells were distributed homogenously in the PN in $WT^{TVA/Rabies-glycoprotein}$ while $Hoxa5^{TVA/Rabies-glycoprotein}$ samples displayed a significant preference to the posterior (Figure 31A, I, Q, n = 4). Next, we turned our attention to layer 5 neurons in the ipsilateral cortical hemisphere, where we observed a high number of marked neurons throughout the cortical areas in $WT^{TVA/Rabies-glycoprotein}$ specimen (Figure 31B, C, n = 3). In contrast, in $Hoxa5^{TVA/Rabies-glycoprotein}$ animals we observed an almost complete absence of labelled neurons from the primary visual area while S1 displayed a high number of marked neurons (Figure

31J, K, n = 3). Quantification of the respective cortical areas revealed a significant change in cortical input connectivity between *Hoxa5*^{TVA/Rabies-glycoprotein} and *WT*^{TVA/Rabies-glycoprotein} animals (Figure 31R, n = 3). We then focused on S1 as topographic connectivity between S1 and the posterior PN has been previously mapped (Leergaard et al., 2006). Comparison of *WT*^{TVA/Rabies-glycoprotein} and *Hoxa5*^{TVA/Rabies-glycoprotein} samples showed significant changes in the connectivity pattern between PN and S1 regions. *Hoxa5* overexpression resulted in an increase in the ratio of neurons connected to hindlimb regions at the expense of neurons connected to the S1 barrel field (Figure 31D-F, L-N and S, n = 3). To understand whether the preference of *Hoxa5* overexpressing cells to connect to hindlimb related regions would be general feature we extended our analysis to the medial lemniscal pathway cuneate and gracile nuclei, which were prominently labelled by our monosynaptic tracing approach (Figure 29J, K). Indeed, upon *Hoxa5* overexpression the ratio of labelled neurons significantly increased in gracile, which conveys mostly hindlimb related information, and decreased in cuneate, a forelimb representation-associated structure (Figure 31G, H, O, P and T). Together, *Hoxa5* overexpression drives PN neurons into a hindlimb specific somatosensory circuitry.

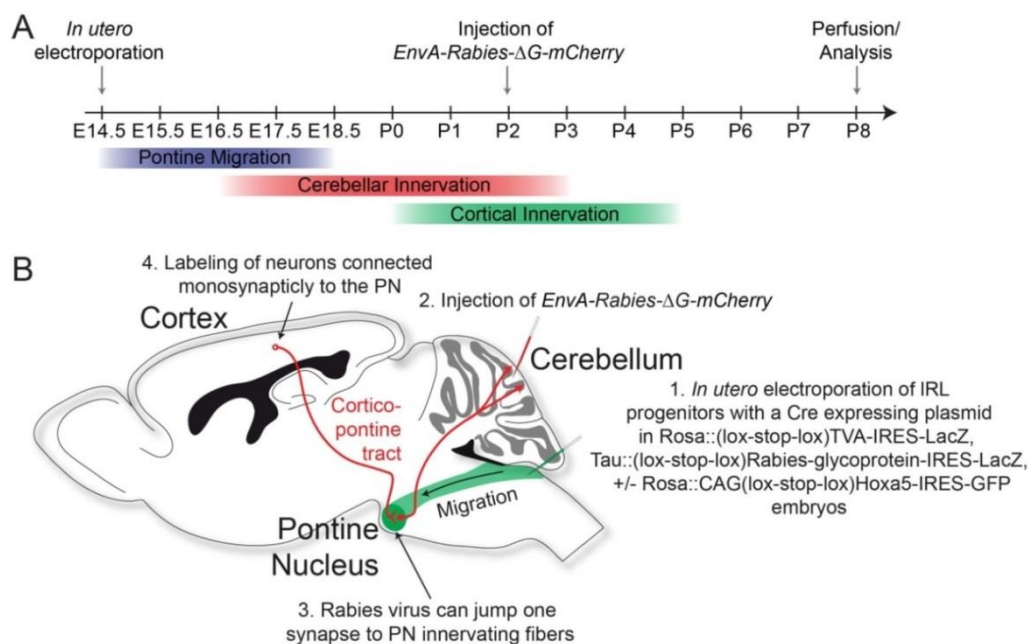


Figure 30: Schematic illustration of the experimental design to initiate trans-synaptic rabies spread from PN neurons

(A) Timeline of experimental steps for initiation of trans-synaptic rabies labelling from PN neurons and phases of PN circuit development. (B) Schematic illustration of the experimental design to initiate trans-synaptic rabies spread from PN neurons. Adapted from (Kratochwil, 2013)

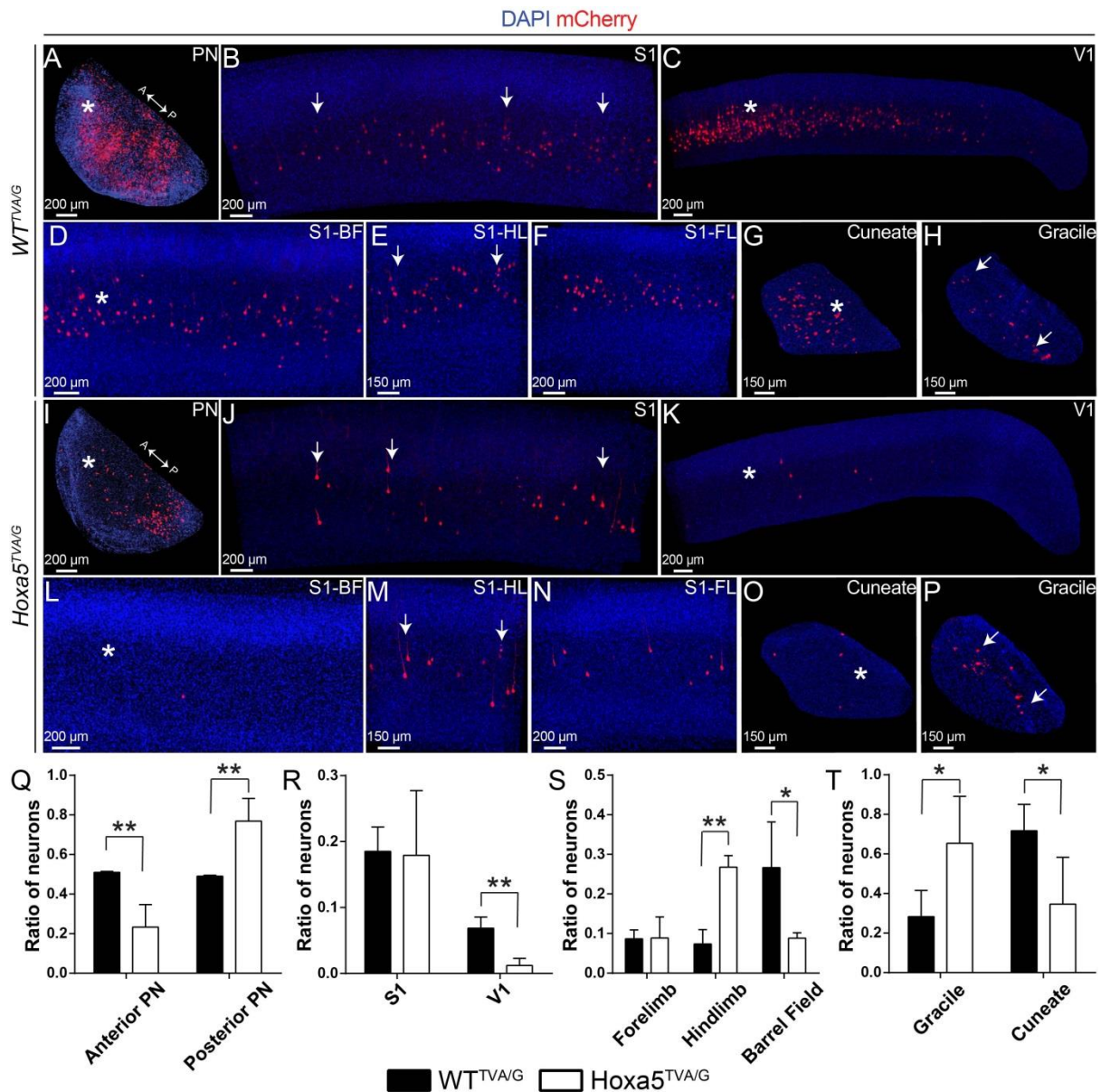


Figure 31: Hoxa5 overexpression is sufficient to reorganize input connectivity of PN neurons

(A-P) Sagittal section at P8 showing the distribution of mCherry⁺ neurons in different regions of the CNS upon a cerebellar injection of *EnvA-Rabies-ΔG-mCherry* in pCAG-iCRE electroporated *WT^{TVA/Rabies-glycoprotein}* and *Hoxa5^{TVA/Rabies-glycoprotein}* animals. Note the change in distribution of mCherry⁺ neurons between the *WT^{TVA/Rabies-glycoprotein}* and *Hoxa5^{TVA/Rabies-glycoprotein}* animals in the PN (Asterisks in A, B), Cortex (Arrows and Asterisks in B-F, J-N) and hindbrain (Arrows and Asterisks in G, H, O, P). (Q-T) Relative quantification of mCherry⁺ neurons found in different cortical and hindbrain regions *WT^{TVA/Rabies-glycoprotein}* and *Hoxa5^{TVA/Rabies-glycoprotein}* animals. The bias of PN neurons to the posterior upon *Hoxa5* overexpression (Q, n = 4, p = 0.003) leads to a change in presynaptic input between cortical areas (R, n = 3, p = 0.004), within cortical areas (S, n = 3, p < 0.001 (hindlimb), p = 0.048 (barrel field)) and hindlimb regions (T, n = 3, p = 0.034). Data are presented as mean + SD.

Altogether, *Hoxa5* overexpression is capable of organising input connectivity in a cell-autonomous manner by providing positional identity to PN neurons. Therefore, our findings support a model in which rostro-caudal origin of PN subsets along the progenitor domain is translated postmitotically into a Hox expression code. This results in stereotyped PN settling positions. In turn, Hox dependent targeted positioning within the nucleus and/or Hox expression select input connectivity from both cortical and subcortical regions.

4. Discussion

The PN connects two of the largest structures in the CNS, cerebral cortex and cerebellum. Motor and multimodal sensory information processing and potentially even higher brain functions like cognition and emotion might critically rely on specific microcircuits formed through the PN relay. In this study, we investigated how PN neuron subsets are formed and establish their connectivity during development. In particular, we identified a specific subset of PN neurons which get specified post-mitotically by the induction of *Hox PG5* genes. *Hox PG5* genes in turn provide positional and transcriptional identity to PN neurons, which is essential for cortico-ponto-cerebellar circuit formation.

4.1. A-P identity is specified post-mitotically in PN neurons

Our work demonstrates that positional information of PN neurons is provided by *Hox PG5* genes largely upon onset of migration and not at the mitotic progenitor stage. This is in contrast to current knowledge, which suggests that A-P identity is defined by Hox transcription factors in mitotic cells and maintained in postmitotic neurons resulting in the generation of distinct neuronal subtypes throughout the CNS (Dasen and Jessell, 2009; Molyneaux et al., 2007; Oury et al., 2006). Hox genes have been known to provide identity to progenitors especially in the spinal cord where they generate motor neuron pools through their combinatorial expression (Dasen et al., 2005). By showing that Hox gene expression can be selectively activated postmitotically within neuronal subsets in order to generate heterogeneous cell populations from a homogenous population of progenitors, we provide insight into the mechanisms that specify positional identity of PN neurons in the hindbrain. Considering the necessity for generating discrete PN neuron subsets to allow for the complex wiring between cortex and cerebellum, this setup has the strong advantage of flexibility over a system with boundaries of *Hox PG5* expression already set at the progenitor stage. The percentage of IRL derived PN neurons, which induce *Hox PG5* genes, could vary over time providing plasticity to the system. Also, the relative contribution and spatial distribution of cells expressing the different paralogue genes *Hoxa5*, *b5*, and *c5* could be variably determined by slightly different exposures to environmental signals during migration and after settling in the forming PN. Thus, throughout development new PN neuron subsets can be formed which would be distinct from each other due to expression of varying combinations and levels of *Hox PG5* genes. By intersecting postmitotic specification of

rostro-caudal identity with distinct birth dating of different subsets (Leergaard et al., 1995) diversity of PN neuron pools can be generated underlying the establishment of complex sub-circuit diversification in the cortico-ponto-cerebellar pathway.

Our findings on the regulation of *Hox PG5* expression in PN neurons is in line with longstanding literature on how RA sets expression domains of Hox genes during early rostral-caudal patterning of the CNS (Gavalas and Krumlauf, 2000; Glover et al., 2006; Walshe et al., 2002). Interestingly, graded *Raldh2* expression in the meninges together with graded *Cyp26b1* expression along the rostral-caudal axis of the hindbrain limits the induction of *Hox PG5* genes to posteriorly derived PN neurons. In this respect, the cross-regulation of *Hoxa5* and *Cyp26b1* presents an entry point to understand how such gradient may be established during late phases of development. Rhombomeric expression of *Hox PG5* genes in the developing hindbrain neuroepithelium is RA dependent and their anterior boundaries are set between E9.5 and E11.5 (Oosterveen et al., 2004). *Wnt1* expression is readily identifiable from E9 onwards (Dymecki and Tomasiewicz, 1998). By linking the exclusion of *Hox PG5* expression in the IRL progenitor domain directly to Wnt signaling we show for the first time a role for Wnt signaling in repressing Hox genes. We show that Wnt signaling (and Ezh2-dependent repression, see below) plays a key role in maintaining plasticity in the precerebellar IRL allowing spatiotemporally distinct postmitotic specification of PN neuron identity. Moreover, *Axin2* shows detectable levels of expression in *Hox PG5* negative postmitotic PN neurons indicating an additional role for Wnt signaling in keeping *Hox PG5* genes repressed in the remainder of the migratory stream after neurons exit from the IRL. Interestingly, we find reduced *Wnt5a* levels in *Hox PG5* positive neurons in our RNA-Seq experiments confirming the maintenance of Wnt signaling in anteriorly derived *Hox PG5* negative IRL progenies. So far, a rather activating role was shown for Wnt in respect to Hox gene expression in the mesoderm (Lengerke et al., 2008) as well as in somite specification (Ikeya and Takada, 2001). At the molecular level the interaction between Wnt and Hox was suggested to involve *Cdx1*. As *Cdx1* has been shown to upregulate Hox genes (Subramanian et al., 1995), we favor a different model for linking Wnt activity and *Hox PG5* repression. Wnt signaling regulates D-V patterning of the neural tube through modulation of Gli3 activity (Alvarez-Medina et al., 2008). Gli3 in turn acts as negative regulator of Hox genes as exemplified by suppressing *Hoxd13* and *Hoxd12* during early limb budding (Zuniga and Zeller, 1999). We envision that Wnt activity in the IRL induces *Gli3* expression which keeps progenitor cells *Hox PG5* negative during their induction in the posterior hindbrain. Thus,

Wnt signaling plays a key role in maintaining precerebellar neuron plasticity in mitotic cells of the IRL ensuring flexibility for precise specification of identity postmitotically. The striking absence of RA responsiveness in the IRL makes it tempting to speculate that Wnt also contributes to the suppression of RA response. However, whether RA terminates Wnt signaling or whether Wnt signaling actively suppresses RA responsiveness remains to be determined.

4.2. H3K27me3 dependent and independent mechanisms of *Hox PG5* gene repression

The dynamic regulation of *Hox PG5* genes in the IRL raises questions about the involvement of epigenetic regulation in such processes. We previously demonstrated that conditional inactivation of *Ezh2* in *Wnt1* expressing progenitor leads to ectopic expression of *Hox PG5* genes in anterior IRL derived migrating PN neurons (Di Meglio et al., 2013). Unexpectedly, we found that inactivation of *Ezh2* does not result in ectopic activation of *Hox PG5* genes in IRL progenitors but only in postmitotic cells. This sheds light on the role of H3K27me3 regulation at developmentally important genes. It is well established that *Ezh2* is associated primarily with developmentally regulated genes and most prominently *Hox* genes in embryonic stem cells (ESCs) (Boyer et al., 2006), *Drosophila* (Ringrose and Paro, 2004), and mammals (Di Meglio et al., 2013; Schwarz et al., 2014). Also the role of H3K27 demethylation during development through *Jmjd3* and *Utx1* has become increasingly understood in recent years (Estaras et al., 2012; Iida et al., 2014; Park et al., 2014). However, only few studies focused on the dynamics of *Hox* de-repression upon H3K27me3 removal during neuronal differentiation and most such studies rely on stem cell culture systems (Kashyap et al., 2011; Laursen et al., 2013). Within our *in vivo* system we demonstrate that *Ezh2* knockout is insufficient to induce premature transcription of *Hox PG5* genes in *Wnt*⁺ progenitor cells. Instead, PN neurons remain plastic until environmental signals are appropriate for their final specification. Yet, H3K27me3 depletion leads to a generalized induction of *Hox PG5* genes throughout IRL progenies suggesting an increased sensitivity to rostro-caudally graded RA levels upon *Ezh2* knockout. Thus, a central function of *Ezh2* during late stages of precerebellar development might be establishing a threshold for RA mediated activation of *Hox PG5* genes in order to allow for diversification of PN neurons. The onset of *Hox* transcription precedes the removal of the H3K27me3 mark upon RA treatment in ESCs, indicating that the removal of the H3K27me3 mark may not be required

for transcriptional activation (Kashyap et al., 2011). Here, we show that conditional inactivation of *Ezh2* results in an increased spatial response to RA and that *Jmjd3* knockout decreases *Hox PG5* expression levels at the onset and during later stages of migration. Even though transcriptional activation of *Hox PG5* genes may be independent of H3K27me3 removal, the presence of H3K27me3 interferes with efficient transcription. High levels of expression can only be achieved upon H3K27me3 depletion. Opposing changes of expression levels of *Ezh2* and *Jmjd3* during differentiation of precerebellar neurons in the IRL are consistent with the idea that remodeling of H3K27me3 is necessary at the onset of migration for the final specification of PN neurons. The regulation of Hox expression through *Jmjd3* and its association to a *Hoxa5* enhancer region is in line with a recent report that described *Jmjd3* binding to 59% of mapped enhancers in the developing neocortex and the necessity of *Jmjd3* for the activation of selected enhancers (Park et al., 2014). Our finding reporting a delay in neuronal differentiation of IRL progenitors in *Jmjd3* knockout animals supports similar findings reported in a number of studies (Jiang et al., 2013; Kartikasari et al., 2013; Ramadoss et al., 2012). Thus, we can extend the function of *Jmjd3* *in vivo* to neuronal differentiation as well as specification of A-P identity in the developing hindbrain.

4.3. Higher order chromatin reorganisation upon RA treatment in the nervous system

We found that RA treatment is sufficient to change not only the epigenetic landscape but also the 3D chromatin organisation of Hox clusters in the mammalian hindbrain in a context dependent manner. Previous work has shown that higher order chromatin organisation at Hox clusters is organised in a way that active and inactive genes form distinct domains (Noordermeer et al., 2011) and that Hox cluster conformation is highly dynamic during differentiation (Chambeyron and Bickmore, 2004; Ferraiuolo et al., 2010; Rousseau et al., 2014). These findings highlight the interplay between spatial and temporal expression of Hox loci and their 3D chromatin topology. However, the nature of signals and specific factors that underlie such structural changes during embryonic neuronal development remain poorly understood. In ESCs, RA induced transcription and chromatin remodelling of the Hox clusters extends up to *Hox PG10* genes (De Kumar et al., 2015; Kashyap et al., 2011). Experimental evidence in the developing CNS on whether RA is sufficient to orchestrate the conformational switch of induced Hox genes loci from a repressed to an active domain is still lacking. Our findings confirm the existence of chromatin domains that accurately separate

inactive and active Hox genes along the rostral-caudal axis of the hindbrain. We demonstrate that the regulation of *Hox PG5* expression through RA signaling is instructive for domain association. We can therefore for the first time directly link transcriptional regulation of Hox genes through environmental signaling molecules to 3D chromatin reorganisation *in vivo*. In our system, unlike in cultured ESCs, we find that the Hox clusters are restricted in their capability to be successively activated beyond *Hox PG5* genes in response to RA. This is illustrated by the lack of any conformational change in r8 upon RA treatment. Insulation of functional chromatin domains within Hox clusters might be a possible mechanism to limit the expansion of active domains to more posterior Hox genes. In fact, CTCF binding has been reported at multiple sites within the *Hoxa* cluster including a site between *Hoxa5* and *Hoxa6* (Narendra et al., 2015). Deletion of two of these binding sites resulted in a posterior spread of Hox gene activation in ESCs after RA mediated differentiation into motor neurons. In this context, it will be interesting to assess which signals determine the CTCF binding *in vivo* within the Hox clusters as RA is an unlikely candidate based on our experimental evidence.

4.4. *Hoxa5* regulates positional and transcriptional identity of specific PN neurons subsets

The tight spatio-temporal regulation of *Hox PG5* expression in PN neurons suggests a substantial role of these transcription factors in consequent developmental processes. Recent work showed that Hox genes regulate guidance molecules critically important for PN neuron migration (Di Meglio et al., 2013). However, direct evidence for the involvement of Hox transcription factors in topographic migration and nucleation of PN neurons was still lacking. Our findings in *Math1^{Hoxa5-IRES-GFP}*, *MafB^{Hoxa5-IRES-GFP;tdTomato}*, and *in utero* electroporated mice demonstrate that *Hoxa5* expression directly correlates with the final position of neurons in the PN showing that the spatial segregation of PN neuron subsets derived from distinct A-P (rhombomere-derived) regions along the IRL progenitor domain is mediated by Hox gene expression. Identity of PN neurons, set through elaborate mechanisms in postmitotic neurons as described above, is thus reflected into its position within the nucleus.

The comparative genomic approach used in this study deepens our understanding of Hox dependent transcriptional programs underlying topographic circuit formation. Virtually all important classes of guidance molecules including Netrins (*Ntn1*), Slits (*Slit3*), Ephrins (*Efn3* and *b3*), Semaphorins (*Sema6a* and *6d*, *Plxn4*, *Nrp1* and *2*), cell adhesion molecules

(*Cdh2* and *23*, *Pcdh9* and *19*) and other signaling factors such as NGFs, FGFs and Wnts are differentially expressed along the A-P axis of the PN. This demonstrates the complexity of molecular gradients that have to be established within the PN to connect two such diverse structures like the cortex and the cerebellum in a meaningful manner. By correlation of the datasets we obtained from the *Math1*^{tdTomato} vs. *Hoxa5*^{tdTomato} and *Math1*^{tdTomato} vs. *Math1*^{Hoxa5-*IRES-GFP*} comparisons we show that some aspects of the molecular gradients within the PN are regulated by a single Hox transcription factor. The relevance of these gradients not only for topographic circuit formation but also higher order brain functions is apparent from the GO analysis of commonly regulated genes. There, the most enriched biological processes are related to connectivity, cognition and behaviour. A potential function in precerebellar circuit formation has actually already been discussed (Chedotal et al., 1996) or shown (Solowska et al., 2002) for a number of identified genes indicating the significance of our datasets in uncovering new molecular players in the development of cortico-ponto-cerebellar circuitry. The modest correlation between the two datasets also indicates that the r8-derived PN neuron transcriptional program depends not only on a single but likely on a combination of several Hox and potentially other transcription factors. In fact, the missing cross-regulation between *Hoxa5* and other Hox factors points towards the necessity of creating pools of PN neurons that do show heterogeneity in terms of their combinatorial *Hox PG5* code. Thus, each *Hox PG5* gene might regulate partially distinct sets of target genes in order to allow for sub-circuit diversification within the r8 derived subset of PN neurons. Further work will be needed to support this prediction.

4.5. *Hoxa5* is sufficient to orchestrate PN neuron input-output connectivity

A topographic connectivity pattern has been described for the cortico-pontine projections (Leergaard and Bjaalie, 2007). Despite a number of publications involving tracing data from the cerebellum, no such clear-cut topography emerged for the ponto-cerebellar connectivity so far (Azizi et al., 1981; Broch-Smith and Brodal, 1990; Mihailoff et al., 1981; Nikundiwe et al., 1994). The defined target zone of *MaifB*^{tdTomato} positive mossy fibers within cerebellar hemispheres provide for the first time a link between rostro-caudal progenitor origin of PN neurons and their projection pattern to the cerebellum. The selective innervation of the paraflocculus is in accordance with retrograde tracing experiments performed from the paraflocculus in cats in which more than 70% of the labelled neurons were found in the

rostral half of the PN (Broch-Smith and Brodal, 1990; Nikundiwe et al., 1994). Besides few studies that addressed the involvement of signaling molecules in ponto-cerebellar circuit formation virtually nothing is known about the involvement of transcription factors in topographic circuit formation between PN and cerebellum. Our findings of the altered projection patterns of r6 derived PN neurons upon ectopic *Hoxa5* expression establish Hox transcription factors as master regulators of ponto-cerebellar connectivity. *Nrp1* has been suggested to be involved in guiding subsets of PN axons to distinct target regions, including the paraflocculus, within the cerebellum (Solowska et al., 2002) showing a potential molecular mechanism underlying such precise targeting of lobules. Interestingly, we find *Nrp1* being significantly down regulated in *Hox PG5* positive and *Hoxa5* overexpressing PN neurons in our RNA-Seq experiments showing *Hoxa5* involvement in setting the *Nrp1* expression domain. How different axon guidance pathways interact to define the final projection area of PN neurons will require more extensive analysis on the respective involvement of differentially regulated genes across the PN and cerebellum.

A-P position within the PN matters in terms of cortical input connectivity for PN neurons. The di-synaptic nature of the communication between cortex and cerebellum has complicated the direct mapping of cerebro-ponto-cerebellar pathway. Few studies have tried to circumvent this issue by the use of trans-synaptic viral markers but they still suffered from technical limitations (Suzuki et al., 2012). By combining *in utero* electroporation with trans-synaptic rabies tracing techniques we established an assay that reliably allows the global assessment of cortical (and sub-cortical) regions which relay information to the cerebellum via the PN. We used this approach to primarily study the spatial connectivity rules between PN and cortex by comparing the 3-D distribution of labelled neurons in both structures. We demonstrate that dependent on their A-P position PN neurons receive input from largely segregated regions of the cortex. The bias of anterior cells to input from regions including visual cortex complements the findings of the projection pattern of *MafB^{tdTomato}* positive neurons to the paraflocculus, a structure associated with visually guided movements (Marple-Horvat and Stein, 1990). Together, this indicates the potential restriction of the anterior, *Hox PG5* negative part of the PN for processing visual information by connecting cortical and cerebellar areas involved in visual processes with each other. Conversely, posterior, *Hox PG5* positive neurons may rather serve somatosensory related circuits as they received primarily input from somatosensory cortex. Moreover, *Hoxa5* overexpression shifted the r6 derived mossy fibers to cerebellar lobules normally receiving cortical somatosensory information

(Apps and Hawkes, 2009). Future experiments will have to employ optogenetic manipulations of identified PN neuron subsets to further address the physiological relevance of these findings. In general, our results are in accordance with the literature (Leergaard and Bjaalie, 2007) and unambiguously proves a topographic organisation at the synaptic levels between cortex and PN. While varying densities of projections from different cortical areas have been reported (Legg et al., 1989) we did not find a strong bias towards any cortical area in those cases showing a homogenous labelling in the PN. The similar dense labelling of regions like the orbitofrontal and retrosplenial cortex as compared to motor and somatosensory areas suggest that the cerebellum might be equally concerned with cognitive tasks like decision making and learning as it is with motor functions (Mar et al., 2011; Vann et al., 2009).

Despite the longstanding knowledge of topographic circuit formation between cortex and PN still very little is known about master regulators that control this complex circuitry. By showing that *Hoxa5* overexpression can shape input connectivity of PN neurons through determining their position within the nucleus we provide a framework for the establishment of functional units in the PN. With our analysis of connectivity patterns between PN and subcortical regions we can further extend the concept of topography as being a general principle in precerebellar circuit formation. The notion that position is the determinant for input connectivity patterns has first been made in the spinal cord (Surmeli et al., 2011). In this study, the settling position of motor neurons was scrambled due to loss of specific identities; in such context sensory afferents maintained their wild-type like innervation pattern which resulted in inappropriate connections. A potential caveat in that study is that as motor neurons do not acquire specific identities, a potentially instructive role on topographic wiring of incoming input could be masked. Here, we show that *Hoxa5* expression dictates a specific positional identity on PN neuron. Cortical input arrives in a defined manner to the PN and different areas connect with neurons present at their respective arborisation site linking neuronal identity to position and position to connectivity patterns. Technically challenging experiments where manipulations of the Hox code are uncoupled from settling position will shed light on an additional implication of Hox genes in shaping cortico-pontine circuitry beyond their role in defining neuronal positional identity. Our RNA-Seq experiments show that a number of molecules involved in such processes are regulated by *Hoxa5*. With this finding we establish neuronal settling position as critical determinant for sub-circuit assembly and diversification in the mammalian hindbrain.

Regardless of a potential cell autonomous role in attracting specific cortical input, our findings suggest that the complex task of connecting cortex and cerebellum in a meaningful manner is achieved through the diversification of PN neurons by the expression of Hox transcriptional codes. It is particularly intriguing that this diversity is established postmitotically, after the progenitor stage, and that the overexpression of a single Hox factor is enough to specify position, input as well as output connectivity of PN neurons.

4.6. Implications for somatosensory map transformation

Do the presented results allow conclusions about the molecular and cellular mechanisms of somatosensory map fracturing? The basis of this fracturing is that somatosensory information is transformed from a continuous, somatotopic body representation to a patchy representation by the pontine relay. Thus, it requires the formation of functional units in the PN that select a specific input from the cortex in the first place. According to our results, the expression of Hox genes selects the input of PN neurons. The forced expression of one single Hox gene, *Hoxa5*, is sufficient to strongly bias PN neurons into a hindlimb somatosensory input circuit. Combinatorial expression of different *Hox PG3*, *Hox PG4* and *Hox PG5* genes might therefore in part constitute the molecular basis for the specification of distinct functional units in the PN relaying somatosensory information representing distinct body regions. A similar combinatorial logic might underlie the specification of PN neuron clusters relaying information from motor cortex or distinct sensory modalities. Further studies will be required to support such predictions. Together with other determinants of PN neuron identity, such as their birthdate, sufficient modules to specify the precise cortical input of a given neuron can be created. Concerning output connectivity, a molecular determinant for the process of somatosensory map fracturing must be capable of inducing a projection pattern that creates multiple patches for the representation of a single body region within a single and across multiple lobules. Along this line, we demonstrate that *Hoxa5* expression is sufficient to change the connectivity pattern of PN neurons from largely targeting one single lobule to the innervation of multiple lobules. This ability of neurons to innervate different lobules of the cerebellum is a pre-requisite for the fracturing of the somatosensory map. Such broadcasting of information allows the formation of patches in the cerebellum, processing the same kind of somatosensory information. Consequently, Hox genes seem to be suitable candidates to orchestrate the basic input-output connectivity of PN neurons that may lay the basics for the fracturing of the cortical somatosensory map.

4.7. Outlook

The results of this thesis establish Hox genes as master regulators of cortico-ponto-cerebellar circuit formation. The analysis and tools described build the foundation to address questions such as the Hox dependent molecular mechanisms that regulate identity, sub-circuit assembly and diversification, and physiological function of PN subsets.

Using the Flag-Tagged *Hoxa5* conditional overexpression mouse line in combination with state-of-the-art techniques like ChIP-Seq (Barski and Zhao, 2009) and ATAC-Seq (Buenrostro et al., 2015) it will be possible to understand how Hox genes regulate chromatin accessibility and expression of target genes in PN neurons, as well as to identify the specific sets of regulatory elements (enhancers) involved. Combinatorial analysis of members from the same and or different PG genes will shed light on how different Hox genes provide specificity despite their high homology.

Bona fide downstream targets of Hox genes as identified by the comparative RNA-Seq approach represent a great selection of genes that are potentially relevant for topographic circuit formation in the cortico-ponto-cerebellar system. In depth analysis of a number of these molecules regarding their capability to attract specific cortical input or direct PN neuron axons to specific lobules in the cerebellum will be required to understand the guidance factors involved in the fracturing of the cortical maps through their relay to the cerebellum. *In utero* electroporation and the combination of this technique with trans-synaptic rabies tracings are the tools required to rapidly assess the functional implication of selected candidate genes. This will also allow addressing the cell autonomous and non-cell autonomous roles of Hox genes once neurons settled in the PN. Some of the presented experiments point towards position being a key determinant of input connectivity. However, data in the literature suggest that PN neurons secrete chemotactically active cues (O'Leary et al., 1991). These two mechanisms are not necessarily mutually exclusive and might be used in combination to strengthen precision and/or generate local sub-circuit diversification. Detailed analysis on single or well defined populations of cells by using mouse genetic tools will answer the contribution of cell autonomous and non-cell autonomous effects on PN circuit formation.

More precise mouse genetic tools through intersectional strategies using Cre and Flp recombinases will allow for the assessment of the input-out connectivity of specific PN

subsets. To this aim, we already generated a *Hoxa5::creERT2* and several *Wnt1::Flp* mouse lines (data not shown). Combining these mouse lines as well as the *MafB::creERT2* with trans-synaptic rabies tracings will give valuable information about the convergence of cortical and subcortical input on defined populations. Co-labelling approaches of PN neurons and identified input regions using multiple colour anterograde and retrograde viral tracings techniques will even give the possibility to look at the integration of inputs on single cells adding significant information to the longstanding question of PN function. Alternatively, adopting the recently developed technique of single cell initiated trans-synaptic rabies tracings would create a valuable tool to assess the precise input connectivity of identified pontine neurons (Wertz et al., 2015). Along these lines, behavioural assessment of mice while manipulating activity of selected PN subsets will reveal possible roles of the PN in a variety of physiological contexts. Optogenetics (Fiala et al., 2010), chemogenetics (Sternson and Roth, 2014) and the selective ablation of cells with diphtheria toxin (Buch et al., 2005) might be appropriate approaches.

Activity dependent mechanisms of cortico-ponto-cerebellar circuit formation remain largely unexplored. There is growing evidence for such mechanisms to be crucially important for topographic map formation. Especially concerning the ponto-cerebellar projections large scale synaptic pruning might be involved in the formation of the fractured map. Mouse genetic tools which affect activity in neurons such as NR1 knockouts or conditional Tetanus toxin and Kir2.1 overexpression lines present in the lab might be useful to start addressing questions in this field of research.

Finally, the evolutionary aspects of PN development are particularly interesting. As cortex and cerebellum grew substantially during evolution the PN had to keep the pace and increase in size as well. In humans the PN is the by far most prominent structure in the hindbrain. Also with the cortex becoming more and more complex it is likely that the PN had to adopt mechanisms to cope with this complexity to allow for sub-circuit diversification. It would be extremely interesting to assess whether the PN attracted neurons from more posterior aspects potentially expressing *Hox PG6* genes to increase the diversity. Transcriptional analysis of PN from different species would provide new insights into the evolutionary mechanisms orchestrating the increasingly complex cross-talk between cortex and cerebellum.

Statement of contribution

I contributed to the design and execution of all experiments shown in this dissertation with help of the different people for the following experiments. The *Math1::Cre* and the *Jmjd3* knock-in mouse lines were generated by Sebastien Ducret. The *Tau::(lox-stop-lox)Rabies-glycoprotein-IRES-nls-LacZ* mouse line was generated by Daisuke Satoh in Silvia Arber's laboratory. FACS sorting was done with the help of Hubertus Kohler. ChIP experiments were done with the help of Vanja Cankovic. 4C-seq experiments were done with the help of Sjoerd Holwerda. RNA-Seq experiments were done with the help of Kirsten Jacobeit, Stéphane Thiry and Tim Roloff. Trans-synaptic rabies tracing experiments were done with the great help of Upasana Maheshwari and technical support by Nicola Maiorano and Kajari Karmakar. Claudius Kratochwil initially described the positioning of r6-derived neurons in the PN and the distribution of mossy fiber terminals in the cerebellum in the *MafB::CreERT2* mouse line and established the trans-synaptic rabies tracing from the PN. Thomas Di Meglio helped in identifying the dynamic regulation of *Hox PG5* gene expression in the RL and with RA treatment experiments. I also performed all statistical analysis and generated all final figures.

Bibliography

Aas, J.E. (1989). Subcortical projections to the pontine nuclei in the cat. *The Journal of comparative neurology* 282, 331-354.

Aberle, H., Bauer, A., Stappert, J., Kispert, A., and Kemler, R. (1997). beta-catenin is a target for the ubiquitin-proteasome pathway. *Embo J* 16, 3797-3804.

Abu-Abed, S., Dolle, P., Metzger, D., Beckett, B., Chambon, P., and Petkovich, M. (2001). The retinoic acid-metabolizing enzyme, CYP26A1, is essential for normal hindbrain patterning, vertebral identity, and development of posterior structures. *Genes Dev* 15, 226-240.

Agger, K., Cloos, P.A., Christensen, J., Pasini, D., Rose, S., Rappsilber, J., Issaeva, I., Canaani, E., Salcini, A.E., and Helin, K. (2007). UTX and JMJD3 are histone H3K27 demethylases involved in HOX gene regulation and development. *Nature* 449, 731-734.

Alder, J., Lee, K.J., Jessell, T.M., and Hatten, M.E. (1999). Generation of cerebellar granule neurons in vivo by transplantation of BMP-treated neural progenitor cells. *Nat Neurosci* 2, 535-540.

Alexander, T., Nolte, C., and Krumlauf, R. (2009). Hox genes and segmentation of the hindbrain and axial skeleton. *Annu Rev Cell Dev Biol* 25, 431-456.

Allen, G.I., and Tsukahara, N. (1974). Cerebrocerebellar communication systems. *Physiol Rev* 54, 957-1006.

Altman, J., and Bayer, S.A. (1987a). Development of the precerebellar nuclei in the rat: I. The precerebellar neuroepithelium of the rhombencephalon. *The Journal of comparative neurology* 257, 477-489.

Altman, J., and Bayer, S.A. (1987b). Development of the precerebellar nuclei in the rat: II. The intramural olivary migratory stream and the neurogenetic organization of the inferior olive. *The Journal of comparative neurology* 257, 490-512.

Altman, J., and Bayer, S.A. (1987c). Development of the precerebellar nuclei in the rat: III. The posterior precerebellar extramural migratory stream and the lateral reticular and external cuneate nuclei. *The Journal of comparative neurology* 257, 513-528.

Altman, J., and Bayer, S.A. (1987d). Development of the precerebellar nuclei in the rat: IV. The anterior precerebellar extramural migratory stream and the nucleus reticularis tegmenti pontis and the basal pontine gray. *The Journal of comparative neurology* 257, 529-552.

Alvarez-Medina, R., Cayuso, J., Okubo, T., Takada, S., and Marti, E. (2008). Wnt canonical pathway restricts graded Shh/Gli patterning activity through the regulation of Gli3 expression. *Development* 135, 237-247.

- Andrey, G., Montavon, T., Mascrez, B., Gonzalez, F., Noordermeer, D., Leleu, M., Trono, D., Spitz, F., and Duboule, D. (2013). A switch between topological domains underlies HoxD genes collinearity in mouse limbs. *Science* *340*, 1234-167.
- Apps, R., and Hawkes, R. (2009). Cerebellar cortical organization: a one-map hypothesis. *Nat Rev Neurosci* *10*, 670-681.
- Ashe, H.L., and Briscoe, J. (2006). The interpretation of morphogen gradients. *Development* *133*, 385-394.
- Azizi, S.A., Mihailoff, G.A., Burne, R.A., and Woodward, D.J. (1981). The pontocerebellar system in the rat: an HRP study. I. Posterior vermis. *J Comp Neurol* *197*, 543-548.
- Barski, A., and Zhao, K. (2009). Genomic location analysis by ChIP-Seq. *J Cell Biochem* *107*, 11-18.
- Bartscherer, K., Pelte, N., Ingelfinger, D., and Boutros, M. (2006). Secretion of Wnt ligands requires Evi, a conserved transmembrane protein. *Cell* *125*, 523-533.
- Bateson, W. (1894). *Materials for the study of variation treated with especial regard to discontinuity in the origin of species*. Macmillan, New York.
- Bechara, A., Laumonnerie, C., Vilain, N., Kratochwil, C.F., Cankovic, V., Maiorano, N.A., Kirschmann, M.A., Ducret, S., and Rijli, F.M. (2015). Hoxa2 Selects Barrelette Neuron Identity and Connectivity in the Mouse Somatosensory Brainstem. *Cell Rep* *13*, 783-797.
- Behrens, J., von Kries, J.P., Kuhl, M., Bruhn, L., Wedlich, D., Grosschedl, R., and Birchmeier, W. (1996). Functional interaction of beta-catenin with the transcription factor LEF-1. *Nature* *382*, 638-642.
- Beier, K.T., Steinberg, E.E., DeLoach, K.E., Xie, S., Miyamichi, K., Schwarz, L., Gao, X.J., Kremer, E.J., Malenka, R.C., and Luo, L. (2015). Circuit Architecture of VTA Dopamine Neurons Revealed by Systematic Input-Output Mapping. *Cell* *162*, 622-634.
- Berkley, K.J., and Hand, P.J. (1978). Projections to the inferior olive of the cat. II. Comparisons of input from the gracile, cuneate and the spinal trigeminal nuclei. *The Journal of comparative neurology* *180*, 253-264.
- Berkley, K.J., and Worden, I.G. (1978). [Projections to the inferior olive of the cat. I. Comparisons of input from the dorsal column nuclei, the lateral cervical nucleus, the spino-olivary pathways, the cerebral cortex and the cerebellum]. *The Journal of comparative neurology* *180*, 237-251.
- Bernstein, B.E., Mikkelsen, T.S., Xie, X., Kamal, M., Huebert, D.J., Cuff, J., Fry, B., Meissner, A., Wernig, M., Plath, K., *et al.* (2006). A bivalent chromatin structure marks key developmental genes in embryonic stem cells. *Cell* *125*, 315-326.
- Bhanot, P., Brink, M., Samos, C.H., Hsieh, J.C., Wang, Y., Macke, J.P., Andrew, D., Nathans, J., and Nusse, R. (1996). A new member of the frizzled family from *Drosophila* functions as a Wingless receptor. *Nature* *382*, 225-230.

- Bjaalie, J.G., and Brodal, P. (1997). Cat pontocerebellar network: numerical capacity and axonal collateral branching of neurones in the pontine nuclei projecting to individual parafloccular folia. *Neurosci Res* 27, 199-210.
- Bjaalie, J.G., Diggle, P.J., Nikundiwe, A., Karagulle, T., and Brodal, P. (1991). Spatial segregation between populations of ponto-cerebellar neurons: statistical analysis of multivariate spatial interactions. *Anat Rec* 231, 510-523.
- Bjaalie, J.G., and Leergaard, T.B. (2000). Functions of the pontine nuclei in cerebro-cerebellar communication. *Trends Neurosci* 23, 152.
- Bloch-Gallego, E., Ezan, F., Tessier-Lavigne, M., and Sotelo, C. (1999). Floor plate and netrin-1 are involved in the migration and survival of inferior olivary neurons. *J Neurosci* 19, 4407-4420.
- Border, B.G., and Mihailoff, G.A. (1990). GABAergic neural elements in the rat basilar pons: electron microscopic immunocytochemistry. *The Journal of comparative neurology* 295, 123-135.
- Boyer, L.A., Plath, K., Zeitlinger, J., Brambrink, T., Medeiros, L.A., Lee, T.I., Levine, S.S., Wernig, M., Tajonar, A., Ray, M.K., *et al.* (2006). Polycomb complexes repress developmental regulators in murine embryonic stem cells. *Nature* 441, 349-353.
- Brand, N., Petkovich, M., Krust, A., Chambon, P., de The, H., Marchio, A., Tiollais, P., and Dejean, A. (1988). Identification of a second human retinoic acid receptor. *Nature* 332, 850-853.
- Broch-Smith, T., and Brodal, P. (1990). Organization of the cortico-ponto-cerebellar pathway to the dorsal paraflocculus. An experimental study with anterograde and retrograde transport of WGA-HRP in the cat. *Arch Ital Biol* 128, 249-271.
- Brodal, P., and Bjaalie, J.G. (1992). Organization of the pontine nuclei. *Neurosci Res* 13, 83-118.
- Brunner, E., Peter, O., Schweizer, L., and Basler, K. (1997). pangolin encodes a Lef-1 homologue that acts downstream of Armadillo to transduce the Wingless signal in *Drosophila*. *Nature* 385, 829-833.
- Buch, T., Heppner, F.L., Tertilt, C., Heinen, T.J., Kremer, M., Wunderlich, F.T., Jung, S., and Waisman, A. (2005). A Cre-inducible diphtheria toxin receptor mediates cell lineage ablation after toxin administration. *Nat Methods* 2, 419-426.
- Buenrostro, J.D., Wu, B., Chang, H.Y., and Greenleaf, W.J. (2015). ATAC-seq: A Method for Assaying Chromatin Accessibility Genome-Wide. *Curr Protoc Mol Biol* 109, 21.29-21.29.
- Bulfone, A., Menguzzato, E., Broccoli, V., Marchitelli, A., Gattuso, C., Mariani, M., Consalez, G.G., Martinez, S., Ballabio, A., and Banfi, S. (2000). Barhl1, a gene belonging to a new subfamily of mammalian homeobox genes, is expressed in migrating neurons of the CNS. *Hum Mol Genet* 9, 1443-1452.

- Burgold, T., Voituron, N., Caganova, M., Tripathi, P.P., Menuet, C., Tusi, B.K., Spreafico, F., Bevingut, M., Gestreau, C., Buontempo, S., *et al.* (2012). The H3K27 demethylase JMJD3 is required for maintenance of the embryonic respiratory neuronal network, neonatal breathing, and survival. *Cell Rep* 2, 1244-1258.
- Cabrera, C.V., Alonso, M.C., Johnston, P., Phillips, R.G., and Lawrence, P.A. (1987). Phenocopies induced with antisense RNA identify the wingless gene. *Cell* 50, 659-663.
- Cammas, L., Romand, R., Fraulob, V., Mura, C., and Dolle, P. (2007). Expression of the murine retinol dehydrogenase 10 (Rdh10) gene correlates with many sites of retinoid signalling during embryogenesis and organ differentiation. *Dev Dynam* 236, 2899-2908.
- Cao, R., Tsukada, Y., and Zhang, Y. (2005). Role of Bmi-1 and Ring1A in H2A ubiquitylation and Hox gene silencing. *Mol Cell* 20, 845-854.
- Carpenter, E.M., Goddard, J.M., Chisaka, O., Manley, N.R., and Capecchi, M.R. (1993). Loss of Hox-A1 (Hox-1.6) function results in the reorganization of the murine hindbrain. *Development* 118, 1063-1075.
- Casali, A., and Struhl, G. (2004). Reading the Hedgehog morphogen gradient by measuring the ratio of bound to unbound Patched protein. *Nature* 431, 76-80.
- Cerminara, N.L., Aoki, H., Loft, M., Sugihara, I., and Apps, R. (2013). Structural basis of cerebellar microcircuits in the rat. *J Neurosci* 33, 16427-16442.
- Chambeyron, S., and Bickmore, W.A. (2004). Chromatin decondensation and nuclear reorganization of the HoxB locus upon induction of transcription. *Genes Dev* 18, 1119-1130.
- Chambeyron, S., Da Silva, N.R., Lawson, K.A., and Bickmore, W.A. (2005). Nuclear re-organisation of the Hoxb complex during mouse embryonic development. *Development* 132, 2215-2223.
- Chambon, P. (1996). A decade of molecular biology of retinoic acid receptors. *Faseb J* 10, 940-954.
- Chapin, J.K., and Lin, C.S. (1984). Mapping the body representation in the SI cortex of anesthetized and awake rats. *The Journal of comparative neurology* 229, 199-213.
- Charite, J., de Graaff, W., Consten, D., Reijnen, M.J., Korving, J., and Deschamps, J. (1998). Transducing positional information to the Hox genes: critical interaction of cdx gene products with position-sensitive regulatory elements. *Development* 125, 4349-4358.
- Chedotal, A., Pourquie, O., Ezan, F., San Clemente, H., and Sotelo, C. (1996). BEN as a presumptive target recognition molecule during the development of the olivocerebellar system. *J Neurosci* 16, 3296-3310.
- Chen, W., ten Berge, D., Brown, J., Ahn, S., Hu, L.A., Miller, W.E., Caron, M.G., Barak, L.S., Nusse, R., and Lefkowitz, R.J. (2003). Dishevelled 2 recruits beta-arrestin 2 to mediate Wnt5A-stimulated endocytosis of Frizzled 4. *Science* 301, 1391-1394.

- Coleman, K.A., Baker, G.E., and Mitrofanis, J. (1997). Topography of fibre organisation in the corticofugal pathways of rats. *The Journal of comparative neurology* 381, 143-157.
- Crick, F. (1970). Diffusion in embryogenesis. *Nature* 225, 420-422.
- D'Angelo, E., and Casali, S. (2012). Seeking a unified framework for cerebellar function and dysfunction: from circuit operations to cognition. *Front Neural Circuits* 6, 116.
- Dahle, O., Kumar, A., and Kuehn, M.R. (2010). Nodal signaling recruits the histone demethylase Jmjd3 to counteract polycomb-mediated repression at target genes. *Sci Signal* 3, ra48.
- Damm, K., Heyman, R.A., Umesono, K., and Evans, R.M. (1993). Functional inhibition of retinoic acid response by dominant negative retinoic acid receptor mutants. *Proc Natl Acad Sci U S A* 90, 2989-2993.
- Danielian, P.S., Muccino, D., Rowitch, D.H., Michael, S.K., and McMahon, A.P. (1998). Modification of gene activity in mouse embryos in utero by a tamoxifen-inducible form of Cre recombinase. *Curr Biol* 8, 1323-1326.
- Dasen, J.S., and Jessell, T.M. (2009). Hox networks and the origins of motor neuron diversity. *Curr Top Dev Biol* 88, 169-200.
- Dasen, J.S., Tice, B.C., Brenner-Morton, S., and Jessell, T.M. (2005). A Hox regulatory network establishes motor neuron pool identity and target-muscle connectivity. *Cell* 123, 477-491.
- Davenne, M., Maconochie, M.K., Neun, R., Pattyn, A., Chambon, P., Krumlauf, R., and Rijli, F.M. (1999). Hoxa2 and Hoxb2 control dorsoventral patterns of neuronal development in the rostral hindbrain. *Neuron* 22, 677-691.
- Davis, A.P., Witte, D.P., Hsieh-Li, H.M., Potter, S.S., and Capecchi, M.R. (1995). Absence of radius and ulna in mice lacking hoxa-11 and hoxd-11. *Nature* 375, 791-795.
- de Diego, I., Kyriakopoulou, K., Karagogeos, D., and Wassef, M. (2002). Multiple influences on the migration of precerebellar neurons in the caudal medulla. *Development* 129, 297-306.
- De Kumar, B., Parrish, M.E., Slaughter, B.D., Unruh, J.R., Gogol, M., Seidel, C., Paulson, A., Li, H., Gaudenz, K., Peak, A., *et al.* (2015). Analysis of dynamic changes in retinoid-induced transcription and epigenetic profiles of murine Hox clusters in ES cells. *Genome Res.*
- De Luca, L., Little, E.P., and Wolf, G. (1969). Vitamin A and protein synthesis by rat intestinal mucosa. *The Journal of biological chemistry* 244, 701-708.
- De Santa, F., Totaro, M.G., Prosperini, E., Notarbartolo, S., Testa, G., and Natoli, G. (2007). The histone H3 lysine-27 demethylase Jmjd3 links inflammation to inhibition of polycomb-mediated gene silencing. *Cell* 130, 1083-1094.

Del Rizzo, P.A., and Trievel, R.C. (2011). Substrate and product specificities of SET domain methyltransferases. *Epigenetics* 6, 1059-1067.

del Toro, E.D., Borday, V., Davenne, M., Neun, R., Rijli, F.M., and Champagnat, J. (2001). Generation of a novel functional neuronal circuit in *Hoxa1* mutant mice. *J Neurosci* 21, 5637-5642.

Deschamps, J. (2007). Ancestral and recently recruited global control of the Hox genes in development. *Curr Opin Genet Dev* 17, 422-427.

Di Bonito, M., Narita, Y., Avallone, B., Sequino, L., Mancuso, M., Andolfi, G., Franze, A.M., Puelles, L., Rijli, F.M., and Studer, M. (2013). Assembly of the auditory circuitry by a Hox genetic network in the mouse brainstem. *PLoS Genet* 9, e1003249.

Di Meglio, T., Kratochwil, C.F., Vilain, N., Loche, A., Vitobello, A., Yonehara, K., Hrycaj, S.M., Roska, B., Peters, A.H., Eichmann, A., *et al.* (2013). *Ezh2* orchestrates topographic migration and connectivity of mouse precerebellar neurons. *Science* 339, 204-207.

Di Meglio, T., Nguyen-Ba-Charvet, K.T., Tessier-Lavigne, M., Sotelo, C., and Chedotal, A. (2008). Molecular mechanisms controlling midline crossing by precerebellar neurons. *J Neurosci* 28, 6285-6294.

Di Meglio, T., and Rijli, F.M. (2013). Transcriptional Regulation of Tangential Neuronal Migration in the Vertebrate Hindbrain. *Comprehensive Developmental Neuroscience: Cellular Migration and Formation of Neuronal Connections vol. 2*, 377-404.

Dolle, P., Dierich, A., LeMeur, M., Schimmang, T., Schuhbauer, B., Chambon, P., and Duboule, D. (1993). Disruption of the *Hoxd-13* gene induces localized heterochrony leading to mice with neotenic limbs. *Cell* 75, 431-441.

Driever, W., and Nusslein-Volhard, C. (1988a). The bicoid protein determines position in the *Drosophila* embryo in a concentration-dependent manner. *Cell* 54, 95-104.

Driever, W., and Nusslein-Volhard, C. (1988b). A gradient of bicoid protein in *Drosophila* embryos. *Cell* 54, 83-93.

Duboule, D., and Morata, G. (1994). Colinearity and Functional Hierarchy among Genes of the Homeotic Complexes. *Trends in Genetics* 10, 358-364.

Dubrulle, J., and Pourquie, O. (2004). *fgf8* mRNA decay establishes a gradient that couples axial elongation to patterning in the vertebrate embryo. *Nature* 427, 419-422.

Dupe, V., Davenne, M., Brocard, J., Dolle, P., Mark, M., Dierich, A., Chambon, P., and Rijli, F.M. (1997). In vivo functional analysis of the *Hoxa-1* 3' retinoic acid response element (3'RARE). *Development* 124, 399-410.

Dupe, V., Matt, N., Garnier, J.M., Chambon, P., Mark, M., and Ghyselinck, N.B. (2003). A newborn lethal defect due to inactivation of retinaldehyde dehydrogenase type 3 is prevented by maternal retinoic acid treatment. *Proc Natl Acad Sci U S A* 100, 14036-14041.

Durston, A.J., Timmermans, J.P., Hage, W.J., Hendriks, H.F., de Vries, N.J., Heideveld, M., and Nieuwkoop, P.D. (1989). Retinoic acid causes an anteroposterior transformation in the developing central nervous system. *Nature* *340*, 140-144.

Dymecki, S.M., and Tomasiewicz, H. (1998). Using Flp-recombinase to characterize expansion of Wnt1-expressing neural progenitors in the mouse. *Dev Biol* *201*, 57-65.

Dyson, S., and Gurdon, J.B. (1998). The interpretation of position in a morphogen gradient as revealed by occupancy of activin receptors. *Cell* *93*, 557-568.

Echelard, Y., Epstein, D.J., St-Jacques, B., Shen, L., Mohler, J., McMahon, J.A., and McMahon, A.P. (1993). Sonic hedgehog, a member of a family of putative signaling molecules, is implicated in the regulation of CNS polarity. *Cell* *75*, 1417-1430.

Erzurumlu, R.S., Murakami, Y., and Rijli, F.M. (2010). Mapping the face in the somatosensory brainstem. *Nat Rev Neurosci* *11*, 252-263.

Estaras, C., Akizu, N., Garcia, A., Beltran, S., de la Cruz, X., and Martinez-Balbas, M.A. (2012). Genome-wide analysis reveals that Smad3 and JMJD3 HDM co-activate the neural developmental program. *Development* *139*, 2681-2691.

Esteve, P., Sandonis, A., Ibanez, C., Shimono, A., Guerrero, I., and Bovolenta, P. (2011). Secreted frizzled-related proteins are required for Wnt/beta-catenin signalling activation in the vertebrate optic cup. *Development* *138*, 4179-4184.

Feller, J., Schneider, A., Schuster-Gossler, K., and Gossler, A. (2008). Noncyclic Notch activity in the presomitic mesoderm demonstrates uncoupling of somite compartmentalization and boundary formation. *Genes Dev* *22*, 2166-2171.

Ferguson, E.L., and Anderson, K.V. (1992). Decapentaplegic acts as a morphogen to organize dorsal-ventral pattern in the *Drosophila* embryo. *Cell* *71*, 451-461.

Ferraiuolo, M.A., Rousseau, M., Miyamoto, C., Shenker, S., Wang, X.Q., Nadler, M., Blanchette, M., and Dostie, J. (2010). The three-dimensional architecture of Hox cluster silencing. *Nucleic Acids Res* *38*, 7472-7484.

Fiala, A., Suska, A., and Schluter, O.M. (2010). Optogenetic approaches in neuroscience. *Curr Biol* *20*, R897-903.

Flora, A., Garcia, J.J., Thaller, C., and Zoghbi, H.Y. (2007). The E-protein Tcf4 interacts with Math1 to regulate differentiation of a specific subset of neuronal progenitors. *Proc Natl Acad Sci U S A* *104*, 15382-15387.

Fromental-Ramain, C., Warot, X., Messadecq, N., LeMeur, M., Dolle, P., and Chambon, P. (1996). Hoxa-13 and Hoxd-13 play a crucial role in the patterning of the limb autopod. *Development* *122*, 2997-3011.

Fu, Y., Tvrdik, P., Makki, N., Machold, R., Paxinos, G., and Watson, C. (2013). The interfascicular trigeminal nucleus: a precerebellar nucleus in the mouse defined by retrograde

neuronal tracing and genetic fate mapping. *The Journal of comparative neurology* 521, 697-708.

Fu, Y., Tvrdik, P., Makki, N., Palombi, O., Machold, R., Paxinos, G., and Watson, C. (2009). The precerebellar linear nucleus in the mouse defined by connections, immunohistochemistry, and gene expression. *Brain Res* 1271, 49-59.

Fujii, H., Sato, T., Kaneko, S., Gotoh, O., Fujii-Kuriyama, Y., Osawa, K., Kato, S., and Hamada, H. (1997). Metabolic inactivation of retinoic acid by a novel P450 differentially expressed in developing mouse embryos. *Embo J* 16, 4163-4173.

Gaidatzis, D., Lerch, A., Hahne, F., and Stadler, M.B. (2015). QuasR: quantification and annotation of short reads in R. *Bioinformatics* 31, 1130-1132.

Gale, E., Zile, M., and Maden, M. (1999). Hindbrain respecification in the retinoid-deficient quail. *Mech Dev* 89, 43-54.

Gale, N.W., Holland, S.J., Valenzuela, D.M., Flenniken, A., Pan, L., Ryan, T.E., Henkemeyer, M., Strebhardt, K., Hirai, H., Wilkinson, D.G., *et al.* (1996). Eph receptors and ligands comprise two major specificity subclasses and are reciprocally compartmentalized during embryogenesis. *Neuron* 17, 9-19.

Gallet, A., Staccini-Lavenant, L., and Therond, P.P. (2008). Cellular trafficking of the glypican Dally-like is required for full-strength Hedgehog signaling and wingless transcytosis. *Dev Cell* 14, 712-725.

Gaufo, G.O., Thomas, K.R., and Capecchi, M.R. (2003). Hox3 genes coordinate mechanisms of genetic suppression and activation in the generation of branchial and somatic motoneurons. *Development* 130, 5191-5201.

Gavalas, A. (2002). ArRAnging the hindbrain. *Trends Neurosci* 25, 61-64.

Gavalas, A., Davenne, M., Lumsden, A., Chambon, P., and Rijli, F.M. (1997). Role of Hoxa-2 in axon pathfinding and rostral hindbrain patterning. *Development* 124, 3693-3702.

Gavalas, A., and Krumlauf, R. (2000). Retinoid signalling and hindbrain patterning. *Curr Opin Genet Dev* 10, 380-386.

Gavalas, A., Ruhrberg, C., Livet, J., Henderson, C.E., and Krumlauf, R. (2003). Neuronal defects in the hindbrain of Hoxa1, Hoxb1 and Hoxb2 mutants reflect regulatory interactions among these Hox genes. *Development* 130, 5663-5679.

Gehring, W.J., Kloter, U., and Suga, H. (2009). Evolution of the Hox gene complex from an evolutionary ground state. *Curr Top Dev Biol* 88, 35-61.

Geisen, M.J., Di Meglio, T., Pasqualetti, M., Ducret, S., Brunet, J.F., Chedotal, A., and Rijli, F.M. (2008). Hox paralog group 2 genes control the migration of mouse pontine neurons through slit-robo signaling. *PLoS Biol* 6, e142.

- Geisler, S.J., and Paro, R. (2015). Trithorax and Polycomb group-dependent regulation: a tale of opposing activities. *Development* *142*, 2876-2887.
- Giguere, V., Ong, E.S., Segui, P., and Evans, R.M. (1987). Identification of a receptor for the morphogen retinoic acid. *Nature* *330*, 624-629.
- Glickstein, M., May, J., and Mercier, B. (1990). Visual corticopontine and tectopontine projections in the macaque. *Arch Ital Biol* *128*, 273-293.
- Glickstein, M., May, J.G., 3rd, and Mercier, B.E. (1985). Corticopontine projection in the macaque: the distribution of labelled cortical cells after large injections of horseradish peroxidase in the pontine nuclei. *The Journal of comparative neurology* *235*, 343-359.
- Glover, J.C., Renaud, J.S., and Rijli, F.M. (2006). Retinoic acid and hindbrain patterning. *J Neurobiol* *66*, 705-725.
- Gregor, T., Wieschaus, E.F., McGregor, A.P., Bialek, W., and Tank, D.W. (2007). Stability and nuclear dynamics of the bicoid morphogen gradient. *Cell* *130*, 141-152.
- Grieneisen, V.A., Scheres, B., Hogeweg, P., and AF, M.M. (2012). Morphogengineering roots: comparing mechanisms of morphogen gradient formation. *BMC Syst Biol* *6*, 37.
- Guthrie, S., and Lumsden, A. (1991). Formation and regeneration of rhombomere boundaries in the developing chick hindbrain. *Development* *112*, 221-229.
- Guthrie, S., Prince, V., and Lumsden, A. (1993). Selective dispersal of avian rhombomere cells in orthotopic and heterotopic grafts. *Development* *118*, 527-538.
- Harikumar, A., and Meshorer, E. (2015). Chromatin remodeling and bivalent histone modifications in embryonic stem cells. *EMBO Rep* *16*, 1609-1619.
- Hart, C.P., Fainsod, A., and Ruddle, F.H. (1987). Sequence analysis of the murine Hox-2.2, -2.3, and -2.4 homeo boxes: evolutionary and structural comparisons. *Genomics* *1*, 182-195.
- Hart, M.J., de los Santos, R., Albert, I.N., Rubinfeld, B., and Polakis, P. (1998). Downregulation of beta-catenin by human Axin and its association with the APC tumor suppressor, beta-catenin and GSK3 beta. *Curr Biol* *8*, 573-581.
- Harterink, M., and Korswagen, H.C. (2012). Dissecting the Wnt secretion pathway: key questions on the modification and intracellular trafficking of Wnt proteins. *Acta Physiol (Oxf)* *204*, 8-16.
- Heintzman, N.D., Hon, G.C., Hawkins, R.D., Kheradpour, P., Stark, A., Harp, L.F., Ye, Z., Lee, L.K., Stuart, R.K., Ching, C.W., *et al.* (2009). Histone modifications at human enhancers reflect global cell-type-specific gene expression. *Nature* *459*, 108-112.
- Helms, A.W., Abney, A.L., Ben-Arie, N., Zoghbi, H.Y., and Johnson, J.E. (2000). Autoregulation and multiple enhancers control Math1 expression in the developing nervous system. *Development* *127*, 1185-1196.

- Herr, P., and Basler, K. (2012). Porcupine-mediated lipidation is required for Wnt recognition by Wls. *Dev Biol* 361, 392-402.
- Herrero, L., Pardoe, J., and Apps, R. (2002). Pontine and lateral reticular projections to the c1 zone in lobulus simplex and paramedian lobule of the rat cerebellar cortex. *Cerebellum* 1, 185-199.
- Hikasa, H., and Sokol, S.Y. (2013). Wnt signaling in vertebrate axis specification. *Cold Spring Harb Perspect Biol* 5, a007955.
- Hippenmeyer, S., Vrieseling, E., Sigrist, M., Portmann, T., Laengle, C., Ladle, D.R., and Arber, S. (2005). A developmental switch in the response of DRG neurons to ETS transcription factor signaling. *PLoS Biol* 3, e159.
- Hirsinger, E., Jouve, C., Dubrulle, J., and Pourquie, O. (2000). Somite formation and patterning. *Int Rev Cytol* 198, 1-65.
- His, W. (1891). Die Entwicklung des menschlichen Rautenhirns vom Ende des ersten bis zum Beginn des dritten Monats Der mathematisch-physischen Classe der Koeniglich Saechsischen Gesellschaft der Wissenschaften 17, 1-74.
- Holland, P.W. (2013). Evolution of homeobox genes. *Wiley Interdiscip Rev Dev Biol* 2, 31-45.
- Horan, G.S., Ramirez-Solis, R., Featherstone, M.S., Wolgemuth, D.J., Bradley, A., and Behringer, R.R. (1995). Compound mutants for the paralogous *hoxa-4*, *hoxb-4*, and *hoxd-4* genes show more complete homeotic transformations and a dose-dependent increase in the number of vertebrae transformed. *Genes Dev* 9, 1667-1677.
- Huang, C.C., Sugino, K., Shima, Y., Guo, C., Bai, S., Menseh, B.D., Nelson, S.B., and Hantman, A.W. (2013). Convergence of pontine and proprioceptive streams onto multimodal cerebellar granule cells. *Elife* 2, e00400.
- Huang, D., Chen, S.W., and Gudas, L.J. (2002). Analysis of two distinct retinoic acid response elements in the homeobox gene *Hoxb1* in transgenic mice. *Dev Dyn* 223, 353-370.
- Huang, D., Chen, S.W., Langston, A.W., and Gudas, L.J. (1998). A conserved retinoic acid responsive element in the murine *Hoxb-1* gene is required for expression in the developing gut. *Development* 125, 3235-3246.
- Huang, X., Ketova, T., Fleming, J.T., Wang, H., Dey, S.K., Litingtung, Y., and Chiang, C. (2009). Sonic hedgehog signaling regulates a novel epithelial progenitor domain of the hindbrain choroid plexus. *Development* 136, 2535-2543.
- Hunter, N.L., and Dymecki, S.M. (2007). Molecularly and temporally separable lineages form the hindbrain roof plate and contribute differentially to the choroid plexus. *Development* 134, 3449-3460.

Hunter, N.L., Hikasa, H., Dymecki, S.M., and Sokol, S.Y. (2006). Vertebrate homologues of Frodo are dynamically expressed during embryonic development in tissues undergoing extensive morphogenetic movements. *Dev Dyn* 235, 279-284.

Iida, A., Iwagawa, T., Kuribayashi, H., Satoh, S., Mochizuki, Y., Baba, Y., Nakauchi, H., Furukawa, T., Koseki, H., Murakami, A., *et al.* (2014). Histone demethylase Jmjd3 is required for the development of subsets of retinal bipolar cells. *Proc Natl Acad Sci U S A* 111, 3751-3756.

Imura, T., and Pourquie, O. (2006). Collinear activation of Hoxb genes during gastrulation is linked to mesoderm cell ingression. *Nature* 442, 568-571.

Ikeya, M., and Takada, S. (2001). Wnt-3a is required for somite specification along the anteroposterior axis of the mouse embryo and for regulation of cdx-1 expression. *Mech Dev* 103, 27-33.

Ingham, P.W. (1985). A clonal analysis of the requirement for the trithorax gene in the diversification of segments in *Drosophila*. *J Embryol Exp Morphol* 89, 349-365.

Itoh, K., Antipova, A., Ratcliffe, M.J., and Sokol, S. (2000). Interaction of dishevelled and Xenopus axin-related protein is required for wnt signal transduction. *Mol Cell Biol* 20, 2228-2238.

Itoh, K., and Sokol, S.Y. (1997). Graded amounts of Xenopus dishevelled specify discrete anteroposterior cell fates in prospective ectoderm. *Mech Dev* 61, 113-125.

Jho, E.H., Zhang, T., Domon, C., Joo, C.K., Freund, J.N., and Costantini, F. (2002). Wnt/beta-catenin/Tcf signaling induces the transcription of Axin2, a negative regulator of the signaling pathway. *Mol Cell Biol* 22, 1172-1183.

Ji, Z., and Hawkes, R. (1994). Topography of Purkinje cell compartments and mossy fiber terminal fields in lobules II and III of the rat cerebellar cortex: spinocerebellar and cuneocerebellar projections. *Neuroscience* 61, 935-954.

Jiang, W., Wang, J., and Zhang, Y. (2013). Histone H3K27me3 demethylases KDM6A and KDM6B modulate definitive endoderm differentiation from human ESCs by regulating WNT signaling pathway. *Cell Res* 23, 122-130.

Johnson, B.C., Kennedy, M., and Chiba, N. (1969). Vitamin A and nuclear RNA synthesis. *Am J Clin Nutr* 22, 1048-1058.

Jung, H., Lacombe, J., Mazzoni, E.O., Liem, K.F., Jr., Grinstein, J., Mahony, S., Mukhopadhyay, D., Gifford, D.K., Young, R.A., Anderson, K.V., *et al.* (2010). Global control of motor neuron topography mediated by the repressive actions of a single hox gene. *Neuron* 67, 781-796.

Jungbluth, S., Bell, E., and Lumsden, A. (1999). Specification of distinct motor neuron identities by the singular activities of individual Hox genes. *Development* 126, 2751-2758.

Kalb, R., Latwiel, S., Baymaz, H.I., Jansen, P.W., Muller, C.W., Vermeulen, M., and Muller, J. (2014). Histone H2A monoubiquitination promotes histone H3 methylation in Polycomb repression. *Nat Struct Mol Biol* 21, 569-571.

Kalinovsky, A., Boukhtouche, F., Blazeski, R., Bornmann, C., Suzuki, N., Mason, C.A., and Scheiffele, P. (2011). Development of axon-target specificity of ponto-cerebellar afferents. *PLoS Biol* 9, e1001013.

Kaprielian, Z., Runko, E., and Imondi, R. (2001). Axon guidance at the midline choice point. *Dev Dyn* 221, 154-181.

Kartikasari, A.E., Zhou, J.X., Kanji, M.S., Chan, D.N., Sinha, A., Grapin-Botton, A., Magnuson, M.A., Lowry, W.E., and Bhushan, A. (2013). The histone demethylase Jmjd3 sequentially associates with the transcription factors Tbx3 and Eomes to drive endoderm differentiation. *Embo J* 32, 1393-1408.

Kashyap, V., Gudas, L.J., Brenet, F., Funk, P., Viale, A., and Scandura, J.M. (2011). Epigenomic reorganization of the clustered Hox genes in embryonic stem cells induced by retinoic acid. *The Journal of biological chemistry* 286, 3250-3260.

Kashyap, V., Laursen, K.B., Brenet, F., Viale, A.J., Scandura, J.M., and Gudas, L.J. (2013). RARgamma is essential for retinoic acid induced chromatin remodeling and transcriptional activation in embryonic stem cells. *J Cell Sci* 126, 999-1008.

Kawaguchi, R., Yu, J.M., Honda, J., Hu, J., Whitelegge, J., Ping, P.P., Wiita, P., Bok, D., and Sun, H. (2007). A membrane receptor for retinol binding protein mediates cellular uptake of vitamin A. *Science* 315, 820-825.

Kawauchi, D., Taniguchi, H., Watanabe, H., Saito, T., and Murakami, F. (2006). Direct visualization of nucleogenesis by precerebellar neurons: involvement of ventricle-directed, radial fibre-associated migration. *Development* 133, 1113-1123.

Kessel, M., and Gruss, P. (1991). Homeotic Transformations of Murine Vertebrae and Concomitant Alteration of Hox Codes Induced by Retinoic Acid. *Cell* 67, 89-104.

Kim, C.H., Oda, T., Itoh, M., Jiang, D., Artinger, K.B., Chandrasekharappa, S.C., Driever, W., and Chitnis, A.B. (2000). Repressor activity of Headless/Tcf3 is essential for vertebrate head formation. *Nature* 407, 913-916.

Kim, H.D., and O'Shea, E.K. (2008). A quantitative model of transcription factor-activated gene expression. *Nat Struct Mol Biol* 15, 1192-1198.

Kishida, S., Yamamoto, H., Ikeda, S., Kishida, M., Sakamoto, I., Koyama, S., and Kikuchi, A. (1998). Axin, a negative regulator of the wnt signaling pathway, directly interacts with adenomatous polyposis coli and regulates the stabilization of beta-catenin. *The Journal of biological chemistry* 273, 10823-10826.

Kmita, M., and Duboule, D. (2003). Organizing axes in time and space; 25 years of colinear tinkering. *Science* 301, 331-333.

- Kmita, M., van der Hoeven, F., Zakany, J., Krumlauf, R., and Duboule, D. (2000). Mechanisms of Hox gene colinearity: transposition of the anterior Hoxb1 gene into the posterior HoxD complex. *Genes Dev* *14*, 198-211.
- Kolmac, C.I., Power, B.D., and Mitrofanis, J. (1998). Patterns of connections between zona incerta and brainstem in rats. *J Comp Neurol* *396*, 544-555.
- Kolodkin, A.L., and Tessier-Lavigne, M. (2011). Mechanisms and molecules of neuronal wiring: a primer. *Cold Spring Harb Perspect Biol* *3*.
- Komiya, Y., and Habas, R. (2008). Wnt signal transduction pathways. *Organogenesis* *4*, 68-75.
- Kosinski, R.J., Neafsey, E.J., and Castro, A.J. (1986). A comparative topographical analysis of dorsal column nuclear and cerebral cortical projections to the basilar pontine gray in rats. *The Journal of comparative neurology* *244*, 163-173.
- Kratochwil, C. (2013). Transcriptional and epigenetic regulation of neuronal migration and circuitry development in the murine hindbrain. Dissertation.
- Krauss, S., Korzh, V., Fjose, A., and Johansen, T. (1992). Expression of four zebrafish wnt-related genes during embryogenesis. *Development* *116*, 249-259.
- Krumlauf, R. (1994). Hox Genes in Vertebrate Development. *Cell* *78*, 191-201.
- Kuhl, M., Sheldahl, L.C., Park, M., Miller, J.R., and Moon, R.T. (2000). The Wnt/Ca²⁺ pathway: a new vertebrate Wnt signaling pathway takes shape. *Trends Genet* *16*, 279-283.
- Kumamoto, T., and Hanashima, C. (2014). Neuronal subtype specification in establishing mammalian neocortical circuits. *Neurosci Res* *86*, 37-49.
- Lan, F., Bayliss, P.E., Rinn, J.L., Whetstine, J.R., Wang, J.K., Chen, S., Iwase, S., Alpatov, R., Issaeva, I., Canaani, E., *et al.* (2007). A histone H3 lysine 27 demethylase regulates animal posterior development. *Nature* *449*, 689-694.
- Landsberg, R.L., Awatramani, R.B., Hunter, N.L., Farago, A.F., DiPietrantonio, H.J., Rodriguez, C.I., and Dymecki, S.M. (2005). Hindbrain rhombic lip is comprised of discrete progenitor cell populations allocated by Pax6. *Neuron* *48*, 933-947.
- Larabell, C.A., Torres, M., Rowning, B.A., Yost, C., Miller, J.R., Wu, M., Kimelman, D., and Moon, R.T. (1997). Establishment of the dorso-ventral axis in *Xenopus* embryos is presaged by early asymmetries in beta-catenin that are modulated by the Wnt signaling pathway. *J Cell Biol* *136*, 1123-1136.
- Laursen, K.B., Mongan, N.P., Zhuang, Y., Ng, M.M., Benoit, Y.D., and Gudas, L.J. (2013). Polycomb recruitment attenuates retinoic acid-induced transcription of the bivalent NR2F1 gene. *Nucleic Acids Res* *41*, 6430-6443.

- Lee, M.G., Villa, R., Trojer, P., Norman, J., Yan, K.P., Reinberg, D., Di Croce, L., and Shiekhatter, R. (2007). Demethylation of H3K27 regulates polycomb recruitment and H2A ubiquitination. *Science* 318, 447-450.
- Leergaard, T.B. (2003). Clustered and laminar topographic patterns in rat cerebro-pontine pathways. *Anat Embryol (Berl)* 206, 149-162.
- Leergaard, T.B., and Bjaalie, J.G. (2007). Topography of the complete corticopontine projection: from experiments to principal Maps. *Front Neurosci* 1, 211-223.
- Leergaard, T.B., Lakke, E.A., and Bjaalie, J.G. (1995). Topographical organization in the early postnatal corticopontine projection: a carbocyanine dye and 3-D computer reconstruction study in the rat. *The Journal of comparative neurology* 361, 77-94.
- Leergaard, T.B., Lillehaug, S., De Schutter, E., Bower, J.M., and Bjaalie, J.G. (2006). Topographical organization of pathways from somatosensory cortex through the pontine nuclei to tactile regions of the rat cerebellar hemispheres. *Eur J Neurosci* 24, 2801-2812.
- Lefebvre, P., Martin, P.J., Flajollet, S., Dedieu, S., Billaut, X., and Lefebvre, B. (2005). Transcriptional activities of retinoic acid receptors. *Vitam Horm* 70, 199-264.
- Legg, C.R., Mercier, B., and Glickstein, M. (1989). Corticopontine projection in the rat: the distribution of labelled cortical cells after large injections of horseradish peroxidase in the pontine nuclei. *J Comp Neurol* 286, 427-441.
- Leid, M., Kastner, P., Lyons, R., Nakshatri, H., Saunders, M., Zacharewski, T., Chen, J.Y., Staub, A., Garnier, J.M., Mader, S., *et al.* (1992). Purification, cloning, and RXR identity of the HeLa cell factor with which RAR or TR heterodimerizes to bind target sequences efficiently. *Cell* 68, 377-395.
- Lein, E.S., Hawrylycz, M.J., Ao, N., Ayres, M., Bensinger, A., Bernard, A., Boe, A.F., Boguski, M.S., Brockway, K.S., Byrnes, E.J., *et al.* (2007). Genome-wide atlas of gene expression in the adult mouse brain. *Nature* 445, 168-176.
- Lengerke, C., Schmitt, S., Bowman, T.V., Jang, I.H., Maouche-Chretien, L., McKinney-Freeman, S., Davidson, A.J., Hammerschmidt, M., Rentzsch, F., Green, J.B., *et al.* (2008). BMP and Wnt specify hematopoietic fate by activation of the Cdx-Hox pathway. *Cell Stem Cell* 2, 72-82.
- Lewis, E.B. (1978). A gene complex controlling segmentation in *Drosophila*. *Nature* 276, 565-570.
- Lewis, W.H. (1904). Experimental studies on the development of the eye in amphibia. I. On the origin of the lens. *Rana palustris*. *American Journal of Anatomy* 3, 505-536.
- Li, S., Qiu, F., Xu, A., Price, S.M., and Xiang, M. (2004). *Barhl1* regulates migration and survival of cerebellar granule cells by controlling expression of the neurotrophin-3 gene. *J Neurosci* 24, 3104-3114.

- Linville, A., Gumusaneli, E., Chandraratna, R.A., and Schilling, T.F. (2004). Independent roles for retinoic acid in segmentation and neuronal differentiation in the zebrafish hindbrain. *Dev Biol* 270, 186-199.
- Liu, Y., Helms, A.W., and Johnson, J.E. (2004). Distinct activities of Msx1 and Msx3 in dorsal neural tube development. *Development* 131, 1017-1028.
- Logan, C.Y., and Nusse, R. (2004). The Wnt signaling pathway in development and disease. *Annu Rev Cell Dev Biol* 20, 781-810.
- Lumsden, A., and Krumlauf, R. (1996). Patterning the vertebrate neuraxis. *Science* 274, 1109-1115.
- Luo, L., and Flanagan, J.G. (2007). Development of continuous and discrete neural maps. *Neuron* 56, 284-300.
- MacLean, G., Abu-Abed, S., Dolle, P., Tahayato, A., Chambon, P., and Petkovich, M. (2001). Cloning of a novel retinoic-acid metabolizing cytochrome P450, Cyp26B1, and comparative expression analysis with Cyp26A1 during early murine development. *Mech Dev* 107, 195-201.
- Maconochie, M.K., Nonchev, S., Studer, M., Chan, S.K., Popperl, H., Sham, M.H., Mann, R.S., and Krumlauf, R. (1997). Cross-regulation in the mouse HoxB complex: the expression of Hoxb2 in rhombomere 4 is regulated by Hoxb1. *Genes Dev* 11, 1885-1895.
- Madisen, L., Mao, T., Koch, H., Zhuo, J.M., Berenyi, A., Fujisawa, S., Hsu, Y.W., Garcia, A.J., 3rd, Gu, X., Zanella, S., *et al.* (2012). A toolbox of Cre-dependent optogenetic transgenic mice for light-induced activation and silencing. *Nat Neurosci* 15, 793-802.
- Madisen, L., Zwingman, T.A., Sunkin, S.M., Oh, S.W., Zariwala, H.A., Gu, H., Ng, L.L., Palmiter, R.D., Hawrylycz, M.J., Jones, A.R., *et al.* (2010). A robust and high-throughput Cre reporting and characterization system for the whole mouse brain. *Nat Neurosci* 13, 133-140.
- Magrotti, E., Borutti, G., Mariani, G., Donati, E., and Faggi, L. (1990). Ataxic hemiparesis syndrome clinical and CT study of 20 new cases. *Funct Neurol* 5, 65-71.
- Mahony, S., Mazzoni, E.O., McCuine, S., Young, R.A., Wichterle, H., and Gifford, D.K. (2011a). Ligand-dependent dynamics of retinoic acid receptor binding during early neurogenesis. *Genome Biol* 12, R2.
- Mahony, S., Mazzoni, E.O., McCuine, S., Young, R.A., Wichterle, H., and Gifford, D.K. (2011b). Ligand-dependent dynamics of retinoic acid receptor binding during early neurogenesis. *Genome Biol* 12.
- Mangelsdorf, D.J., Borgmeyer, U., Heyman, R.A., Zhou, J.Y., Ong, E.S., Oro, A.E., Kakizuka, A., and Evans, R.M. (1992). Characterization of three RXR genes that mediate the action of 9-cis retinoic acid. *Genes Dev* 6, 329-344.
- Mangelsdorf, D.J., Ong, E.S., Dyck, J.A., and Evans, R.M. (1990). Nuclear receptor that identifies a novel retinoic acid response pathway. *Nature* 345, 224-229.

- Manley, N.R., and Capecchi, M.R. (1997). Hox group 3 paralogous genes act synergistically in the formation of somitic and neural crest-derived structures. *Dev Biol* 192, 274-288.
- Manzanares, M., Bel-Vialar, S., Ariza-McNaughton, L., Ferretti, E., Marshall, H., Maconochie, M.M., Blasi, F., and Krumlauf, R. (2001). Independent regulation of initiation and maintenance phases of *Hoxa3* expression in the vertebrate hindbrain involve auto- and cross-regulatory mechanisms. *Development* 128, 3595-3607.
- Mar, A.C., Walker, A.L., Theobald, D.E., Eagle, D.M., and Robbins, T.W. (2011). Dissociable effects of lesions to orbitofrontal cortex subregions on impulsive choice in the rat. *J Neurosci* 31, 6398-6404.
- Marcos, S., Backer, S., Causeret, F., Tessier-Lavigne, M., and Bloch-Gallego, E. (2009). Differential roles of Netrin-1 and its receptor DCC in inferior olivary neuron migration. *Mol Cell Neurosci* 41, 429-439.
- Margueron, R., and Reinberg, D. (2011). The Polycomb complex PRC2 and its mark in life. *Nature* 469, 343-349.
- Marillat, V., Sabatier, C., Failli, V., Matsunaga, E., Sotelo, C., Tessier-Lavigne, M., and Chedotal, A. (2004). The slit receptor Rig-1/Robo3 controls midline crossing by hindbrain precerebellar neurons and axons. *Neuron* 43, 69-79.
- Marin, O., Valdeolmillos, M., and Moya, F. (2006). Neurons in motion: same principles for different shapes? *Trends Neurosci* 29, 655-661.
- Mark, M., Ghyselinck, N.B., and Chambon, P. (2009). Function of retinoic acid receptors during embryonic development. *Nucl Recept Signal* 7, e002.
- Marple-Horvat, D.E., and Stein, J.F. (1990). Neuronal activity in the lateral cerebellum of trained monkeys, related to visual stimuli or to eye movements. *J Physiol* 428, 595-614.
- Marshall, H., Studer, M., Popperl, H., Aparicio, S., Kuroiwa, A., Brenner, S., and Krumlauf, R. (1994). A conserved retinoic acid response element required for early expression of the homeobox gene *Hoxb-1*. *Nature* 370, 567-571.
- McIntyre, D.C., Rakshit, S., Yallowitz, A.R., Loken, L., Jeannotte, L., Capecchi, M.R., and Wellik, D.M. (2007). Hox patterning of the vertebrate rib cage. *Development* 134, 2981-2989.
- McLaughlin, T., and O'Leary, D.D. (2005). Molecular gradients and development of retinotopic maps. *Annu Rev Neurosci* 28, 327-355.
- Mengeling, B.J., Goodson, M.L., Bourguet, W., and Privalsky, M.L. (2012). SMRTepsilon, a corepressor variant, interacts with a restricted subset of nuclear receptors, including the retinoic acid receptors alpha and beta. *Mol Cell Endocrinol* 351, 306-316.
- Mihailoff, G.A. (1983). Intra- and interhemispheric collateral branching in the rat pontocerebellar system, a fluorescence double-label study. *Neuroscience* 10, 141-160.

- Mihailoff, G.A. (1993). Cerebellar nuclear projections from the basilar pontine nuclei and nucleus reticularis tegmenti pontis as demonstrated with PHA-L tracing in the rat. *The Journal of comparative neurology* 330, 130-146.
- Mihailoff, G.A., Burne, R.A., Azizi, S.A., Norell, G., and Woodward, D.J. (1981). The pontocerebellar system in the rat: an HRP study. II. Hemispherical components. *The Journal of comparative neurology* 197, 559-577.
- Mihailoff, G.A., Kosinski, R.J., Azizi, S.A., and Border, B.G. (1989). Survey of noncortical afferent projections to the basilar pontine nuclei: a retrograde tracing study in the rat. *The Journal of comparative neurology* 282, 617-643.
- Moazed, D., and O'Farrell, P.H. (1992). Maintenance of the engrailed expression pattern by Polycomb group genes in *Drosophila*. *Development* 116, 805-810.
- Mock, M., Schwarz, C., and Thier, P. (1997). Electrophysiological properties of rat pontine nuclei neurons In vitro II. Postsynaptic potentials. *J Neurophysiol* 78, 3338-3350.
- Molenaar, M., van de Wetering, M., Oosterwegel, M., Peterson-Maduro, J., Godsave, S., Korinek, V., Roose, J., Destree, O., and Clevers, H. (1996). XTcf-3 transcription factor mediates beta-catenin-induced axis formation in *Xenopus* embryos. *Cell* 86, 391-399.
- Molotkov, A., Molotkova, N., and Duester, G. (2006). Retinoic acid guides eye morphogenetic movements via paracrine signaling but is unnecessary for retinal dorsoventral patterning. *Development* 133, 1901-1910.
- Molyneaux, B.J., Arlotta, P., Menezes, J.R., and Macklis, J.D. (2007). Neuronal subtype specification in the cerebral cortex. *Nat Rev Neurosci* 8, 427-437.
- Montavon, T., and Duboule, D. (2013). Chromatin organization and global regulation of Hox gene clusters. *Philos Trans R Soc Lond B Biol Sci* 368, 20120367.
- Moon, R.T., Campbell, R.M., Christian, J.L., McGrew, L.L., Shih, J., and Fraser, S. (1993). Xwnt-5A: a maternal Wnt that affects morphogenetic movements after overexpression in embryos of *Xenopus laevis*. *Development* 119, 97-111.
- Morriss, G.M. (1972). Morphogenesis of the malformations induced in rat embryos by maternal hypervitaminosis A. *Journal of Anatomy* 113, 241-250.
- Mulligan, K.A., and Cheyette, B.N. (2012). Wnt signaling in vertebrate neural development and function. *J Neuroimmune Pharmacol* 7, 774-787.
- Murthy, V.N. (2011). Olfactory maps in the brain. *Annu Rev Neurosci* 34, 233-258.
- Nadarajah, B., and Parnavelas, J.G. (2002). Modes of neuronal migration in the developing cerebral cortex. *Nat Rev Neurosci* 3, 423-432.
- Narendra, V., Rocha, P.P., An, D., Raviram, R., Skok, J.A., Mazzoni, E.O., and Reinberg, D. (2015). Transcription. CTCF establishes discrete functional chromatin domains at the Hox clusters during differentiation. *Science* 347, 1017-1021.

- Narita, Y., and Rijli, F.M. (2009). Hox genes in neural patterning and circuit formation in the mouse hindbrain. *Curr Top Dev Biol* 88, 139-167.
- Neumann, C.J., and Cohen, S.M. (1997). Long-range action of Wingless organizes the dorsal-ventral axis of the Drosophila wing. *Development* 124, 871-880.
- Neumann, S., Coudreuse, D.Y., van der Westhuyzen, D.R., Eckhardt, E.R., Korswagen, H.C., Schmitz, G., and Sprong, H. (2009). Mammalian Wnt3a is released on lipoprotein particles. *Traffic* 10, 334-343.
- Niederreither, K., and Dolle, P. (2008). Retinoic acid in development: towards an integrated view. *Nat Rev Genet* 9, 541-553.
- Niederreither, K., McCaffery, P., Drager, U.C., Chambon, P., and Dolle, P. (1997). Restricted expression and retinoic acid-induced downregulation of the retinaldehyde dehydrogenase type 2 (RALDH-2) gene during mouse development. *Mech Dev* 62, 67-78.
- Niederreither, K., Subbarayan, V., Dolle, P., and Chambon, P. (1999). Embryonic retinoic acid synthesis is essential for early mouse post-implantation development. *Nat Genet* 21, 444-448.
- Niederreither, K., Vermot, J., Le Roux, I., Schuhbaur, B., Chambon, P., and Dolle, P. (2003). The regional pattern of retinoic acid synthesis by RALDH2 is essential for the development of posterior pharyngeal arches and the enteric nervous system. *Development* 130, 2525-2534.
- Nikundiwe, A.M., Bjaalie, J.G., and Brodal, P. (1994). Lamellar organization of pontocerebellar neuronal populations. A multi-tracer and 3-D computer reconstruction study in the cat. *Eur J Neurosci* 6, 173-186.
- Noordermeer, D., Leleu, M., Splinter, E., Rougemont, J., De Laat, W., and Duboule, D. (2011). The dynamic architecture of Hox gene clusters. *Science* 334, 222-225.
- Nusse, R., and Varmus, H.E. (1982). Many tumors induced by the mouse mammary tumor virus contain a provirus integrated in the same region of the host genome. *Cell* 31, 99-109.
- O'Byrne, S.M., and Blaner, W.S. (2013). Retinol and retinyl esters: biochemistry and physiology. *J Lipid Res* 54, 1731-1743.
- O'Leary, D.D., Heffner, C.D., Kutka, L., Lopez-Mascaraque, L., Missias, A., and Reinoso, B.S. (1991). A target-derived chemoattractant controls the development of the corticopontine projection by a novel mechanism of axon targeting. *Development Suppl* 2, 123-130.
- Odeh, F., Ackerley, R., Bjaalie, J.G., and Apps, R. (2005). Pontine maps linking somatosensory and cerebellar cortices are in register with climbing fiber somatotopy. *J Neurosci* 25, 5680-5690.
- Oka, H., Sasaki, K., Matsuda, Y., Yasuda, T., and Mizuno, N. (1975). Responses of pontocerebellar neurones to stimulation of the parietal association and the frontal motor cortices. *Brain Res* 93, 399-407.

- Okada, T., Keino-Masu, K., and Masu, M. (2007). Migration and nucleogenesis of mouse precerebellar neurons visualized by in utero electroporation of a green fluorescent protein gene. *Neurosci Res* 57, 40-49.
- Oosterveen, T., Meijlink, F., and Deschamps, J. (2004). Expression of retinaldehyde dehydrogenase II and sequential activation of 5' Hoxb genes in the mouse caudal hindbrain. *Gene Expr Patterns* 4, 243-247.
- Oosterveen, T., Niederreither, K., Dolle, P., Chambon, P., Meijlink, F., and Deschamps, J. (2003). Retinoids regulate the anterior expression boundaries of 5' Hoxb genes in posterior hindbrain. *Embo J* 22, 262-269.
- Oury, F., Murakami, Y., Renaud, J.S., Pasqualetti, M., Charnay, P., Ren, S.Y., and Rijli, F.M. (2006). Hoxa2- and rhombomere-dependent development of the mouse facial somatosensory map. *Science* 313, 1408-1413.
- Palstra, R.J., Tolhuis, B., Splinter, E., Nijmeijer, R., Grosveld, F., and de Laat, W. (2003). The beta-globin nuclear compartment in development and erythroid differentiation. *Nat Genet* 35, 190-194.
- Panakova, D., Sprong, H., Marois, E., Thiele, C., and Eaton, S. (2005). Lipoprotein particles are required for Hedgehog and Wingless signalling. *Nature* 435, 58-65.
- Papalopulu, N., Clarke, J.D., Bradley, L., Wilkinson, D., Krumlauf, R., and Holder, N. (1991a). Retinoic acid causes abnormal development and segmental patterning of the anterior hindbrain in *Xenopus* embryos. *Development* 113, 1145-1158.
- Papalopulu, N., Lovell-Badge, R., and Krumlauf, R. (1991b). The expression of murine Hox-2 genes is dependent on the differentiation pathway and displays a collinear sensitivity to retinoic acid in F9 cells and *Xenopus* embryos. *Nucleic Acids Res* 19, 5497-5506.
- Park, D.H., Hong, S.J., Salinas, R.D., Liu, S.J., Sun, S.W., Sgualdino, J., Testa, G., Matzuk, M.M., Iwamori, N., and Lim, D.A. (2014). Activation of neuronal gene expression by the JMJD3 demethylase is required for postnatal and adult brain neurogenesis. *Cell Rep* 8, 1290-1299.
- Pasini, D., Malatesta, M., Jung, H.R., Walfridsson, J., Willer, A., Olsson, L., Skotte, J., Wutz, A., Porse, B., Jensen, O.N., *et al.* (2010). Characterization of an antagonistic switch between histone H3 lysine 27 methylation and acetylation in the transcriptional regulation of Polycomb group target genes. *Nucleic Acids Res* 38, 4958-4969.
- Patel, N.S., Rhinn, M., Semprich, C.I., Halley, P.A., Dolle, P., Bickmore, W.A., and Storey, K.G. (2013). FGF signalling regulates chromatin organisation during neural differentiation via mechanisms that can be uncoupled from transcription. *PLoS Genet* 9, e1003614.
- Perissi, V., Staszewski, L.M., McInerney, E.M., Kurokawa, R., Krones, A., Rose, D.W., Lambert, M.H., Milburn, M.V., Glass, C.K., and Rosenfeld, M.G. (1999). Molecular determinants of nuclear receptor-corepressor interaction. *Genes Dev* 13, 3198-3208.

- Perla Cota, M.S., Derrick E. Rancourt (2013). Stem Cells and Epigenetic Reprogramming. Pluripotent Stem Cells.
- Perrimon, N., and Mahowald, A.P. (1987). Multiple functions of segment polarity genes in *Drosophila*. *Dev Biol* 119, 587-600.
- Petkovich, M., Brand, N.J., Krust, A., and Chambon, P. (1987). A human retinoic acid receptor which belongs to the family of nuclear receptors. *Nature* 330, 444-450.
- Pfeiffer, S., Ricardo, S., Manneville, J.B., Alexandre, C., and Vincent, J.P. (2002). Producing cells retain and recycle Wingless in *Drosophila* embryos. *Curr Biol* 12, 957-962.
- Philippidou, P., and Dasen, J.S. (2013). Hox genes: choreographers in neural development, architects of circuit organization. *Neuron* 80, 12-34.
- Pijpers, A., Apps, R., Pardoe, J., Voogd, J., and Ruigrok, T.J. (2006). Precise spatial relationships between mossy fibers and climbing fibers in rat cerebellar cortical zones. *J Neurosci* 26, 12067-12080.
- Pivetta, C., Esposito, M.S., Sigrist, M., and Arber, S. (2014). Motor-circuit communication matrix from spinal cord to brainstem neurons revealed by developmental origin. *Cell* 156, 537-548.
- Proville, R.D., Spolidoro, M., Guyon, N., Dugue, G.P., Selimi, F., Isope, P., Popa, D., and Lena, C. (2014). Cerebellum involvement in cortical sensorimotor circuits for the control of voluntary movements. *Nat Neurosci* 17, 1233-1239.
- Puschendorf, M., Terranova, R., Boutsma, E., Mao, X., Isono, K., Brykczynska, U., Kolb, C., Otte, A.P., Koseki, H., Orkin, S.H., *et al.* (2008). PRC1 and Suv39h specify parental asymmetry at constitutive heterochromatin in early mouse embryos. *Nat Genet* 40, 411-420.
- Ramadoss, S., Chen, X., and Wang, C.Y. (2012). Histone demethylase KDM6B promotes epithelial-mesenchymal transition. *J Biol Chem* 287, 44508-44517.
- Raper, J., and Mason, C. (2010). Cellular strategies of axonal pathfinding. *Cold Spring Harb Perspect Biol* 2, a001933.
- Ray, R.S., and Dymecki, S.M. (2009). Rautenlippe Redux -- toward a unified view of the precerebellar rhombic lip. *Curr Opin Cell Biol* 21, 741-747.
- Rhinn, M., and Dolle, P. (2012). Retinoic acid signalling during development. *Development* 139, 843-858.
- Richards, G.S., and Degnan, B.M. (2009). The dawn of developmental signaling in the metazoa. *Cold Spring Harb Symp Quant Biol* 74, 81-90.
- Rijsewijk, F., Schuermann, M., Wagenaar, E., Parren, P., Weigel, D., and Nusse, R. (1987). The *Drosophila* homolog of the mouse mammary oncogene int-1 is identical to the segment polarity gene wingless. *Cell* 50, 649-657.

- Ringrose, L., and Paro, R. (2004). Epigenetic regulation of cellular memory by the Polycomb and Trithorax group proteins. *Annu Rev Genet* 38, 413-443.
- Rodriguez, C.I., Buchholz, F., Galloway, J., Sequerra, R., Kasper, J., Ayala, R., Stewart, A.F., and Dymecki, S.M. (2000). High-efficiency deleter mice show that FLPe is an alternative to Cre-loxP. *Nat Genet* 25, 139-140.
- Rodriguez, C.I., and Dymecki, S.M. (2000). Origin of the precerebellar system. *Neuron* 27, 475-486.
- Rogers, K.W., and Schier, A.F. (2011). Morphogen gradients: from generation to interpretation. *Annu Rev Cell Dev Biol* 27, 377-407.
- Romand, R., Kondo, T., Cammas, L., Hashino, E., and Dolle, P. (2008). Dynamic expression of the retinoic acid-synthesizing enzyme retinol dehydrogenase 10 (*rdh10*) in the developing mouse brain and sensory organs. *J Comp Neurol* 508, 879-892.
- Romanes, G.J. (1949). Neurological Anatomy in relation to Clinical Medicine. *Journal of Anatomy* 83, 385-385.
- Rosenfeld, M.G., Lunyak, V.V., and Glass, C.K. (2006). Sensors and signals: a coactivator/corepressor/epigenetic code for integrating signal-dependent programs of transcriptional response. *Genes Dev* 20, 1405-1428.
- Rosina, A., and Provini, L. (1984). Pontocerebellar system linking the two hemispheres by intracerebellar branching. *Brain Res* 296, 365-369.
- Rossant, J., Zirngibl, R., Cado, D., Shago, M., and Giguere, V. (1991). Expression of a retinoic acid response element-hsplacZ transgene defines specific domains of transcriptional activity during mouse embryogenesis. *Genes Dev* 5, 1333-1344.
- Rousseau, M., Crutchley, J.L., Miura, H., Suderman, M., Blanchette, M., and Dostie, J. (2014). Hox in motion: tracking HoxA cluster conformation during differentiation. *Nucleic Acids Res* 42, 1524-1540.
- Ruegg, D., and Wiesendanger, M. (1975). Corticofugal effects from sensorimotor area I and somatosensory area II on neurones of the pontine nuclei in the cat. *J Physiol* 247, 745-757.
- Saint-Cyr, J.A. (1983). The projection from the motor cortex to the inferior olive in the cat. An experimental study using axonal transport techniques. *Neuroscience* 10, 667-684.
- Sandell, L.L., Sanderson, B.W., Moiseyev, G., Johnson, T., Mushegian, A., Young, K., Rey, J.P., Ma, J.X., Staehling-Hampton, K., and Trainor, P.A. (2007). RDH10 is essential for synthesis of embryonic retinoic acid and is required for limb, craniofacial, and organ development. *Genes Dev* 21, 1113-1124.
- Santagati, F., Minoux, M., Ren, S.Y., and Rijli, F.M. (2005). Temporal requirement of *Hoxa2* in cranial neural crest skeletal morphogenesis. *Development* 132, 4927-4936.

- Schmid, T., Kruger, M., and Braun, T. (2007). NSCL-1 and -2 control the formation of precerebellar nuclei by orchestrating the migration of neuronal precursor cells. *J Neurochem* *102*, 2061-2072.
- Schubeler, D. (2015). Function and information content of DNA methylation. *Nature* *517*, 321-326.
- Schuettengruber, B., Martinez, A.M., Iovino, N., and Cavalli, G. (2011). Trithorax group proteins: switching genes on and keeping them active. *Nat Rev Mol Cell Biol* *12*, 799-814.
- Schwarz, C., Horowski, A., Mock, M., and Thier, P. (2005). Organization of tectopontine terminals within the pontine nuclei of the rat and their spatial relationship to terminals from the visual and somatosensory cortex. *The Journal of comparative neurology* *484*, 283-298.
- Schwarz, C., Mock, M., and Thier, P. (1997). Electrophysiological properties of rat pontine nuclei neurons In vitro. I. Membrane potentials and firing patterns. *J Neurophysiol* *78*, 3323-3337.
- Schwarz, C., and Thier, P. (1995). Modular organization of the pontine nuclei: dendritic fields of identified pontine projection neurons in the rat respect the borders of cortical afferent fields. *J Neurosci* *15*, 3475-3489.
- Schwarz, C., and Thier, P. (1999). Binding of signals relevant for action: towards a hypothesis of the functional role of the pontine nuclei. *Trends Neurosci* *22*, 443-451.
- Schwarz, C., and Thier, P. (2000). Reply. *Trends Neurosci* *23*, 152-153.
- Schwarz, D., Varum, S., Zemke, M., Scholer, A., Baggiolini, A., Draganova, K., Koseki, H., Schubeler, D., and Sommer, L. (2014). Ezh2 is required for neural crest-derived cartilage and bone formation. *Development* *141*, 867-877.
- Schwarz, L.A., Miyamichi, K., Gao, X.J., Beier, K.T., Weissbourd, B., DeLoach, K.E., Ren, J., Ibanes, S., Malenka, R.C., Kremer, E.J., *et al.* (2015). Viral-genetic tracing of the input-output organization of a central noradrenaline circuit. *Nature* *524*, 88-92.
- Seidler, B., Schmidt, A., Mayr, U., Nakhai, H., Schmid, R.M., Schneider, G., and Saur, D. (2008). A Cre-loxP-based mouse model for conditional somatic gene expression and knockdown in vivo by using avian retroviral vectors. *Proc Natl Acad Sci U S A* *105*, 10137-10142.
- Seo, H.C., Edvardsen, R.B., Maeland, A.D., Bjordal, M., Jensen, M.F., Hansen, A., Flaate, M., Weissenbach, J., Lehrach, H., Wincker, P., *et al.* (2004). Hox cluster disintegration with persistent anteroposterior order of expression in *Oikopleura dioica*. *Nature* *431*, 67-71.
- Shambes, G.M., Gibson, J.M., and Welker, W. (1978). Fractured somatotopy in granule cell tactile areas of rat cerebellar hemispheres revealed by micromapping. *Brain Behav Evol* *15*, 94-140.
- Sharma, R.P., and Chopra, V.L. (1976). Effect of the Wingless (wg1) mutation on wing and haltere development in *Drosophila melanogaster*. *Dev Biol* *48*, 461-465.

- Shimizu, K., and Gurdon, J.B. (1999). A quantitative analysis of signal transduction from activin receptor to nucleus and its relevance to morphogen gradient interpretation. *Proc Natl Acad Sci U S A* *96*, 6791-6796.
- Shinohara, M., Zhu, Y., and Murakami, F. (2013). Four-dimensional analysis of nucleogenesis of the pontine nucleus in the hindbrain. *The Journal of comparative neurology* *521*, 3340-3357.
- Siegfried, E., Chou, T.B., and Perrimon, N. (1992). wingless signaling acts through zeste-white 3, the *Drosophila* homolog of glycogen synthase kinase-3, to regulate engrailed and establish cell fate. *Cell* *71*, 1167-1179.
- Simeone, A., Acampora, D., Arcioni, L., Andrews, P.W., Boncinelli, E., and Mavilio, F. (1990). Sequential activation of HOX2 homeobox genes by retinoic acid in human embryonal carcinoma cells. *Nature* *346*, 763-766.
- Simeone, A., Acampora, D., Nigro, V., Faiella, A., D'Esposito, M., Stornaiuolo, A., Mavilio, F., and Boncinelli, E. (1991). Differential regulation by retinoic acid of the homeobox genes of the four HOX loci in human embryonal carcinoma cells. *Mech Dev* *33*, 215-227.
- Simonis, M., Kooren, J., and de Laat, W. (2007). An evaluation of 3C-based methods to capture DNA interactions. *Nat Methods* *4*, 895-901.
- Solowska, J.M., Mazurek, A., Weinberger, L., and Baird, D.H. (2002). Pontocerebellar axon guidance: neuropilin-1- and semaphorin 3A-sensitivity gradients across basilar pontine nuclei and semaphorin 3A variation across cerebellum. *Mol Cell Neurosci* *21*, 266-284.
- Sommer, A. (2008). Vitamin a deficiency and clinical disease: An historical overview. *J Nutr* *138*, 1835-1839.
- Soshnikova, N., and Duboule, D. (2009). Epigenetic temporal control of mouse Hox genes in vivo. *Science* *324*, 1320-1323.
- Sotelo, C. (2004). Cellular and genetic regulation of the development of the cerebellar system. *Prog Neurobiol* *72*, 295-339.
- Stamatakis, D., Ulloa, F., Tsoni, S.V., Mynett, A., and Briscoe, J. (2005). A gradient of Gli activity mediates graded Sonic Hedgehog signaling in the neural tube. *Genes Dev* *19*, 626-641.
- Stein, E., and Tessier-Lavigne, M. (2001). Hierarchical organization of guidance receptors: silencing of netrin attraction by slit through a Robo/DCC receptor complex. *Science* *291*, 1928-1938.
- Stein, J.F., and Glickstein, M. (1992). Role of the cerebellum in visual guidance of movement. *Physiol Rev* *72*, 967-1017.
- Sternson, S.M., and Roth, B.L. (2014). Chemogenetic tools to interrogate brain functions. *Annu Rev Neurosci* *37*, 387-407.

- Storm, R., Cholewa-Waclaw, J., Reuter, K., Brohl, D., Sieber, M., Treier, M., Muller, T., and Birchmeier, C. (2009). The bHLH transcription factor Olig3 marks the dorsal neuroepithelium of the hindbrain and is essential for the development of brainstem nuclei. *Development* *136*, 295-305.
- Stornaiuolo, A., Acampora, D., Pannese, M., D'Esposito, M., Morelli, F., Migliaccio, E., Rambaldi, M., Faiella, A., Nigro, V., Simeone, A., *et al.* (1990). Human HOX genes are differentially activated by retinoic acid in embryonal carcinoma cells according to their position within the four loci. *Cell Differ Dev* *31*, 119-127.
- Studer, M., Gavalas, A., Marshall, H., Ariza-McNaughton, L., Rijli, F.M., Chambon, P., and Krumlauf, R. (1998). Genetic interactions between Hoxa1 and Hoxb1 reveal new roles in regulation of early hindbrain patterning. *Development* *125*, 1025-1036.
- Studer, M., Lumsden, A., Ariza-McNaughton, L., Bradley, A., and Krumlauf, R. (1996). Altered segmental identity and abnormal migration of motor neurons in mice lacking Hoxb-1. *Nature* *384*, 630-634.
- Studer, M., Popperl, H., Marshall, H., Kuroiwa, A., and Krumlauf, R. (1994). Role of a conserved retinoic acid response element in rhombomere restriction of Hoxb-1. *Science* *265*, 1728-1732.
- Subramanian, V., Meyer, B.I., and Gruss, P. (1995). Disruption of the murine homeobox gene Cdx1 affects axial skeletal identities by altering the mesodermal expression domains of Hox genes. *Cell* *83*, 641-653.
- Surmeli, G., Akay, T., Ippolito, G.C., Tucker, P.W., and Jessell, T.M. (2011). Patterns of spinal sensory-motor connectivity prescribed by a dorsoventral positional template. *Cell* *147*, 653-665.
- Suzuki, D.A., May, J.G., Keller, E.L., and Yee, R.D. (1990). Visual motion response properties of neurons in dorsolateral pontine nucleus of alert monkey. *J Neurophysiol* *63*, 37-59.
- Suzuki, L., Coulon, P., Sabel-Goedknecht, E.H., and Ruigrok, T.J. (2012). Organization of cerebral projections to identified cerebellar zones in the posterior cerebellum of the rat. *J Neurosci* *32*, 10854-10869.
- Swenson, R.S., Kosinski, R.J., and Castro, A.J. (1984). Topography of spinal, dorsal column nuclear, and spinal trigeminal projections to the pontine gray in rats. *J Comp Neurol* *222*, 301-311.
- Szymanski, P., and Levine, M. (1995). Multiple modes of dorsal-bHLH transcriptional synergy in the *Drosophila* embryo. *Embo J* *14*, 2229-2238.
- Tamai, K., Semenov, M., Kato, Y., Spokony, R., Liu, C., Katsuyama, Y., Hess, F., Saint-Jeannet, J.P., and He, X. (2000). LDL-receptor-related proteins in Wnt signal transduction. *Nature* *407*, 530-535.

- Tamariz, E., and Varela-Echavarria, A. (2015). The discovery of the growth cone and its influence on the study of axon guidance. *Front Neuroanat* 9, 51.
- Taniguchi, H., Kawauchi, D., Nishida, K., and Murakami, F. (2006). Classic cadherins regulate tangential migration of precerebellar neurons in the caudal hindbrain. *Development* 133, 1923-1931.
- Tarchini, B., and Duboule, D. (2006). Control of Hoxd genes' collinearity during early limb development. *Dev Cell* 10, 93-103.
- Terenzi, M.G., Zagon, A., and Roberts, M.H. (1995). Efferent connections from the anterior pretectal nucleus to the diencephalon and mesencephalon in the rat. *Brain Res* 701, 183-191.
- Tessier-Lavigne, M. (1994). Axon guidance by diffusible repellants and attractants. *Curr Opin Genet Dev* 4, 596-601.
- Tessier-Lavigne, M., and Goodman, C.S. (1996). The molecular biology of axon guidance. *Science* 274, 1123-1133.
- Testa, G., Schaft, J., van der Hoeven, F., Glaser, S., Anastassiadis, K., Zhang, Y., Hermann, T., Stremmel, W., and Stewart, A.F. (2004). A reliable lacZ expression reporter cassette for multipurpose, knockout-first alleles. *Genesis* 38, 151-158.
- Thaller, C., and Eichele, G. (1987). Identification and Spatial-Distribution of Retinoids in the Developing Chick Limb Bud. *Nature* 327, 625-628.
- Thier, P., Bachor, A., Faiss, J., Dichgans, J., and Koenig, E. (1991). Selective impairment of smooth-pursuit eye movements due to an ischemic lesion of the basal pons. *Ann Neurol* 29, 443-448.
- Thomke, F., and Hopf, H.C. (1999). Pontine lesions mimicking acute peripheral vestibulopathy. *J Neurol Neurosurg Psychiatry* 66, 340-349.
- Tie, F., Banerjee, R., Conrad, P.A., Scacheri, P.C., and Harte, P.J. (2012). Histone demethylase UTX and chromatin remodeler BRM bind directly to CBP and modulate acetylation of histone H3 lysine 27. *Mol Cell Biol* 32, 2323-2334.
- Tolwinski, N.S., and Wieschaus, E. (2004). A nuclear function for armadillo/beta-catenin. *PLoS Biol* 2, E95.
- Tomasch, J. (1969). Numerical capacities of cerebellar cell and fiber systems. *Experientia* 25, 377-378.
- Tumpel, S., Wiedemann, L.M., and Krumlauf, R. (2009). Hox genes and segmentation of the vertebrate hindbrain. *Curr Top Dev Biol* 88, 103-137.
- Turing, A.M. (1952). THE CHEMICAL BASIS OF MORPHOGENESIS. *Philosophical Transactions of the Royal Society of London* 237, 37-72.

- Turner, R.S., and German, W.J. (1941). FUNCTIONAL ANATOMY OF BRACHIUM PONTIS. *J Neurophysiol* 4, 196-206.
- Urvalek, A., Laursen, K.B., and Gudas, L.J. (2014). The roles of retinoic acid and retinoic acid receptors in inducing epigenetic changes. *Subcell Biochem* 70, 129-149.
- van de Werken, H.J., Landan, G., Holwerda, S.J., Hoichman, M., Klous, P., Chachik, R., Splinter, E., Valdes-Quezada, C., Oz, Y., Bouwman, B.A., *et al.* (2012). Robust 4C-seq data analysis to screen for regulatory DNA interactions. *Nat Methods* 9, 969-972.
- van den Akker, E., Forlani, S., Chawengsaksophak, K., de Graaff, W., Beck, F., Meyer, B.I., and Deschamps, J. (2002). Cdx1 and Cdx2 have overlapping functions in anteroposterior patterning and posterior axis elongation. *Development* 129, 2181-2193.
- vanderHoeven, F., Zakany, J., and Duboule, D. (1996). Gene transpositions in the HoxD complex reveal a hierarchy of regulatory controls. *Cell* 85, 1025-1035.
- Vann, S.D., Aggleton, J.P., and Maguire, E.A. (2009). What does the retrosplenial cortex do? *Nat Rev Neurosci* 10, 792-802.
- Vitobello, A., Ferretti, E., Lampe, X., Vilain, N., Ducret, S., Ori, M., Spetz, J.F., Selleri, L., and Rijli, F.M. (2011). Hox and Pbx factors control retinoic acid synthesis during hindbrain segmentation. *Dev Cell* 20, 469-482.
- Voiculescu, O., Charnay, P., and Schneider-Maunoury, S. (2000). Expression pattern of a Krox-20/Cre knock-in allele in the developing hindbrain, bones, and peripheral nervous system. *Genesis* 26, 123-126.
- Vollmer, J.Y., and Clerc, R.G. (1998). Homeobox genes in the developing mouse brain. *J Neurochem* 71, 1-19.
- Waddington (1942). The Epigenotype. *Endeavour* 18–20
- Waddington (1957). The strategy of the genes: a discussion of some aspects of theoretical biology. Allen & Unwin.
- Walshe, J., Maroon, H., McGonnell, I.M., Dickson, C., and Mason, I. (2002). Establishment of hindbrain segmental identity requires signaling by FGF3 and FGF8. *Curr Biol* 12, 1117-1123.
- Wang, H., Wang, L., Erdjument-Bromage, H., Vidal, M., Tempst, P., Jones, R.S., and Zhang, Y. (2004). Role of histone H2A ubiquitination in Polycomb silencing. *Nature* 431, 873-878.
- Wang, S., Krinks, M., Lin, K., Luyten, F.P., and Moos, M., Jr. (1997). Frzb, a secreted protein expressed in the Spemann organizer, binds and inhibits Wnt-8. *Cell* 88, 757-766.
- Wang, V.Y., Rose, M.F., and Zoghbi, H.Y. (2005). Math1 expression redefines the rhombic lip derivatives and reveals novel lineages within the brainstem and cerebellum. *Neuron* 48, 31-43.

- Warming, S., Costantino, N., Court, D.L., Jenkins, N.A., and Copeland, N.G. (2005). Simple and highly efficient BAC recombineering using galK selection. *Nucleic Acids Res* 33, e36.
- Wellik, D.M. (2009). Hox genes and vertebrate axial pattern. *Curr Top Dev Biol* 88, 257-278.
- Wertz, A., Trenholm, S., Yonehara, K., Hillier, D., Raics, Z., Leinweber, M., Szalay, G., Ghanem, A., Keller, G., Rozsa, B., *et al.* (2015). Single-cell-initiated monosynaptic tracing reveals layer-specific cortical network modules. *Science* 349, 70-74.
- White, J.A., Guo, Y.D., Baetz, K., Beckett-Jones, B., Bonasoro, J., Hsu, K.E., Dilworth, F.J., Jones, G., and Petkovich, M. (1996). Identification of the retinoic acid-inducible all-trans-retinoic acid 4-hydroxylase. *The Journal of biological chemistry* 271, 29922-29927.
- White, R.J., Nie, Q., Lander, A.D., and Schilling, T.F. (2007). Complex regulation of *cyp26a1* creates a robust retinoic acid gradient in the zebrafish embryo. *PLoS Biol* 5, e304.
- White, R.J., and Schilling, T.F. (2008). How degrading: Cyp26s in hindbrain development. *Dev Dyn* 237, 2775-2790.
- Wickersham, I.R., Lyon, D.C., Barnard, R.J., Mori, T., Finke, S., Conzelmann, K.K., Young, J.A., and Callaway, E.M. (2007). Monosynaptic restriction of transsynaptic tracing from single, genetically targeted neurons. *Neuron* 53, 639-647.
- Wickersham, I.R., Sullivan, H.A., and Seung, H.S. (2010). Production of glycoprotein-deleted rabies viruses for monosynaptic tracing and high-level gene expression in neurons. *Nat Protoc* 5, 595-606.
- Wieschaus, E., and Riggleman, R. (1987). Autonomous requirements for the segment polarity gene *armadillo* during *Drosophila* embryogenesis. *Cell* 49, 177-184.
- Wiesendanger, R., and Wiesendanger, M. (1982). The corticopontine system in the rat. I. Mapping of corticopontine neurons. *The Journal of comparative neurology* 208, 215-226.
- Wilson, L., Gale, E., Chambers, D., and Maden, M. (2004). Retinoic acid and the control of dorsoventral patterning in the avian spinal cord. *Dev Biol* 269, 433-446.
- Wingate, R.J., and Hatten, M.E. (1999). The role of the rhombic lip in avian cerebellum development. *Development* 126, 4395-4404.
- Wolpert, L. (1969). Positional information and the spatial pattern of cellular differentiation. *J Theor Biol* 25, 1-47.
- Xu, Q., Mellitzer, G., and Wilkinson, D.G. (2000). Roles of Eph receptors and ephrins in segmental patterning. *Philos Trans R Soc Lond B Biol Sci* 355, 993-1002.
- Yamada, M., Terao, M., Terashima, T., Fujiyama, T., Kawaguchi, Y., Nabeshima, Y., and Hoshino, M. (2007). Origin of climbing fiber neurons and their developmental dependence on *Ptf1a*. *J Neurosci* 27, 10924-10934.

- Yamamoto, A., Nagano, T., Takehara, S., Hibi, M., and Aizawa, S. (2005). Shisa promotes head formation through the inhibition of receptor protein maturation for the caudalizing factors, Wnt and FGF. *Cell* *120*, 223-235.
- Yan, D., Wiesmann, M., Rohan, M., Chan, V., Jefferson, A.B., Guo, L., Sakamoto, D., Caothien, R.H., Fuller, J.H., Reinhard, C., *et al.* (2001). Elevated expression of axin2 and hnk2 mRNA provides evidence that Wnt/beta-catenin signaling is activated in human colon tumors. *Proc Natl Acad Sci U S A* *98*, 14973-14978.
- Yanagawa, S., Matsuda, Y., Lee, J.S., Matsubayashi, H., Sese, S., Kadowaki, T., and Ishimoto, A. (2002). Casein kinase I phosphorylates the Armadillo protein and induces its degradation in *Drosophila*. *Embo J* *21*, 1733-1742.
- Yanagawa, S., van Leeuwen, F., Wodarz, A., Klingensmith, J., and Nusse, R. (1995). The dishevelled protein is modified by wingless signaling in *Drosophila*. *Genes Dev* *9*, 1087-1097.
- Yashiro, K., Zhao, X., Uehara, M., Yamashita, K., Nishijima, M., Nishino, J., Saijoh, Y., Sakai, Y., and Hamada, H. (2004). Regulation of retinoic acid distribution is required for proximodistal patterning and outgrowth of the developing mouse limb. *Dev Cell* *6*, 411-422.
- Yost, C., Torres, M., Miller, J.R., Huang, E., Kimelman, D., and Moon, R.T. (1996). The axis-inducing activity, stability, and subcellular distribution of beta-catenin is regulated in *Xenopus* embryos by glycogen synthase kinase 3. *Genes Dev* *10*, 1443-1454.
- Young, T., Rowland, J.E., van de Ven, C., Bialecka, M., Novoa, A., Carapuco, M., van Nes, J., de Graaff, W., Duluc, I., Freund, J.N., *et al.* (2009). Cdx and Hox genes differentially regulate posterior axial growth in mammalian embryos. *Dev Cell* *17*, 516-526.
- Yu, V.C., Delsert, C., Andersen, B., Holloway, J.M., Devary, O.V., Naar, A.M., Kim, S.Y., Boutin, J.M., Glass, C.K., and Rosenfeld, M.G. (1991). RXR beta: a coregulator that enhances binding of retinoic acid, thyroid hormone, and vitamin D receptors to their cognate response elements. *Cell* *67*, 1251-1266.
- Zachman, R.D. (1967). The stimulation of RNA synthesis in vivo and in vitro by retinol (vitamin A) in the intestine of vitamin A deficient rats. *Life Sci* *6*, 2207-2213.
- Zakany, J., and Duboule, D. (2007). The role of Hox genes during vertebrate limb development. *Curr Opin Genet Dev* *17*, 359-366.
- Zakany, J., Gerard, M., Favier, B., Potter, S.S., and Duboule, D. (1996). Functional equivalence and rescue among group 11 hox gene products in vertebral patterning. *Dev Biol* *176*, 325-328.
- Zelent, A., Krust, A., Petkovich, M., Kastner, P., and Chambon, P. (1989). Cloning of murine alpha and beta retinoic acid receptors and a novel receptor gamma predominantly expressed in skin. *Nature* *339*, 714-717.
- Zhang, J., Smith, D., Yamamoto, M., Ma, L., and McCaffery, P. (2003). The meninges is a source of retinoic acid for the late-developing hindbrain. *J Neurosci* *23*, 7610-7620.

Zhang, M., Kim, H.J., Marshall, H., Gendron-Maguire, M., Lucas, D.A., Baron, A., Gudas, L.J., Gridley, T., Krumlauf, R., and Grippo, J.F. (1994). Ectopic Hoxa-1 induces rhombomere transformation in mouse hindbrain. *Development* *120*, 2431-2442.

Zhu, Y., Matsumoto, T., Mikami, S., Nagasawa, T., and Murakami, F. (2009). SDF1/CXCR4 signalling regulates two distinct processes of precerebellar neuronal migration and its depletion leads to abnormal pontine nuclei formation. *Development* *136*, 1919-1928.

Zuniga, A., and Zeller, R. (1999). Gli3 (Xt) and formin (ld) participate in the positioning of the polarising region and control of posterior limb-bud identity. *Development* *126*, 13-21.

Acknowledgments

At the end I'd like to thank some people who supported me during the time I was working on this thesis. Without them this work would probably not exist in the present form. More importantly, I do want to thank those people that I will miss to mention personally, despite them having been there during certain aspects of my time in- and outside of FMI.

I want to thank Filippo Rijli for the opportunity to conduct my PhD work in this very stimulating environment and who provided me with the necessary support to pursue this exciting project. I will always remember the inspiring scientific and non-scientific discussion that taught me many important lessons also beyond the lab. I also want to thank the members of my thesis committee, Peter Scheiffele and Botond Roska for their helpful comments and suggestions and Roger Clerc for chairing the examination.

Of course I want to especially thank all current and former members of the Rijli Lab. I will truly take many memories from my time with all of you. Despite everybody having a significant contribution, some people should be pointed out in particular: Thomas Di Meglio who supported me especially in the initial phases of my PhD and for stimulating discussions that shaped this exciting project in large parts; Claudius Kratochwil for his essential scientific input on the connectivity part of the project, for very many enjoyable moments in- and outside the lab, for proofreading of this manuscript and for his ongoing support over the last years; Upasana Maheshwari for joining the project when it was needed the most, proofreading this manuscript and being a great person to work with; Sjoerd Holwerda for his help on the 4C part; Nicola Maiorano and Kajari Karmakar for their technical support with the rabies viruses; Nathalie Vilain and Sebastien Ducret for their excellent scientific and technical contributions, Sebastien especially for his help in generating transgenic lines.

I also want to thank the entire FMI and particularly the FMI facility members. Much of the work would have not been feasible without their extraordinary technical support. Steve Bourke, Moritz Kirschbaum, Jan Eglinger, Raphael Thierry and Laurent Gelman (FAIM); Hubertur Kohler (FACS and Tee); Kirsten Jacobeit, Stéphane Thiry and Tim Roloff (Functional Genomics); Augustyn Bogucki and Sandrine Bichet (Histo); Jean-Francois Spetz (Transgenic Mouse Facility); the entire administration staff of the FMI, particularly Elida Keller and Sandra Ziegler; Marc Bühler for his support as Dean of students and of course

Susan Gasser for her dedication as director of the FMI. You make the FMI being a great place to do science.

Many thanks to all members of the Student reps, the Skiing weekend and Life Science Beach Cup organization committees, the FMI soccer team members, the entire SC Novartis II team, the Wednesday climbing group, everybody I meet over the past years on the Basel Beach volleyball courts, the Rhine swimmers, the Flora Beach BBQ companions and lots of very good friends in- and outside the FMI, with whom I shared countless wonderful moments. All of you made my time in Basel being absolutely amazing!

I owe a very big and very special ‘thank you’ to Lisa Adelfinger. With her critical input she contributed significantly to this thesis and many other parts of my PhD. More importantly, she kept me on track in difficult times and reminded me about the important things in life, by always having a sympathetic ear and providing unconditional support. It is great to have such a wonderful person in my life.

Last but not least I want to thank my parents for supporting me during all these years.